Seasonal Variability of the Upper Ocean Driven by the Atmospheric Forcing and its Regulation of Nutrients and Chlorophyll in the Bay of Bengal

Thesis submitted to

Goa University

For the degree of

Doctor of Philosophy

in

Marine Sciences

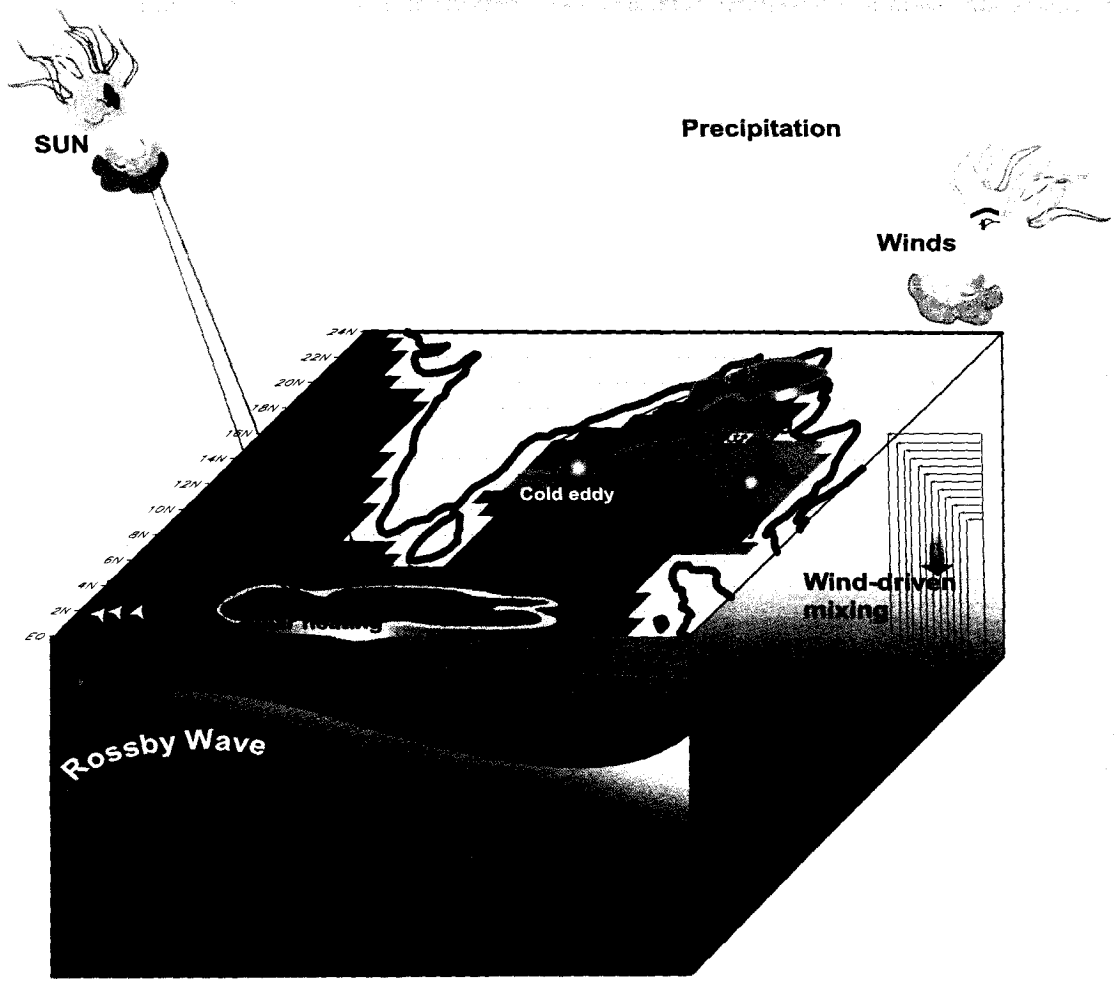

by

Jayu Narvekar

Reg.no: 200404816

National Institute of Oceanography,

Goa, India.

August 2008

Seasonal variability of the upper ocean driven by the atmospheric forcing and its regulation of nutrients and chlorophyll in the Bay of Bengal

Thesis submitted to

Goa University

For the degree of

Doctor of Philosophy

in

Marine Sciences

by

Jayu Narvekar
Reg.no: 200404816

National Institute of Oceanography,
Goa, India.

August 2008

List of Contents

Chapter 4 – Atmospheric Forcing and Remote Forcing

Chapter 5 – Eddies and mixed layer variability

Chapter 6 – Nitrate and Chlorophyll

Statement

As required under the University ordinance 0.19.8(vi), I state that this thesis entitled "Seasonal variability of the upper ocean driven by the atmospheric forcing and its regulation of nutrients and chlorophyll in the Bay of Bengal" is my original contribution and it has not been submitted on any previous occasion.

The literature related to the problem investigated has been cited. Due acknowledgements have been made wherever facilities and suggestions have been availed off.

Jayu Narvekar

National Institute of Oceanography
Dona Paula, Goa

Place: Dona Paula

Date: 20 August 2008

Certificate

This is to certify that the thesis entitled "Seasonal variability of the upper ocean driven by the atmospheric forcing and its regulation of nutrients and chlorophyll in the Bay of Bengal" submitted by Ms. Jayu Narvekar for the award of the degree of Doctor of Philosophy in Marine Science is based on original studies carried out by her under my supervision. The thesis or any part thereof has not been previously submitted for any other degree or diploma in any institution.

Dr. S. Prasanna Kumar

Research Supervisor

National Institute of Oceanography

Dona Paula, Goa

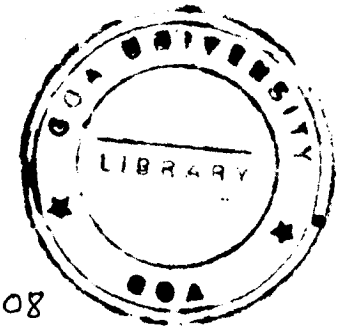

Place: Dona Paula

Date: 20 August 2008

All the suggestions of the reviewers are incorporated.

Basil Mathew, Sc F
(External Examiner)

Acknowledgements

Guru Brahma Guru Vishnu Guru Devo Maheshwarah |

Guru Saakshaat Par-Brahma Tasmei Shree Gurave Namah ||

Indian tradition has given a great place for Guru. As the creator of knowledge he takes the place Brahma, as the protector of our intellectual faculty he takes the place of Vishnu and as the destroyer of our ignorance he takes the place of Maheshwara. He is the Supreme Being, the Para Brahma, in binding us all with the feeling of universal oneness hence I offer my salutation to my Guru, to Dr. S. Prasanna Kumar, Scientist, National Institute of Oceanography (NIO), Goa, who guided me in my quest to understand the fascinating ways in which the Bay of Bengal changes with season. Dr. Aftab Can, Reader, Marine Sciences served as my Co-guide and his valuable suggestions from time to time helped me to a great extent in my research work. Dr. Harilal B. Menon, Professor, Marine Sciences was always there to encourage me. Dr. G. N. Nayak, Head of the Department of Marine Sciences was very kind and provided all the administrative support in fulfilling the formalities of the University for the smooth completion of my thesis work.

I am grateful to Council of Scientific and Industrial Research (CSIR), New Delhi for providing me the Junior Research Fellowship and the total financial support in completing my thesis work. A special thanks to Dr. S. R. Shetye, Director, National Institute of Oceanography, Goa, for providing all the necessary the facilities without which I would not have completed my thesis work successfully. Dr. Vethamony,

Scientist, NIO monitored my thesis work as VC's nominee and was very kind and supportive in providing me with his constructive criticism which helped me immensely. I thank Dr. M.R. Ramesh Kumar and Dr. V.S.N. Murty for their discussions and suggestions which helped me in my thesis work.

Two departments in NIO are the lifeline for Ph.D students – The Data Division and the Library. Since my Ph.D work was based on observational data, I have to greatly rely upon the Data Division. Dr. G.V. Reddy was very kind and was always there to help me with any kind of data request that I had, and I had a large number of them. I have no words to express my gratitude. Dr. M. Tapaswi, Documentation officer, NIO Library and his team helped me greatly with reference material not only from NIO resources, but from other Institute as well. Similarly Mr. A. Mahale and his team helped me with several of my difficult diagrams. In fact Mr. Mahale and Mr. Shyam helped me in designing the cover page of my thesis. My special thanks to Dr. Tapaswi, Mr. Mahale and their teams.

In my thesis I have used physical, chemical and biological data collected under Bay of Bengal Process Studies (BOBPS). I wish to thank each and every individual members of the BOBPS team who meticulously and painstakingly collected the data onboard ORV Sagar Kanya and FORV Sagar Sampada. My special thanks to Dr. N. Ramaiah, Dr. S. Sardesai and Dr. Mangesh Gauns of BOBPS for the chlorophyll and nitrate data.

During the course of my thesis work I encountered several difficulties working with LINUX and also programming for data processing. Whether it is the difficulty with computer hardware or software, Mr. Gourish Salgaonkar was always there to help me

out. He was my friend and well-wisher. I have no words to express my gratitude to Mr. Gourish Salgaonkar for his all-out support and help. I am also thankful to Dr. Nuncio Murukesh for helping me with sea-level anomaly data and with discussions from time to time.

I am also thankful to all my friends for the help they rendered during the course of my thesis work.

I wish to express my whole-hearted thanks to my parents, my grandmother, my sister Teja, my brother Indrajeet and other members of my family for their constant moral support and encouragement without which I would not have completed my thesis work.

Last but not least to the Almighty God for giving me the courage and confidence in executing the work.

Abstract

The upper ocean is the most variable and dynamically active part of the marine environment that couples the underlying ocean to the atmosphere above through the transfer of mass, momentum and energy. The thickness of mixed layer is an important parameter in determining the quantity of heat that is available for exchange with atmosphere which is capable of triggering several ocean-atmosphere coupled processes. Mixed layer also plays an important role in determining the chlorophyll biomass and biological productivity of the upper ocean. The present thesis is an attempt to decipher the basin-scale variability of the mixed layer in the Bay of Bengal on a seasonal scale and the factors responsible for it. The aim is also to understand how the changes in water column nitrate and chlorophyll are linked to the upper ocean variability.

A suite of *in situ* as well as remote sensing data was used. The *in situ* data consisted of temperature, salinity, nitrate and chlorophyll *a* profiles derived from World Ocean Data Base and Responsible National Oceanographic Data Centre (RNODC) at National Institute of Oceanography, which archives the data collected by Indian research ships. In addition temperature and salinity profiles from Argo were also used. These data were used to prepare the monthly mean temperature and salinity climatology, while seasonal climatology was prepared for nitrate and chlorophyll *a* on a 1°x1° spatial grid. In addition to this, the high resolution *in situ* data collected during Bay of Bengal Process Studies (BOBPS) during summer (6 July to 2 August, 2001), fall intermonsoon (14 September to 12 October, 2002), spring intermonsoon (12 April to 7 May, 2003), and winter (25

November 2005 to 4 January 2006) were also utilized to delineate the effect of meso-scale variability on mixed layer depth.

As the salinity changed rapidly in the upper layers in the Bay of Bengal due to freshening by river runoff as well as precipitation, density criteria was used to define mixed layer for the present study. Mixed layer was defined as the depth at which the density (sigma-t) exceeds 0.2 kg m^{-3} from its surface value. The barrier layer was numerically calculated by subtracting the mixed layer depth (MLD) from the isothermal layer. The isothermal layer for the present study was defined as the depth at which the temperature decreased by 1°C from its surface value.

The atmospheric data used was monthly mean climatology of the incoming short wave radiation, wind speed, evaporation, precipitation and net heat flux on 1° x 1° grid, which was obtained from National Oceanographic Centre (NOC), Southampton for the period 1980-1993. The remote sensing data used for the study was the chlorophyll pigment concentrations from SeaWiFS during the period September 1997 to December 2007 and the merged sea-level anomalies of Topex/Poseidon ERS1/2 series of satellites obtained from AVISO live access server during the period October 1992 to January 2006. From the sea-level height anomalies, velocities were computed assuming geostrophic balance.

The mixed layer and barrier layer variability were examined in the light of heat flux, momentum flux (wind-stress curl) and fresh water flux (evaporation-precipitation) to decipher the factors that are responsible for their changes.

The mixed layer depth (MLD) during the spring intermonsoon (March-April-May) was the shallowest in the Bay of Bengal compared to the rest of the season. It varied between 10 and 25 m in March and April. This shallow MLD was driven by the strong stratification induced by peak solar heating (280-290 W/m^2) and subsequent highest net heat gain by the ocean (150-160 W/m^2). The low salinity waters (< 32.5 psu) in the northern Bay (north of 18°N) during March-April made the upper ocean highly stratified. The weak winds during this period were unable to drive deep wind-mixing due to strong stratification and hence resulted in the formation of shallow mixed layer.

In the south, the comparatively deeper mixed layer (~ 35 m) seen west of 90°E was due to the presence of high salinity waters (>34.5 psu) which made the water column less stable and the moderate winds were able to initiate greater mixing leading to the observed deep MLD. However, the deep MLD east of Sri Lanka was linked to the development of anti-cyclonic circulation associated with the formation of subtropical gyre which begins in May. This anti-cyclonic circulation drives down-welling and deepens the mixed layer. The co-location of comparatively deep MLD (>25 m) and strong negative wind stress curl (~ -20×10^{-8} Pascal/m) along the western boundary in April suggested the role of wind stress curl in deepening the mixed layer. Note that the subtropical gyre was well developed in April in the central and western Bay of Bengal, which also leads to down-welling and augments the deepening of the mixed layer. The deep MLD in May in the south, south of 4°N, was related to the downward Ekman pumping due to the negative wind stress curl. In addition to this the time-longitude plot of sea-level height anomaly along 4°N showed the propagation of Rossby waves during spring intermonsoon, which also contributed in deepening the mixed layer.

During summer monsoon (June-July-August) though the wind speed was the highest in the entire basin, the MLD was the shallowest in the northern Bay (~ 5m). An examination of E-P showed that it was negative and the highest of all the season, implying excess precipitation (in excess of 440 mm/month), in the northern Bay. In addition to the oceanic precipitation, the influx of freshwaters from the rivers adjoing the Bay of Bengal also contributed towards freshening of the surface waters of the Bay. The spreading of low salinity waters (<32 psu) were seen from the northern Bay towards the south and east with the progress of summer monsoon. The vertical profiles of stability parameter showed that these low salinity waters strongly stratified the upper ocean. The warm upper ocean with SST in excess of 28.5°C also contributed towards strengthening the stratification. Hence, the winds though were the strongest of all the season, were unable to break the stratification to initiate wind-driven mixing and deepen the mixed layer. The shallow MLD seen around Sri Lanka was driven by the positive wind stress curl. The positive wind stress curl was seen developing in May, which peaked in June and collapsed by September. The upwelling associated with the positive wind stress curl drives an upward Ekman pumping and this led to the observed shallow mixed layer during summer monsoon. The band of deep mixed layer seen extending from the southwestern region into the central Bay was linked to the advection of high salinity waters from the Arabian Sea. This high salinity waters reduced the stratification of the upper ocean as could be inferred from the stability parameter. Thus, the strong winds of the summer monsoon combined with the less stratified upper ocean in the southern Bay due to the intrusion of high salinity waters from the Arabian Sea were able to drive strong wind-driven mixing. This was the mechanism which led to the formation of deep MLD in

the south. In addition to this, the high sea-level anomaly in the central and eastern part of the southern Bay associated with the propagating Rossby waves also contributed towards deep MLD.

As the summer monsson tapers off and the fall intermonsoon (September-October) sets in, the shallow MLD which was confined to northern Bay, north of 18°N, was seen extending southward to 15°N in October. This could be explained in the context of changing atmospheric forcing from summer monsoon to fall intermonsoon. The short wave radiation as well as net heat flux showed a secondary heating of the upper ocean during fall intermonsoon and accordingly the SST was in excess of 29°C in October. Though the E-P showed a rapidly decreasing precipitation, the surface salinity showed a progressive decrease from that of summer monsoon and also a further southward extension of the low salinity waters. This indicated that the shallow MLD in the northern Bay and its further southward extension was linked to the presence of low salinity waters and its advection southward. The winds over the Bay showed a drastic reduction in their speed in the north during fall intermonsoon with the high wind speed confined to the southern Bay. Thus, the deep MLD in the southern Bay was driven by a combination of comparatively high wind speed and the presence of high salinity waters both of which destabilized the water column.

The winter monsoon (November-February), in general, showed comparatively deep MLD (~30-40 m) all over the Bay except in the north and eastern Bay. The shallow MLD (~5-15 m) in the north and eastern Bay could be explained in the context of the presence of low salinity waters (<32 psu) during November-December and associated strong

stratification. As the winter progressed, the E-P showed a net evaporation and with no substantial input from rivers discharge the low salinity waters were confined to the northern part during January-February. As a result the area of deeper mixed layer expands further towards eastern boundary. The shallow MLD observed near the Sumatra coast in January was driven by the strengthened positive wind stress curl and the associated upward Ekman pumping. The deep MLD in the rest of the Bay was related to the weakest stratification that occurred in the Bay during winter monsoon compared to all other seasons. The wind speed, which showed a secondary peak in winter were able to initiate deeper wind-mixing as the stratification of the water column was the weakest and this gave rise to the deep mixed layer.

The seasonal variability of the barrier layer (BL) thickness showed strong coupling with wind stress curl, freshwater flux and prevailing circulation of the basin. The nutrient concentrations as well as chlorophyll a showed close correspondence with the changes in the mixed layer. During spring intermonsoon the upper ocean was oligotropic and showed very low chlorophyll *a* concentrations (~ 0.1 - 0.3 mg/m^3). This was because of the strongly stratified upper ocean due to the peak heating by incoming shortwave radiation. The mixed layer was very shallow as the weak winds during spring intermonsoon were unable to initiate strong wind-driven mixing. As a result there was no vertical transport of nutrients to the surface layer from subsurface making the upper ocean oligotrophic.

During summer monsoon the high nitrate as well as the chlorophyll *a* concentrations in the Indo-Sri Lanka region was driven by the upwelling. The upward Ekman pumping

associated with upwelling transports sub-surface nutrients from the nitracline to the surface layers and supports high biological productivity. In the northern Bay the higher concentration of nitrate was supplied by the river runoff. The observed enhanced chlorophyll *a* was supported by this nutrient input. Away from this region, the high stratification of the upper layers due to the freshwater input from precipitation as well as river runoff inhibited wind-driven mixing though the winds were strongest in summer monsoon. Accordingly, the nutrient input from sub-surface to the upper ocean also was curtailed. Thus, the shallow MLD and the oligotrophic upper ocean lead to the observed low chlorophyll concentrations (~ 0.2 mg/m^3) in the rest of the Bay. In fall intermonsoon, the satellite-derived chlorophyll pigment concentrations showed pattern similar to that of summer monsoon with a reduced concentration indicating the tapering effect of summer monsoon. In winter, both the nitrate concentrations and the chlorophyll *a* concentrations were high along the western boundary. The EICC which moved southward during winter was capable of transporting some of the nutrients from the northern Bay towards the south along the western boundary and could explain the nutrient enhancement which in turn supported observed chlorophyll *a* concentrations.

Chapter 1 – Introduction

1.1 Oceanic Mixed Layer

The Ocean's effect on weather and climate is governed by processes that occur in the upper few tens of meters of the water column at the air-sea interface. The upper ocean is the most variable and dynamically active part of the marine environment that couples the underlying ocean to the atmosphere above through the transfer of mass, momentum and energy. It is through this layer that the atmosphere feels the ocean and hence the changes within this layer will regulate the ocean-atmosphere as a coupled system. Hence a correct representation of the processes occurring in ocean-atmosphere interface is absolutely essential for determining the large-scale upper ocean variability. In addition bulk of the biological productivity of the World Oceans, which is closely linked to climate through CO_2 regulation, critically depends on the physical and chemical changes taking place within this layer. Thus, on a global scale the upper ocean is one of the most important factors in determining climate of the earth system [*Kraus*, 1977]. The air-sea boundary processes and their relation to the upper ocean changes have been an ever-increasing subject of interest to the oceanographers and climate researchers.

Oceanic surface layer is a region of intense mixing and hence the properties within this layer are nearly homogeneous. This nearly homogeneous upper ocean layer is referred to as the mixed layer. The thickness of mixed layer is an important parameter in determining the quantity of heat that is available for exchange with atmosphere which is capable of triggering several ocean-atmosphere coupled processes such as convection, generation of tropical cyclones, etc. In order to model the ocean's climate variability

accurately information on the space-time variability of mixed layer is a prerequisite.

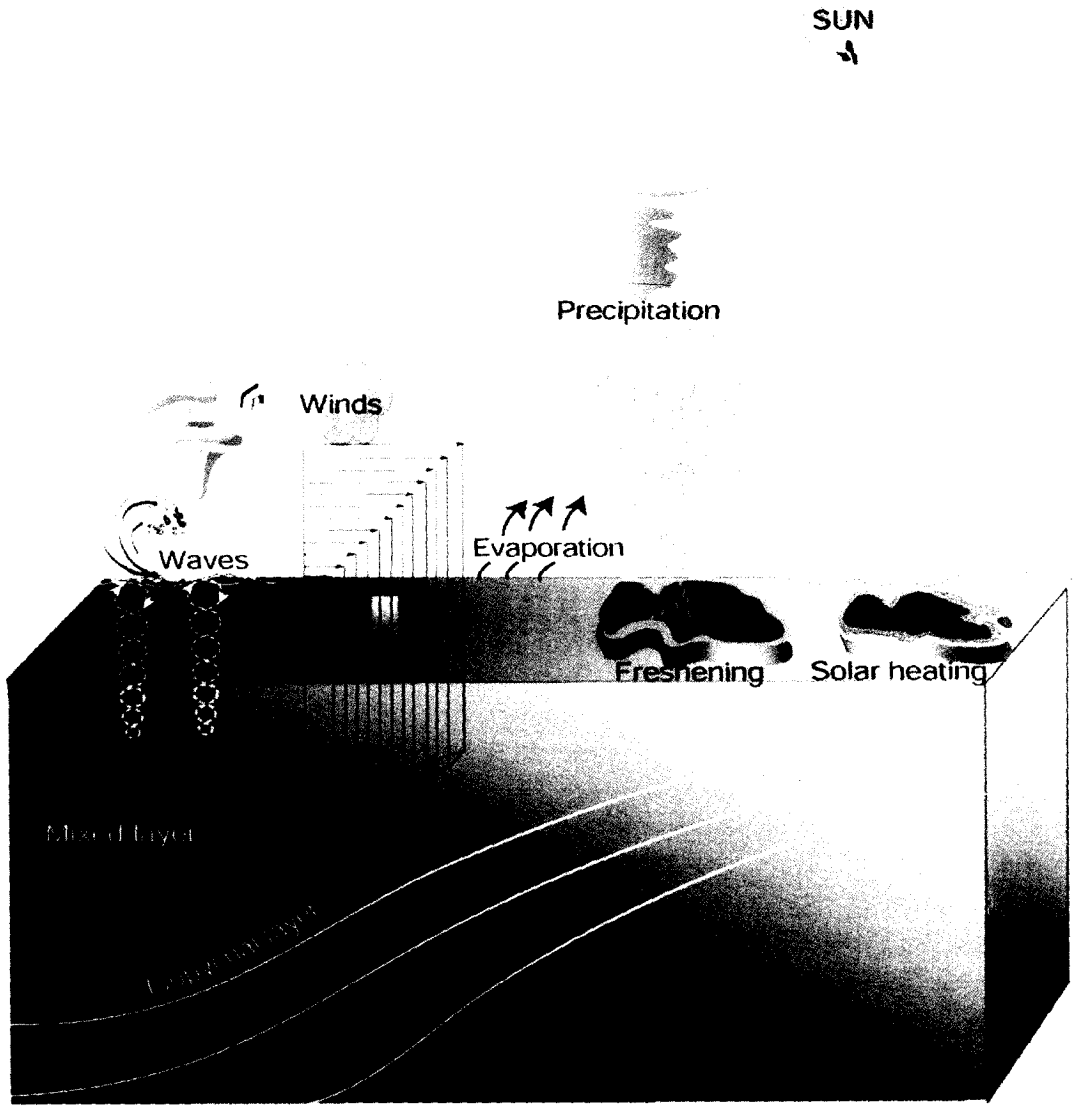

Fig.1.1.1 Schematic representation of various factors that influence the upper ocean mixed layer (redrawn from *Prasanna Kumar and Narvekar*, 2005).

The mixed layer depth (MLD) also is an important parameter in determining the chlorophyll biomass and biological productivity of the upper ocean [*Morel and Andre*, 1991; *Longhurst*, 1995]. The MLD varies on several temporal scales ranging from diurnal, intra-seasonal, seasonal to inter-annual [*Weller and Farmer*, 1992; *Fischer*, 1997

& 2000] and the variability of MLD is directly linked to processes occurring in the mixed layer [*Brainerd and Gregg*, 1995].

Atmospheric forcing that regulates mixing in the upper ocean are winds, waves, solar heating, evaporation and precipitation. Fig.1.1.1 gives a schematic picture of various factors affecting the mixed layer. The solar heating and precipitation stratify and stabilize the upper ocean, while the wind, wave action and evaporation destabilize it through mixing. Since the atmospheric forcing is highly variable on space-time scales, the geographical location, to a great extent, decides the structure and variability of the upper mixed layer.

1.2 Geographic Location and Oceanography of the Study Area

The Bay of Bengal, situated in the eastern part of the northern Indian Ocean, is a tropical basin, which is landlocked in the north and is forced by semi-annually reversing wind system -- the monsoon. During winter (northeast) monsoon (November-February), the winds are weak (~5 m/s) and from northeasterly direction. These northeast trade winds bring cool and dry continental air mass to the Bay of Bengal. In contrast, during the summer (southwest) monsoon (June-September) the strong (~10 m/s) southwesterly winds bring humid maritime air into the Bay of Bengal. The unique feature of the Bay of Bengal is the large seasonal freshwater pulse, which makes the waters of the upper layers less saline and highly stratified. It also is a region of excess precipitation over evaporation [~ 2 m yr^{-1}, *Prasad,* 1997]. This fresh water input leads to the formation of strong halocline within the upper isothermal layer known as 'barrier layer' [*Lukas and*

Linderstrom, 1991; *Sprintall and Tomczak*, 1992]. Strong stratification associated with the barrier layer [*Vinayachandran et al.*, 2002] curtails the vertical mixing leading to the formation of shallow mixed layers. Along with the fresh water the rivers also brings large sediment load (1387 x 10^6 tons of suspended solids annually) [*Subramanian*, 1993] in the northern Bay of Bengal making the surface waters turbid which curtails the light penetration. The fresh water input induces estuarine characteristics with reduced surface salinities over most of the Bay, which intern hampers exchange processes between the atmosphere, surface and deep waters and consequently affects the biological and biogeochemical processes.

The semi-enclosed nature of the Bay of Bengal and its proximity to the equator together with immense quantity of fresh water [1.625 x 10^{12} m^3 yr^{-1}, *Subramanian*, 1993] influx from Ganges, Brahmaputra and several peninsular Indian rivers contribute to the formation of a highly complex system of circulation in the Bay. The surface circulation within the basin, though reverses semi-annually, is not strictly in accordance with the wind reversal but appears to lead it. During the end of winter, in February, when the winds are still northeasterly, the current along the western boundary reverses and flows northward. This northward flowing East India Coastal current (EICC) peaks during March-April (spring intermonsoon), when the winds are weak but possess anticyclonic curl [*Shetye et al.*, 1993]. Open-ocean circulation during this period is the best organized with an anticyclonic, subtropical gyre, and EICC forms the western limb of this circulation (Fig.1.2.1). In May, prior to the intensification of summer (southwest) monsoon, the spring-time anticyclonic circulation collapses and the EICC weakens. In July, when the southwest monsoon is at its full strength, the EICC weakens further and

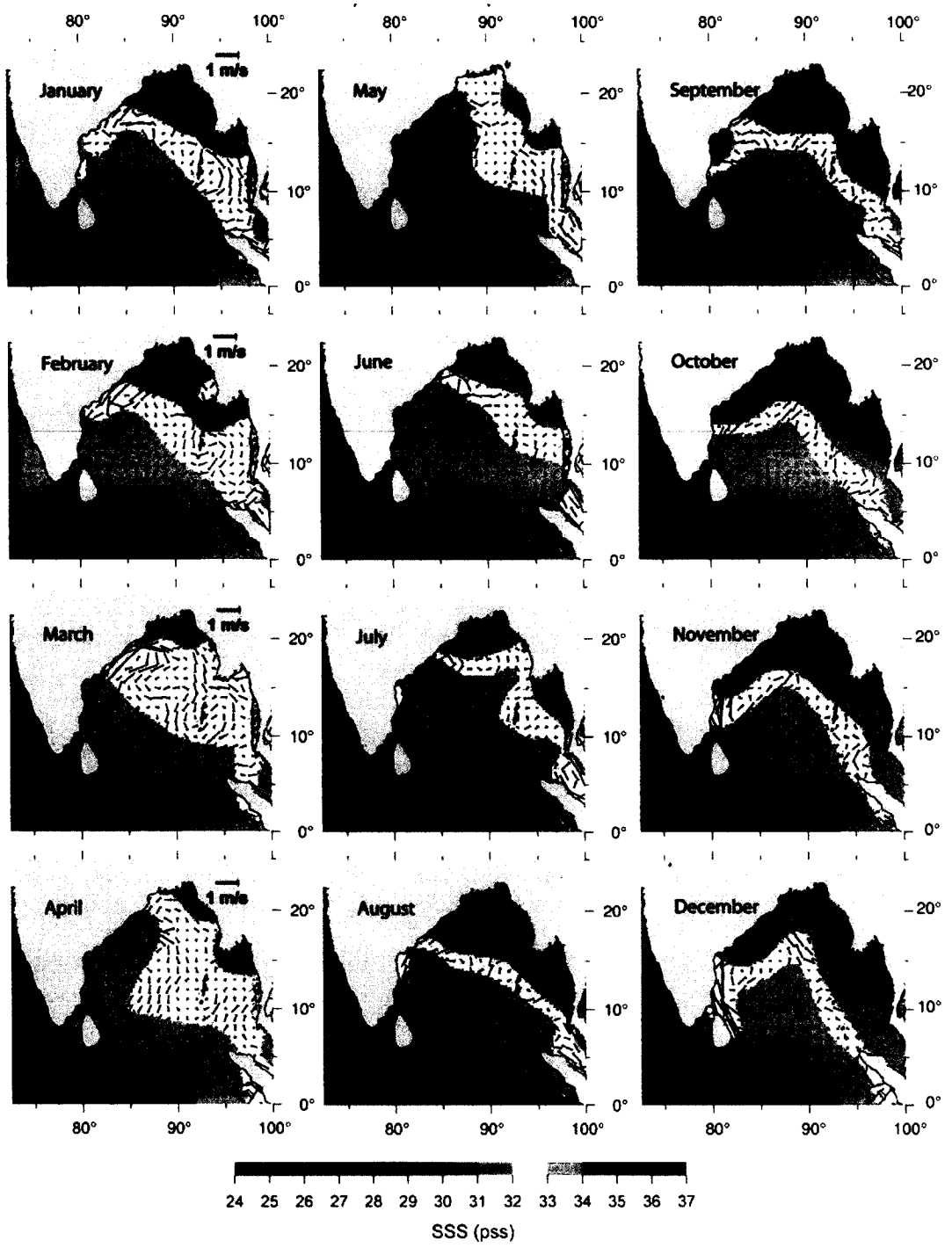

Fig.1.2.1 Monthly mean climatology of sea surface salinity from WOA05 [*Antonov et al.*, 2006] overlaid with geostrophic current vectors computed from sea-level anomaly (SLA). The merged SLA climatology was derived from Topex/Poseidon ERS1/2 satellites during the period 1992-2006.

even reverses to a southward flow in the northern part [*Shetye et al.*, 1991]. The open-ocean circulation at this time of the year consists of multiple gyres, re-circulations, meanders and eddies. In September, when the southwest monsoon weakens, the EICC reverses, flowing towards the south almost along the entire coast, forming a part of the cyclonic gyre. The southward EICC peaks in December and decays in January, completing its annual cycle.

The Bay of Bengal is traditionally considered to have low surface chlorophyll and low biological productivity compared to the Arabian Sea though both the basins are located in similar latitudinal belt and subjected to similar seasonally reversing atmospheric forcing. The reason for this is attributed to the strong near-surface stratification due to excess freshwater flux (low salinity) and relatively weaker winds during the summer monsoon, which makes the surface layers of the Bay of Bengal devoid of nutrients [*Prasanna Kumar et al., 2002*]. Despite the low chlorophyll and primary productivity pattern in the Bay, sediment trap data shows that annual fluxes of organic carbon reach comparable rates in both the Arabian Sea and Bay of Bengal [*Ramaswamy and Nair*, 1994]. This is intriguing as there is no evidence of strong upwelling in the Bay of Bengal except for much localized ones close to the southwestern boundary during summer and traditional mechanisms of nutrient supply to the upper ocean waters cannot account for the observed annual flux of organic carbon from sediment trap. Recent studies indicated the presence of several cyclonic and anticyclonic eddies which alters the hydrography and biogeochemistry of the Bay of Bengal [*Prasanna Kumar et al.*, 2004; *Nuncio*, 2007]. These eddies (cyclonic) enhances the biological productivity by more than double (2 to 8 times) compared to the oligotrophic non-eddy region [*Prasanna Kumar et al.*, 2007].

Though the surface chlorophyll concentration remains low, the enhanced subsurface chlorophyll concentrations result in net increased biological production in the Bay. In addition to these eddies, the Bay of Bengal also is a site of severe tropical cyclones. The cyclones are generated during the spring (April-May) and fall (October) intermonsoons, and are associated with large-scale air-sea exchange, deepening of mixed layer and increased biological productivity through subsurface nutrient injection to euphotic zone.

1.3 Historical Background and Relevance of Present Work

In the past, several studies attempted to understand the complex nature of the circulation and hydrography in the Bay of Bengal [*Varkey et al.*, 1996 and the references therein; *Schott et al.*, 2001; *Shankar et al.*, 2002]. An increasing number of recent studies suggested the role of remote forcing in aiding the semi-annual variability of the upper-layer circulation in the Bay of Bengal [*Potemra et al.*, 1991; *Yu et al.*, 1991; *Perigaud and Delecluse*, 1993; *Prasanna Kumar and Unnikrishnan*, 1995; *McCreary et al.*, 1993 & 1996, *Shetye et al.*, 1996; *Vinayachandran et al.*, 1996; *Shankar et al., 1996*; *Eigenheer and Quadfasel,* 2000]. The remote forcing could arise due to a variety of mechanisms, such as planetary waves originating at the eastern boundary excited by the energy radiated by the coastal Kelvin wave, planetary waves generated by the variability in the local alongshore winds, and the interior Ekman pumping during the peak of summer and winter monsoons. It is natural to expect that these semiannual atmospheric forcing as well as the remote forcing would modulate the thickness of the upper ocean by altering the thermal and mechanical inertia of the layer.

Compared to the studies on circulation and hydrography, studies on the mixed layer in the Bay of Bengal are very few. A limited number of researchers studied the variability of the mixed layer depth for the global ocean [*Monterey and Levitus*, 1997; *Kara et al.*, 2003; *de Boyer Montegut et al.*, 2004 & 2007a] including the Bay of Bengal, while the rest of the studies were aimed at understanding the mixed layer variability of the Indian Ocean of which the Bay of Bengal formed a part. These studies can be categorized into three – studies based on (1) climatological data, (2) data from individual cruises, and (3) ocean models. *Rao et al.* [1989] studied the evolution of mixed layer depth in the tropical Indian Ocean (30°N-30°S, 30°E-120°E) based on monthly mean climatology on 2° latitude by 2° longitude grid from the Master Oceanographic Data Set (MOODS), which contains hydrographic data during the period 1948 to 1981. Subsequently *Rao and Sivakumar* [2000] using a subset of the World Ocean Atlas 1994 [*Levitus and Boyer*, 1994], which contains hydrographic data up to 1993, studied the annual and semi-annual variability of the thermal structure and heat budget of the mixed layer of the tropical Indian Ocean. *Shenoi et al.* [2002] using data from World Ocean Atlas 1994 [*Levitus and Boyer*, 1994; *Levitus et al.*, 1994;] compared various processes that are responsible for the mixed layer heat budget for both the Arabian Sea as well as the Bay of Bengal. Later using World Ocean Atlas 1998 [*Conkright et al.*, 1998], which contains hydrographic data up to 1998, *Rao and Sivakumar* [2003] studied the seasonal cycle of salinity and its influence on the seasonal evolution of near-surface mixed layer depth in the northern Indian Ocean (0-30°N, 40°E-100°E). More recently, *Narvekar and Prasanna Kumar* [2006] studied the seasonal variability of the mixed layer in the central Bay of Bengal using a 2° latitude by 4° longitude climatology prepared from a comprehensive data base

extracted from National Oceanographic Data Centre (NODC, Washington) CD-ROM [*Levitus et al.*, 1994] which contained data during 1900-92, Responsible National Oceanographic Data Centre (RNODC, Goa) which contained data during 1976-2003 collected by Indian research ships, and ARGO data during the period 2001-2004. *Thadathil et al.* [2007] used World Ocean 2001 data along with data from Indian Oceanographic Data Centre (IODC) and Argo data up to September 2006 to generate monthly mean maps of MLD in the Bay of Bengal as a part of the study on the formation and seasonal variability of barrier layer.

Based on the individual *in situ* data collected during MONSOON-77 and MONEX-79 experiments *Gopalakrishna et al.* [1988] studied the influence of wind on the variability of the mixed layer in the northern Indian Ocean during different phases of summer monsoon. *Murty et al.* [1996] studied the time evolution of mixed layer at a stationary location in the northern Bay of Bengal (20°N, 89°E) during southwest monsoon of 1990 (18-31August & 9-19 September) based on the data collected under Monsoon Trough Boundary Layer Experiment (MONTBLEX) programme. Subsequently, based on the data collected during summer monsoon (11-24 July) of 1991 in the northwestern Bay of Bengal *Gopalakrishna et al.* [2002] studied the impact of fresh water plume on the mixed layer depth and surface circulation. *Swain et al.* [2003] used a time series measurements of winds and waves at 13°N, 87°E during 15 July to 30 August 1999 as a part of the Bay of Bengal Monsoon Experiment (BOBMEX-99) to study the effect of wind and waves on the mixed layer depth due to forced mixing in the central Bay of Bengal. Using data collected from the Indian Exclusive Economic Zone (EEZ) under the Marine Research-Living Resources (MRLR) programme as well as data from National Institute of

Oceanography (NIO) hydro CD *Maheswarn* [2004] studied the mixed layer and hydrographic characteristics off the west and east coast of India.

In addition to the above mentioned studies on mixed layer variability based on climatology and *in situ* data, there were also few modeling studies. Using 1.5 layer reduced gravity model *Behera* [1998] studied the response of mixed layer to Bay of Bengal cyclone. *Han et al.* [2001] studied the influence of precipitation minus evaporation (P-E) and river runoff in the Bay of Bengal on the dynamics, thermodynamics and mixed layer physics in the upper Indian Ocean. They showed that in the regions where precipitation exceeds evaporation (P-E > 0) the model mixed layer was found to be thin because of decreased entrainment and increased barrier layer. Using a one-dimensional turbulent closure model *Prasad* [2004] studied the physical mechanism governing the seasonal evolution of mixed layer depth (MLD) along the two open ocean transect in the Arabian Sea and the Bay of Bengal and concluded that the surface forcing controls the MLD in the Bay of Bengal rather than the vertical salinity stratification. Using Ocean General Circulation Model (OGCM) as well as *in situ* hydrographic observations during BOBMEX-99 *Vinaychandran and Kurian* [2007] studied the structure and variability of mixed layer and barrier layer during summer monsoon. *de Boyer Montegut et al.* [2007b] studied the seasonal and inter-annual variability of mixed layer heat budget in the northern Indian Ocean using a OGCM and concluded that salinity stratification plays a clear role in maintaining a high winter SST in the Bay of Bengal and the presence of freshwater near the surface allows heat storage below the surface layer that can be recovered later by entrainment warming during winter cooling.

All of the above studies examined the role of wind-mixing, net heat flux and fresh water flux in explaining the mixed layer variability. None of the earlier studies addressed the role of advection, remote forcing and eddies in regulating the mixed layer on a basin-scale. The present thesis is an attempt to understand basin-wide variability of the mixed-layer in the Bay of Bengal on a seasonal scale not only by local forcing but also by remote forcing, advection and meso-scale eddies along with its coupling to nutrients and chlorophyll.

Chapter 2 – Data and Methodology

In order to study the seasonal variability of mixed layer in the Bay of Bengal and its regulation of nutrients and chlorophyll in response to the atmospheric forcing, a suite of oceanographic, atmospheric and remote sensing data were used.

2.1 Hydrographic Data

The major data set used in the study was the hydrographic data containing profiles of temperature, salinity, nitrate and chlorophyll *a*.

2.1.1 Temperature and Salinity Data

The hydrographic data containing the profiles of temperature and salinity for the Bay of Bengal region (0-25°N, 75-100°E) were extracted from the following 3 sources:

1. The World Ocean Data base 2005 [*Boyer et al.*, 2006] which contained temperature and salinity data from Hydro-cast for the period 1919-2000 and conductivity temperature-depth (CTD) profiles for the period 1972–2003 (http://www.nodc.noaa.gov/OC5/WOD05/pr_wod05.html).

2. Responsible National Oceanographic Data Center (RNODC) at National Institute of Oceanography (NIO), Goa which contained temperature and salinity data from Hydro-cast for the period 1972-1996 and CTD profiles for the period 1979-2006.

3. Argo data which contained the temperature and salinity profiles for the period 2002-2007 was extracted from http://www.usgodae.org/argo/argo.html.

From the above 3 sources 7197 profiles of temperature and salinity from Hydro-cast, 2714 profiles from CTD and 4569 profiles from Argo were extracted. These profiles were subjected to the following quality control procedures to obtain quality data for further analysis.

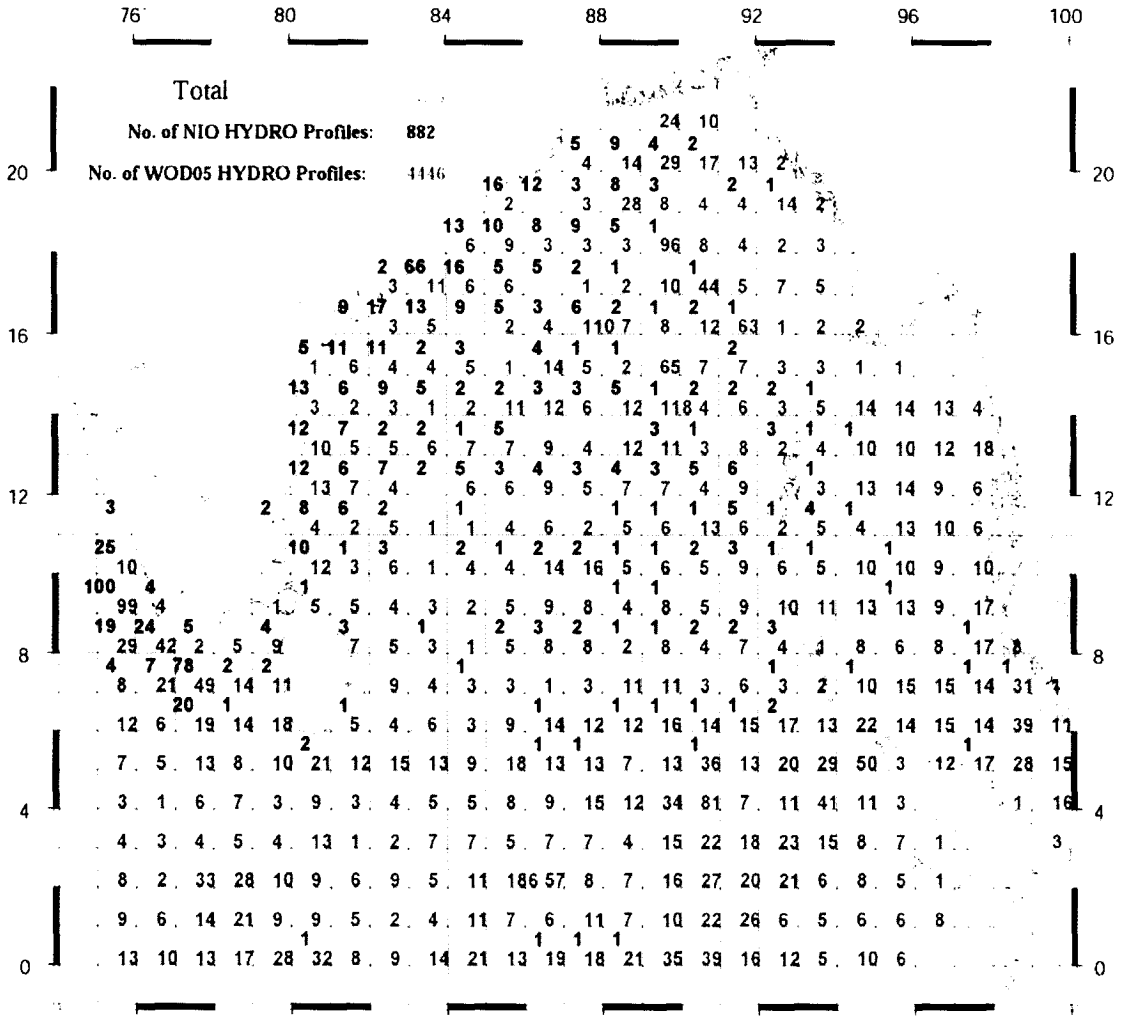

Fig.2.1.1.1 Spatial distribution of number of Hydro-cast profiles from WOD05 and RNODC (NIO) after quality check in 1°latitude x 1°longitude in the Bay of Bengal.

At first the profiles with depth less then 50m were eliminated, as the objective of the study is to determine mixed layer depth, which may exceed 50m. The remaining data were physically examined and duplicate profiles as well as those with obvious errors

were excluded. After the quality control, the total number of Hydro-cast profiles were reduced to 5328, CTD profiles were reduced to 2656 and Argo profiles were reduced to 4203. From the quality checked data total number of profiles available under each category, such as Hydro, CTD and Argo were posted on a 1°latitude by 1° longitude grids and presented in Fig.2.1.1.1 to Fig.2.1.1.3.

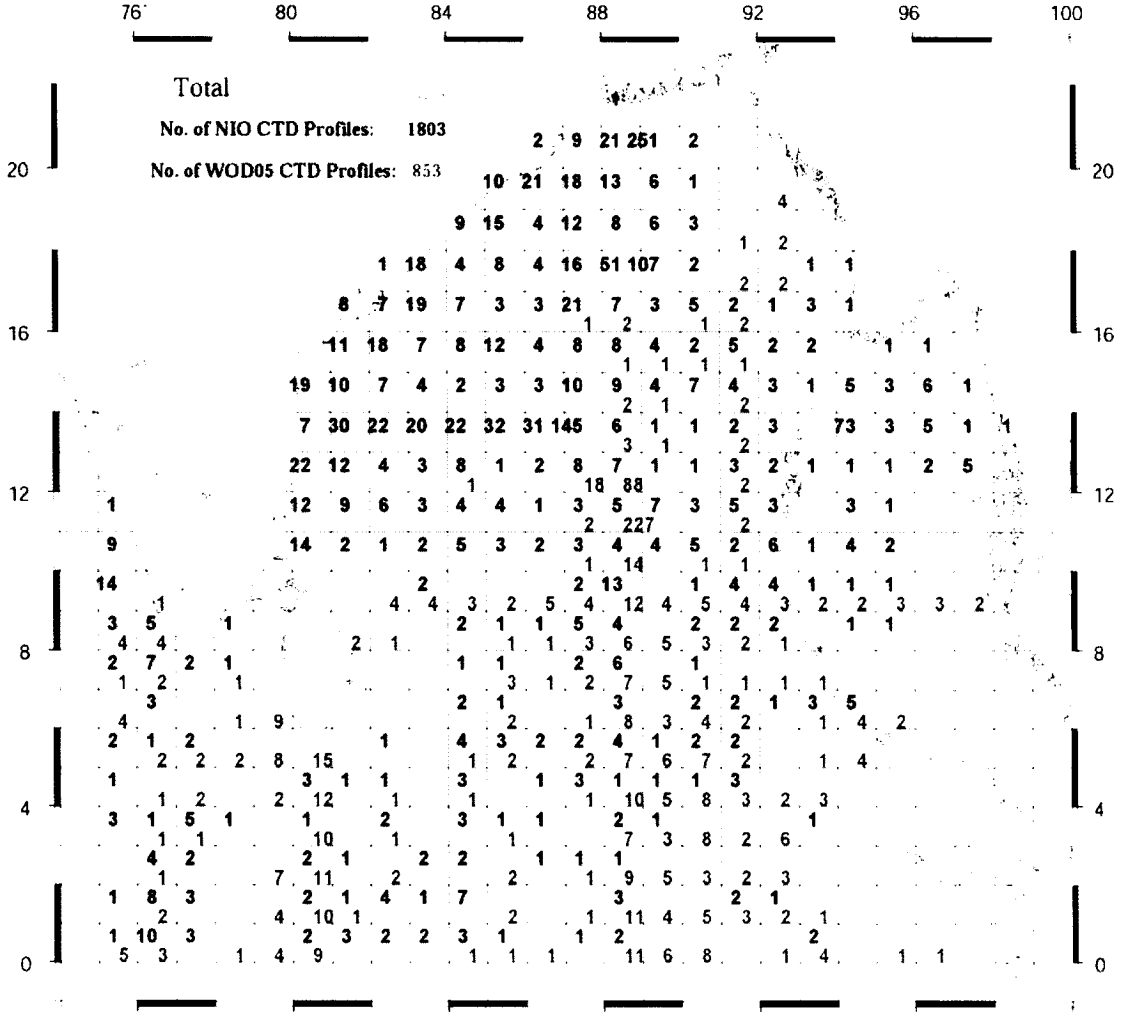

Fig.2.1.1.2 Spatial distribution of number of CTD profiles from WOD05 and RNODC (NIO) after quality check in 1°latitude x 1°longitude in the Bay of Bengal.

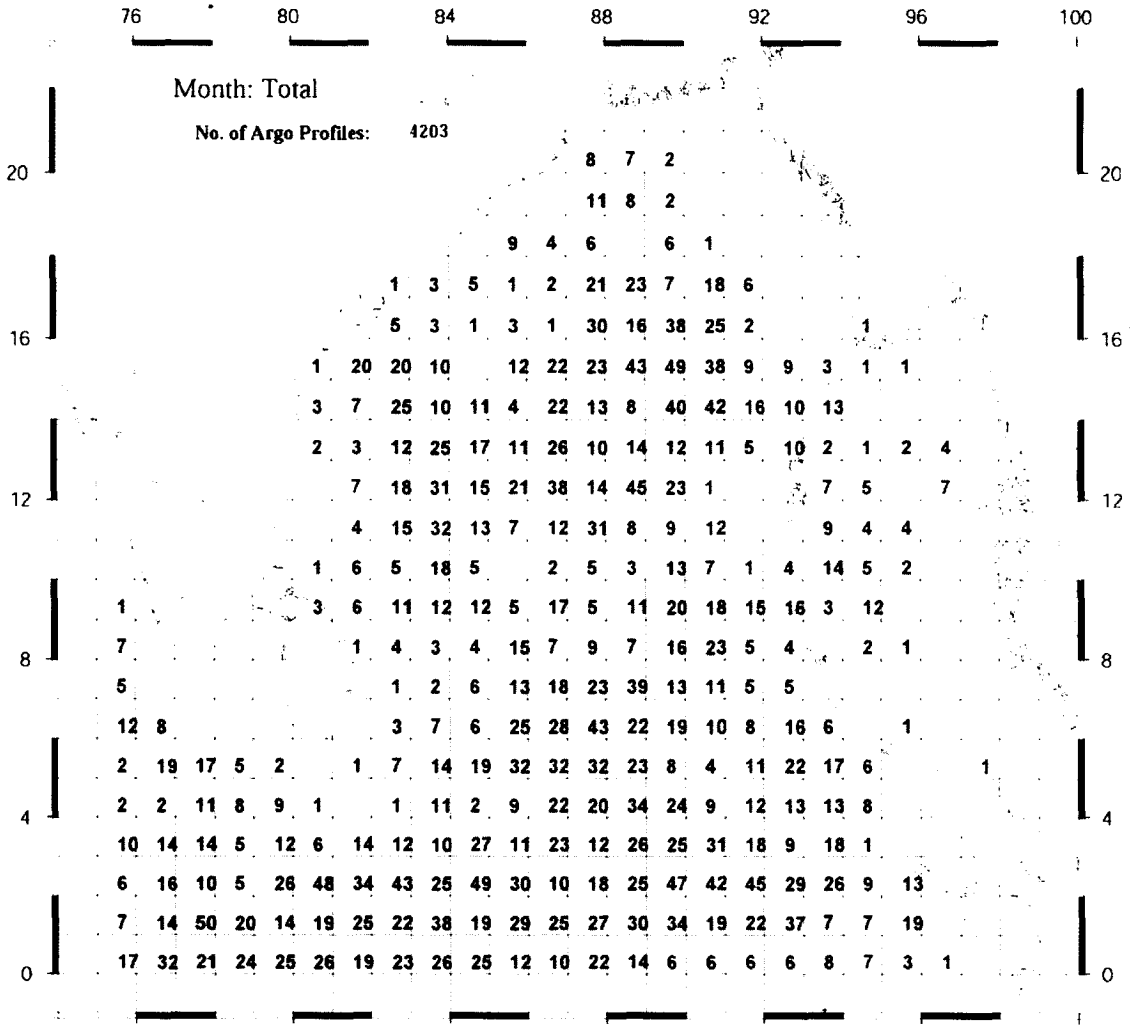

Fig.2.1.1.3 Spatial distribution of number of Argo profiles after quality check in 1°latitude x 1°longitude in the Bay of Bengal.

From the above temperature and salinity profiles density (sigma-t) was calculated [*UNESCO*, 1981] up to a depth of 500 m. The monthly mean climatology of temperature, salinity and sigma-t were prepared on a 1° x 1° grid. These profiles were further used to determine sea surface temperature (SST) and sea surface salinity (SSS). The mixed layer depth (MLD), isothermal depth and barrier layer thickness were calculated from the monthly mean data as descried in the following section.

2.1.2 Definition of Mixed Layer, Isothermal Layer and Barrier Layer

Two types of mixed layer depth (MLD) definitions have been most commonly used in the literature – (1) based on specifying a difference in temperature or density from the surface value [*Wyrtki*, 1964; *Levitus*, 1982; *Schneider and Muller*, 1990] and, (2) based on specifying a gradient in temperature or density [*Bathen*, 1972; *Lukas and Lindstrom*, 1991]. It is important to examine the distribution of properties within the upper layer before any such criteria are applied. Since the Bay of Bengal comes under the semi-annual forcing of monsoons, the vertical profiles of temperature, salinity and sigma-t are presented for a 1-degree grid centered at 9°N and 19°N latitude along 89°E for the month of August and February (Fig.2.1.2.1), which represents the summer and winter conditions respectively.

The vertical profiles indicated that the isothermal, isohaline and isopycnal layers, in general, coincided in the upper ocean irrespective of the season in the southern part of the Bay of Bengal (Fig.2.1.2.1 left panels), but in the northern Bay temperature and salinity showed a different vertical structure (Fig.2.1.2.1 right panels). In the northern Bay, the temperature showed an isothermal layer within which the salinity increased rapidly with depth. This is associated with freshening due to the river runoff as well as precipitation during summer. Hence, the criteria for defining the MLD should take into account the density variation rather than temperature or salinity. Since in the northern Bay density is controlled by salinity more than temperature, in the present study MLD is defined as the depth at which the density (sigma-t) exceeds 0.2 kg m^{-3} from its surface value. To numerically determine MLD, the monthly mean temperature, salinity and sigma-t profiles were interpolated onto 1 m-depth intervals by the cubic spline method.

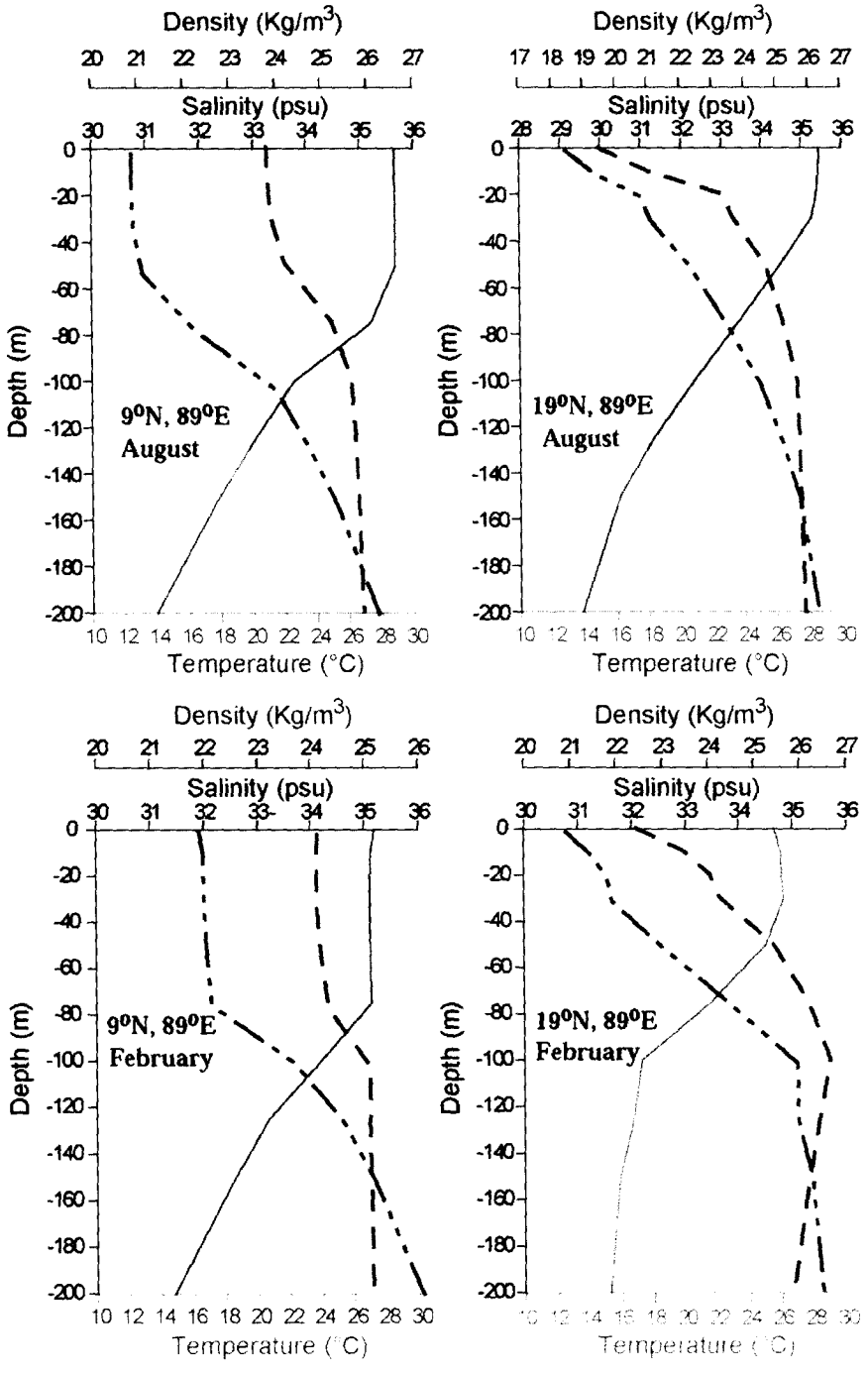

Fig.2.1.2.1 Vertical profiles of temperature (solid line, pink), salinity (broken line, purple) and density (sigma-t; dash-dot line, green) for August (top) and February (bottom) at 9°N (left) and 19°N (right) along 89°E.

Isothermal layer for the present study is defined as the depth at which the temperature decreased by 1°C from its surface value (Fig.2.1.2.2). The barrier layer is the layer within

the isothermal layer and below the mixed layer within which the salinity increased rapidly (blue stippled region in Fig.2.1.2.2). Barrier layer was numerically calculated by subtracting the MLD from the isothermal layer.

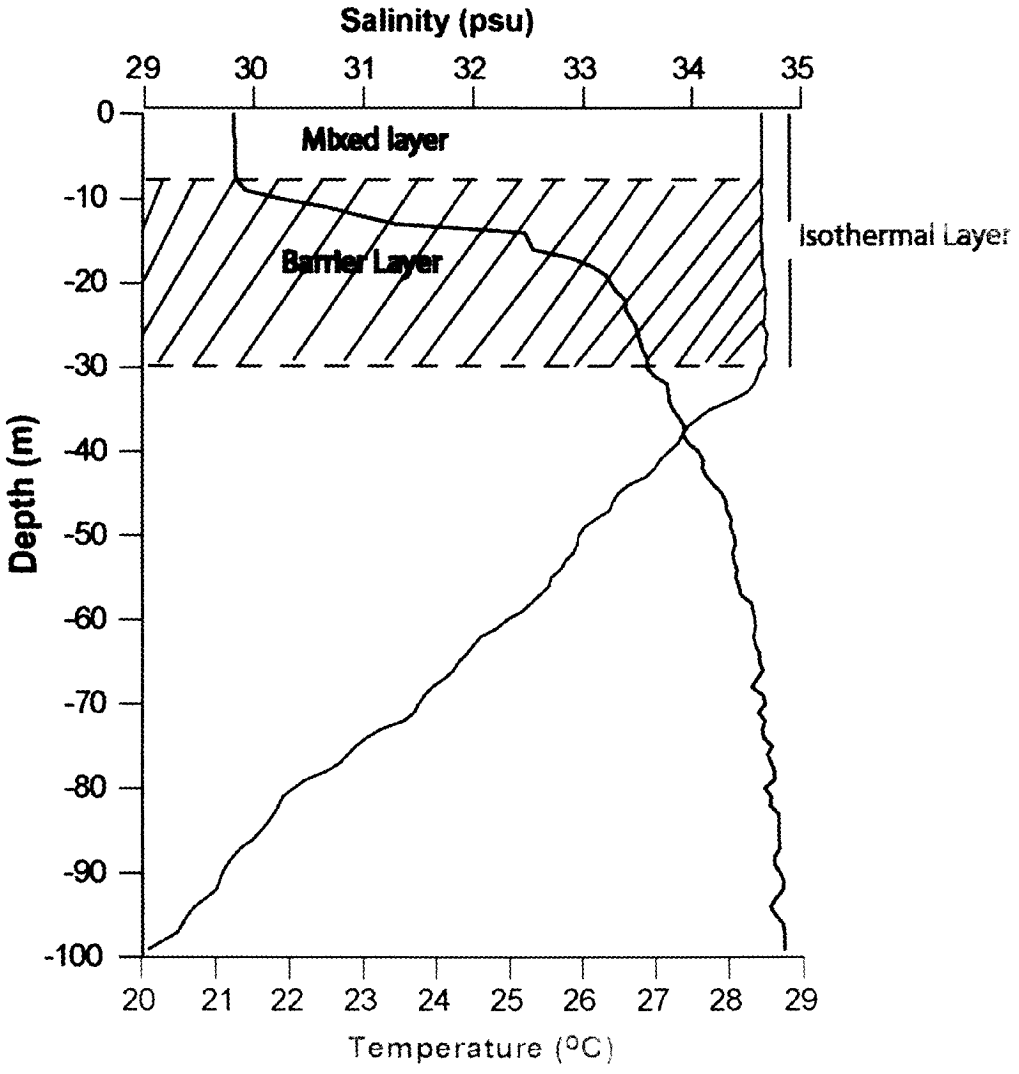

Fig.2.1.2.2 Vertical profiles of temperature and salinity in the northern Bay of Bengal (19°N, 88°E) during August 2001 depicting the isothermal layer and barrier layer.

2.1.3 Nutrient Data

In this study only nitrate profiles from the nutrient database were used. The World Ocean Data base 2005 [*Boyer et al.*, 2006] contained the nitrate data for the period 1906-1999

while the RNODC (NIO) had the data for the period 1973-2006. The total number of nitrate profiles extracted from the above sources was 7406. From these the duplicate profiles were removed first and then the rest of the profiles were physically checked for any obvious ambiguity, which was removed subsequently. The quality control procedure

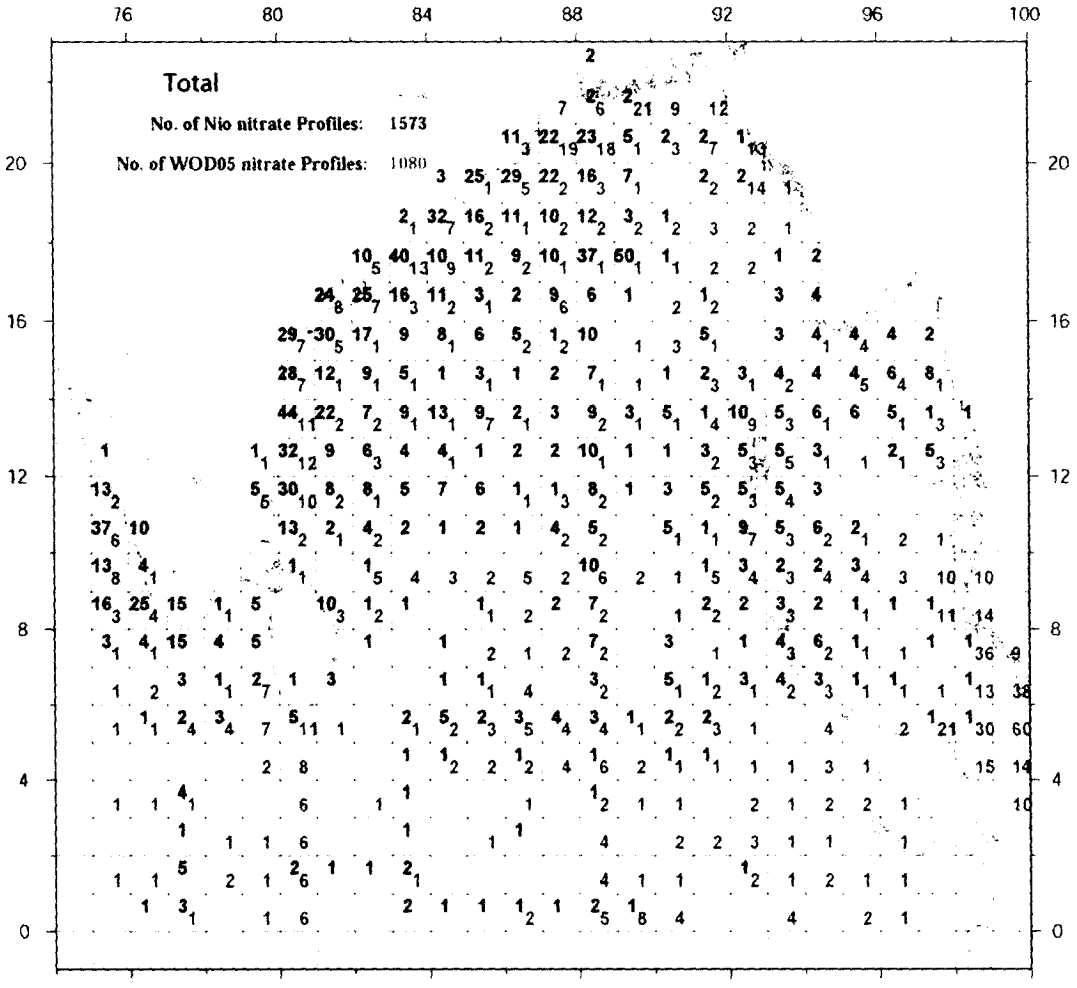

Fig.2.1.3.1 Spatial distribution of number of nitrate profiles from WOD05 and RNODC (NIO) after quality check in 1°latitude x 1°longitude in the Bay of Bengal.

reduced the total number of profiles to 2653. The number of profiles available at each of the 1° latitude x 1° longitude grid is shown in Fig.2.1.3.1 Since the total number of profiles in each of the one-degree grid itself were less, these data were grouped together

in time to produce seasonal mean. The seasons considered for this purpose is defined as

Spring intermonsoon	*March-May*
Summer monsoon	*June-August*
Fall intermonsoon	*September-October*
Winter monsoon	*November-February*

Since spatial coverage of data during fall intermonsoon was very poor and was confined to western Bay of Bengal, this season was not considered.

2.1.4 Chlorophyll Data

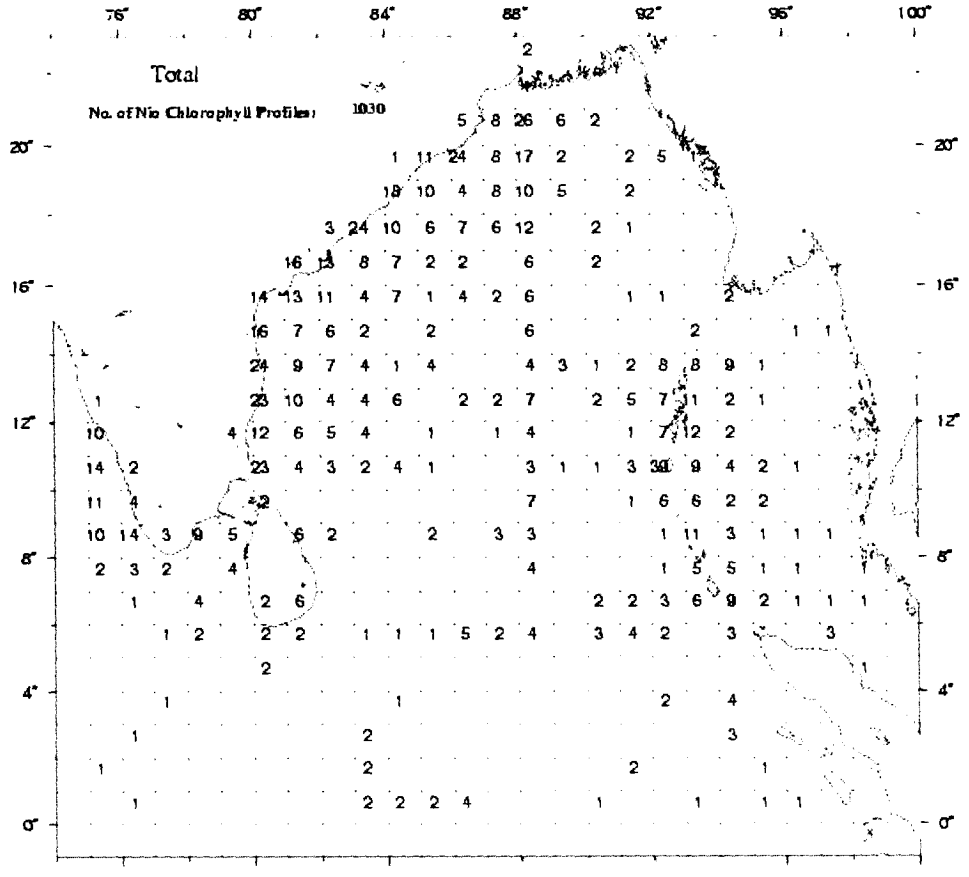

Fig.2.1.4.1 Total number of Chlorophyll *a* data after quality check in the Bay of Bengal during 1951- 2006

The chlorophyll *a* profiles were taken from RNODC (NIO), which contained data for the period 1951-2006. The total number of chlorophyll *a* profiles were 1060 and after the quality control procedure, similar to that of nitrate, the number of profiles reduced to 1030. The number of chlorophyll *a* profiles available in each of the 1^{o} latitude x 1^{o} longitude grid was shown in Fig.2.1.4.1. Since the total number of profiles in each of the one-degree grid itself was less, these data were grouped together in time to produce seasonal mean. During fall intermonsoon spatial coverage of data was very poor and was confined to western Bay of Bengal, hence this season was not considered.

2.1.5 Hydrographic data for studying effect of meso-scale variability on mixed layer depth

Apart from the above mentioned hydrographic data, a set of high resolution *in situ* data collected during Bay of Bengal Process Studies (BOBPS) has been utilized to delineate the effect of meso-scale variability on mixed layer depth. The data includes the vertical profiles of temperature and salinity collected using SeaBird CTD during four seasons along $88^{o}E$ and along the western boundary of the Bay of Bengal (Fig.2.1.5.1). The measurements were carried out during summer (6 July to 2 August, 2001), fall intermonsoon (14 September to 12 October, 2002), spring intermonsoon (12 April to 7 May, 2003), and winter (25 November 2005 to 4 January 2006). CTD salinities were calibrated against water samples collected simultaneously by a rosette sampler and analysed with ship-board Guildline 8400 Autosal.

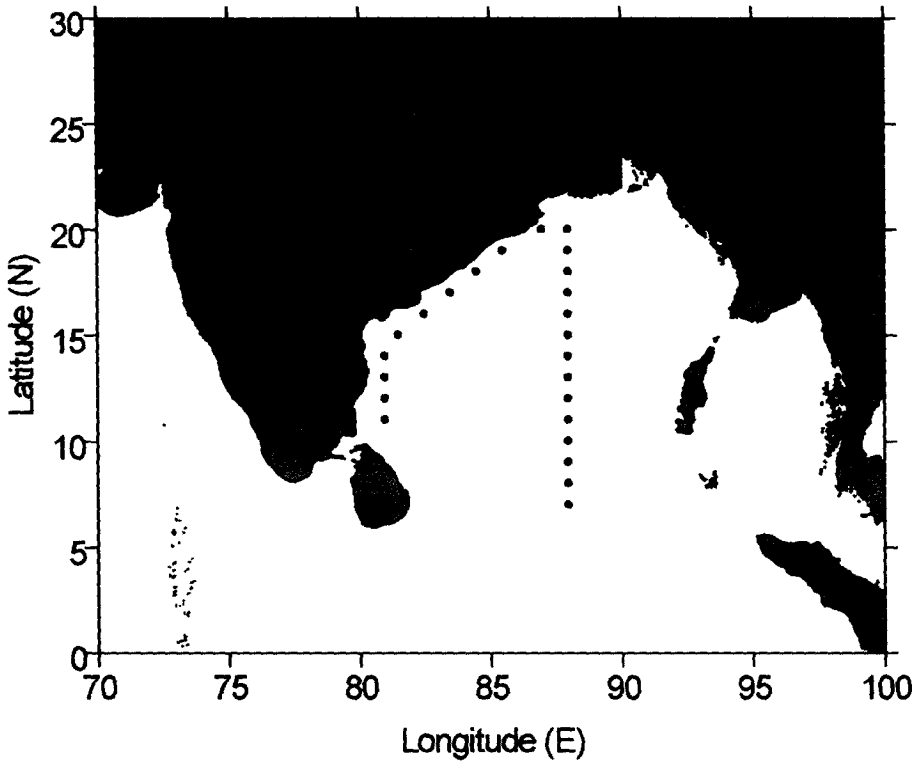

Fig.2.1.5.1 Map showing station location (dark filled circles) along the central (88°E) and western Bay of Bengal where temperature and salinity profiles were collected.

From the temperature and salinity profiles, static stability parameter was computed following *Pond and Pickard* [1983]

$$E = -\frac{1}{\rho}\frac{\partial \rho}{\partial z}$$

Where E is the static stability parameter (m^{-1}), ρ is the density (kg m^{-3}) of the water and z is the depth (m).

2.1.6 River Runoff Data

The monthly mean climatology of river discharge of 6 major rivers Ganges, Brahmaputra, Irrawady, Godavari, Krishna and Cauvery were taken from Global Runoff data Centre, Germany (http://grdc.bafg.de/servlet/is/2781).

2.2 Atmospheric Data

Meteorological data were extracted from the National Oceanographic Centre (NOC), Southampton, climatology (formerly Southampton Oceanographic Centre, SOC) (http://www.noc.soton.ac.uk/ooc/_CLIMATOLOGY/noc11.php) in the domain (0-25°N and 75-100°E) for the period 1980-1993, which contained the monthly mean climatology of meteorological parameters such as incoming short wave radiation, wind speed, evaporation, precipitation and net heat flux on 1° longitude by 1° latitude grid.

2.3 Remote Sensing Data

Since the *in situ* chlorophyll data was limited in both space and time, chlorophyll pigment concentrations derived from global 9-km monthly mean imagery of Sea-viewing Wide Field-of-view Sensor (SeaWiFS) for the period September 1997 to December 2007 (http://reason.gsfc.nasa.gov/OPS/Giovanni/ocean.seawifs.shtml) were used in addition to *in situ* chlorophyll *a* profiles to compare with surface distributions. From these data the climatological seasonal means were calculated for spring intermonsoon, summer monsoon, fall inter monsoon and winter monsoon. Merged sea-level anomalies of Topex/Poseidon ERS1/2 series satellites obtained from AVISO live access server (http://las.aviso.oceanobs.com) was also used for the period October 1992 to January 2006, which gives 7-day snapshots having a spatial resolution of 1/3rd of a degree, to prepare monthly mean climatology of sea-level anomaly. From the sea-level height anomalies velocities were computed assuming the geostrophic relation [*Pond and Pickard*, 1983]

$$2\Omega \sin(\phi).V = g \tan(i)$$

where Ω is the earth's angular velocity, ϕ is the latitude, V is the velocity and tan(i) is the slope of the sea surface.

Chapter 3 – Seasonal Variability of Mixed Layer and Barrier Layer

The seasonal variability of upper ocean parameters such as sea surface temperature (SST), sea surface salinity (SSS), mixed-layer depth (MLD) and barrier layer thickness in the Bay of Bengal is presented in this chapter.

3.1 Sea Surface Temperature

The spatial distribution of sea surface temperature (SST) in the Bay of Bengal during January showed a decrease from south to north (Fig. 3.1.1a). The lowest SST of 25°C was in the north, while the highest SST of 29°C was near the equator. The spatial distribution, thus, showed a 4°C cooling from equator to north. In February the SST distribution was similar to that of January except that the region of 29°C, which was located close to the equator had expanded (Fig.3.1.1b). The temperature in the northern Bay also showed an increase. The coldest temperature in the north was 26°C, which was 1°C warmer than that of January. The meridional difference in SST also reduced to 3°C from its January value of 4°C. During March the basin-wide SST showed a general warming of about 0.5°C compared to previous month (Fig.3.1.1c), though the variation from equator to head Bay remained the same as that of February (~3°C). The warming trend seen during March further intensified in April with northern Bay SST reaching up to 28.5°C (Fig.3.1.1d). Near the equatorial region SST was 30°C. The highest SST of 30.5°C occurred along the central part of the eastern boundary and a tongue of warm SST (~30°C) extended from this region offshore into the central Bay of Bengal. With the

basin-wide warming, a further reduction of the spatial contrast of SST from 3°C in March to 2.5°C in April was noticed.

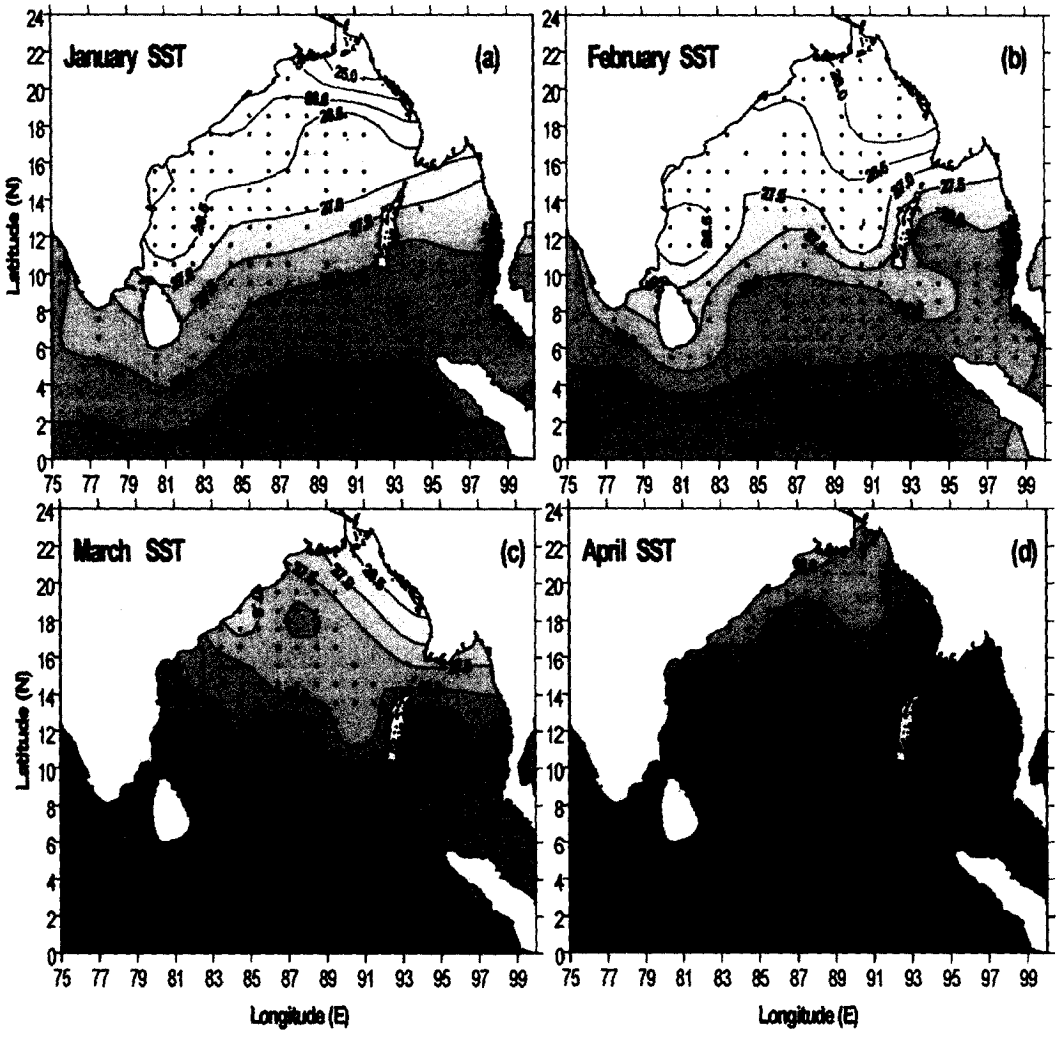

Fig.3.1.1 Monthly mean distribution of SST (°C) in the Bay of Bengal during January to April.

The basin-wide SST was the warmest in May with highest value of 31°C near the northeastern Bay (Fig.3.1.2a). The band of high SST (30°C) seen extending up to the central Bay in April, extends up to the western boundary in May. The SST, in general, was in excess of 29.5°C in the basin, except in the region surrounding southern part of Sri

Lanka where a distinct cold water patch (28.5°C) was seen. Another region of cold SST (29.0°C) was seen near southern part of central Bay. The meridional variation of basin-wide SST further reduced to 1.5°C indicating the continued warming in May.

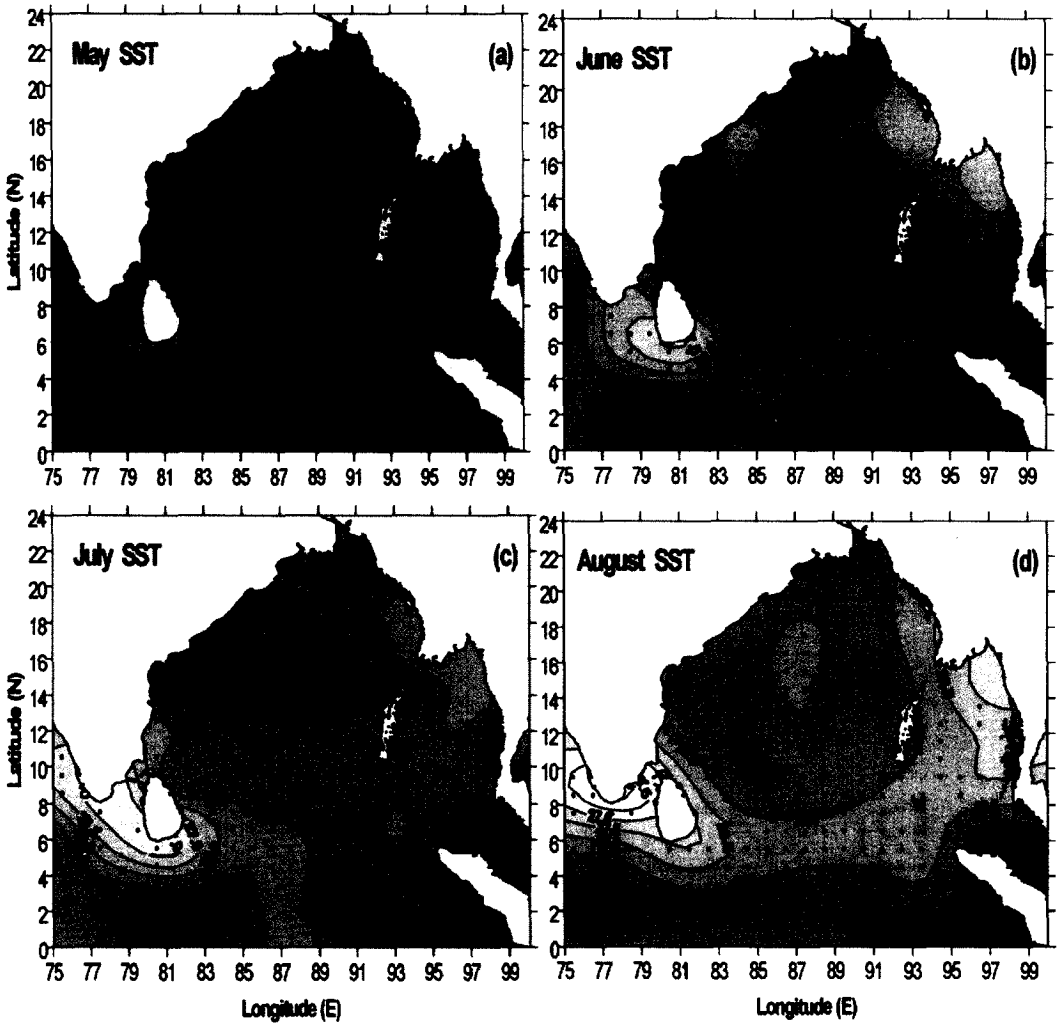

Fig.3.1.2 Monthly mean distribution of SST (°C) in the Bay of Bengal during May to August.

In June the basin-wide SST showed a cooling with values less than 29.5°C, except in a small patch extending from central to northwestern Bay (Fig.3.1.2b). The most prominent feature of the SST distribution was a region of cold water patch surrounding southern part

of Sri Lanka with a sharp thermal front. This patch (~27.5°C) was 1°C colder than the ambient temperature. The meridional difference of SST reduced further to 1°C. This reduction was brought about by the general cooling in the basin-wide SST. In July, the basin-wide SST varied between 28.5 to 29°C (Fig.3.1.2c), except in the region surrounding Sri Lanka, which showed further cooling of SST. The lowest SST was 27°C, which was 1.5°C colder than the ambient waters. The cold water region appeared to spread northward towards the peninsular India and southern part of the west cost of India. The basin-wide SST was about 28.5°C in the Bay during August, which increased towards equator with the highest value of 29.5°C (Fig.3.1.2d). The region of coldest SST moved from the southern part of Sri Lanka towards the tip of peninsular India in August. The lowest SST was about 26.5°C and it was 2.5°C colder than the ambient waters.

The basin-wide SST pattern remained the same in September as that of the previous month except for the warming near the head Bay (Fig.3.1.3a). The cold SST region, which encompassed the southern tip of the peninsular India and Sri Lanka diminished. The associated thermal front also weakened considerably. In October this cold water completely vanished and the basin-wide SST showed a warming once again (Fig.3.1.3b). The northwestern Bay showed cooling in November with SST of about 27.5°C (Fig.3.1.3c). This SST was about 1 to 1.5°C colder than the rest of the basin. This cooling intensified in December with lowest SST of 26.5°C in the northern Bay (Fig.3.1.3d). The meridional temperature difference was about 2.5°C with warmest waters (29°C) near the equator.

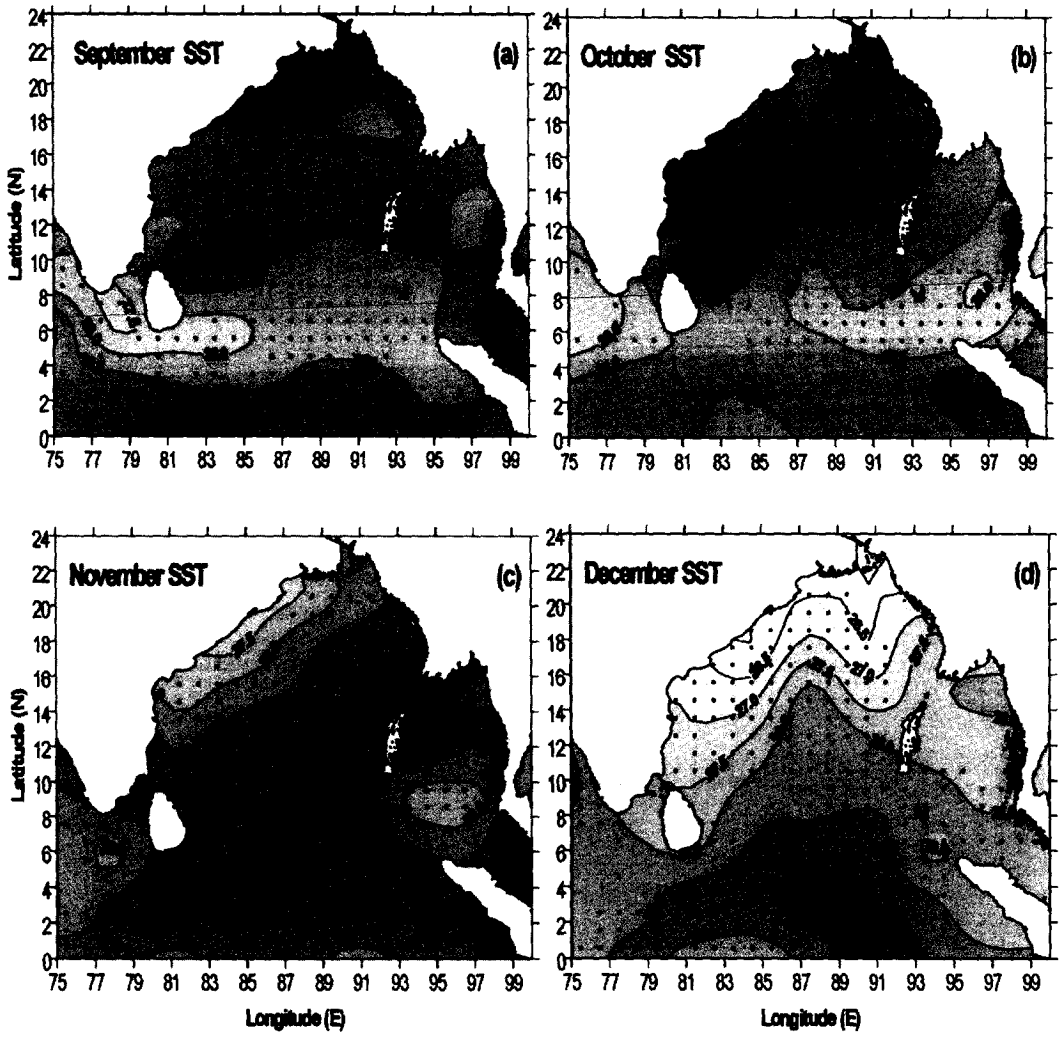

Fig.3.1.3 Monthly mean distribution of SST (°C) in the Bay of Bengal during September to December.

In summary, the SST showed a strong seasonal (semi-annual) cycle. The amplitude of the seasonal cycle was about 6°C with coldest SST of about 25°C in the north during January and warmest SST of about 31°C in the central part of the eastern boundary during May. The seasonal cycle of SST showed two warming period with warm SST during April-May and October. The period of low SST was during January-February. The highest spatial variability occurred during January when SST varied 4°C from south to north. The

least spatial variability occurred during October, which was about 1.5°C. An interesting feature of the SST distribution in the southwestern Bay was the appearance of a thermal front with a region of cold water around Sri Lanka in May. This thermal front further developed in June-July and peaked in August. In July, the cold water region moved northward towards the peninsular India and along the southern part of the west cost of India. The coldest SST of 26.5°C was noticed in August with a thermal gradient of about 3°C from southern tip of peninsular India to south of Sri Lanka. By September this feature diminished. This feature must be associated with Indo-Sri Lankan upwelling system and the Sri Lankan dome.

3.2 Sea Surface Salinity

The distribution of sea surface salinity (SSS) in January showed the presence of low salinity waters close to the northeastern Bay with an increase towards south (Fig.3.2.1a). The lowest salinity was 31 psu while the highest value was about 35 psu. Along the eastern and western boundary also the salinity was low (~32.5-33.5 psu). The spatial variation of SSS from north to south was about 4 psu. In February the spatial distribution was similar to that of January with the lowest salinity of 30 psu in the north and highest salinity of 34.5 psu in the south (Fig.3.2.1b). However, the region of 31 psu salinity reduced in its spatial extent considerably, compared to January, and was confined very close to head Bay (Fig.3.2.1b). The meridional variation of SSS was about 4.5 psu in February. The SSS distribution in March showed an increase of 1 psu in the northern Bay with lowest salinity being 32 psu (Fig.3.2.1c). In the south, south of 10°N the spatial distribution of SSS was similar to that of February. The north-south variation of SSS was ~ 2.5 psu. During April the SSS distribution showed a 0.5 psu reduction in the salinity in

the head Bay (~31.5 psu) from that of March, while that along the western boundary was more than 33.5 psu (Fig.3.2.1d). The meridional variation in SSS was about 3 psu.

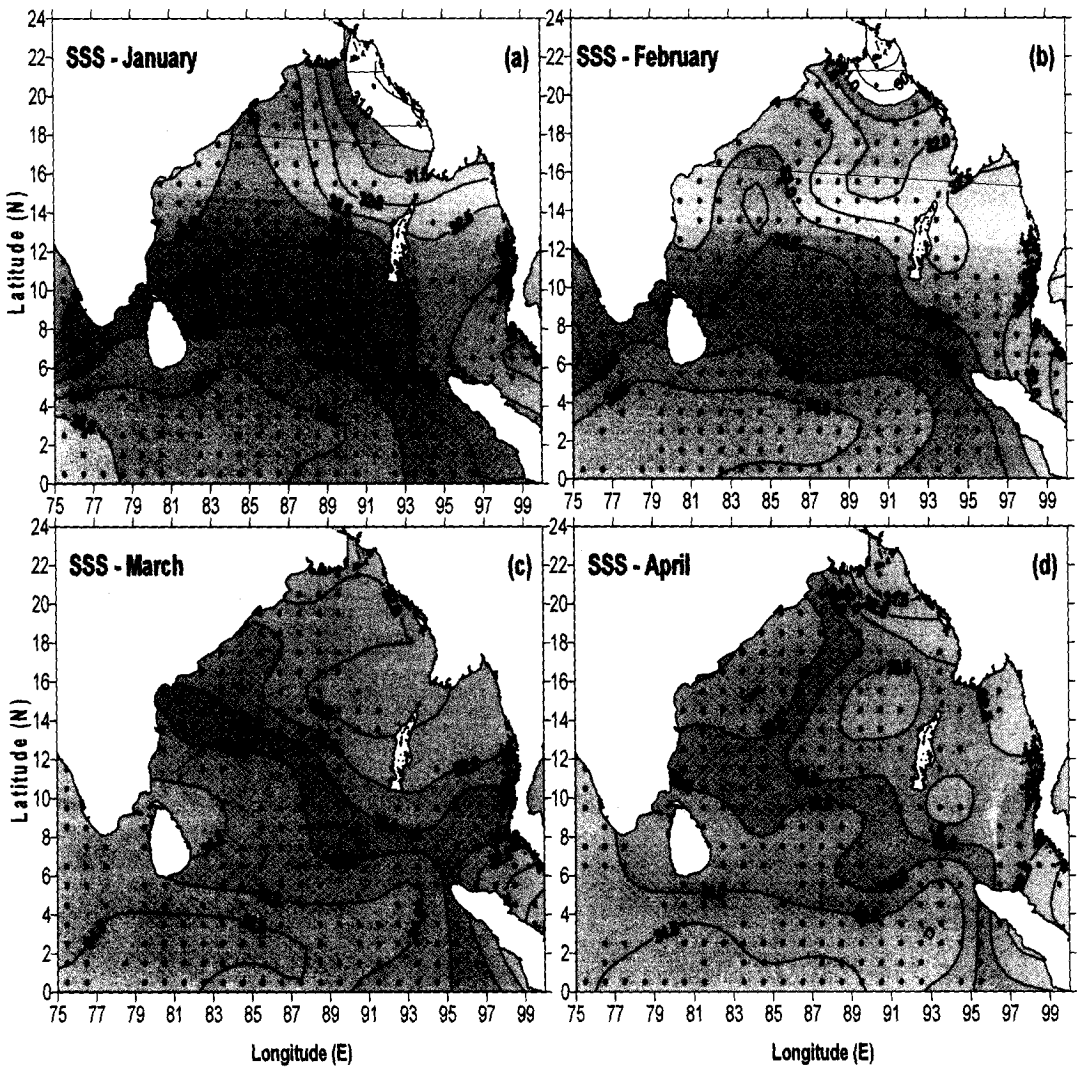

Fig.3.2.1 Monthly mean distribution of SSS (psu) in the Bay of Bengal during January to April.

The SSS distribution showed the least spatial variation of about 2 psu in May with low salinity waters confined to the eastern boundary of the Bay of Bengal (Fig.3.2.2a). Along the western boundary salinity was highest in May (33.5-34 psu). The lowest salinity was

32.5 psu while the highest was 34.5 psu. In June a low salinity patch appeared in the head Bay with a distinct salinity front north of 15°N showing the lowest salinity of 30.5 psu (Fig.3.2.2b). The salinity variation across the front was about 2.5 psu. In the south the distribution remained similar to that of previous month. The meridional variation of salinity was about 4 psu. A tongue of high salinity water (35 psu) was seen close to the

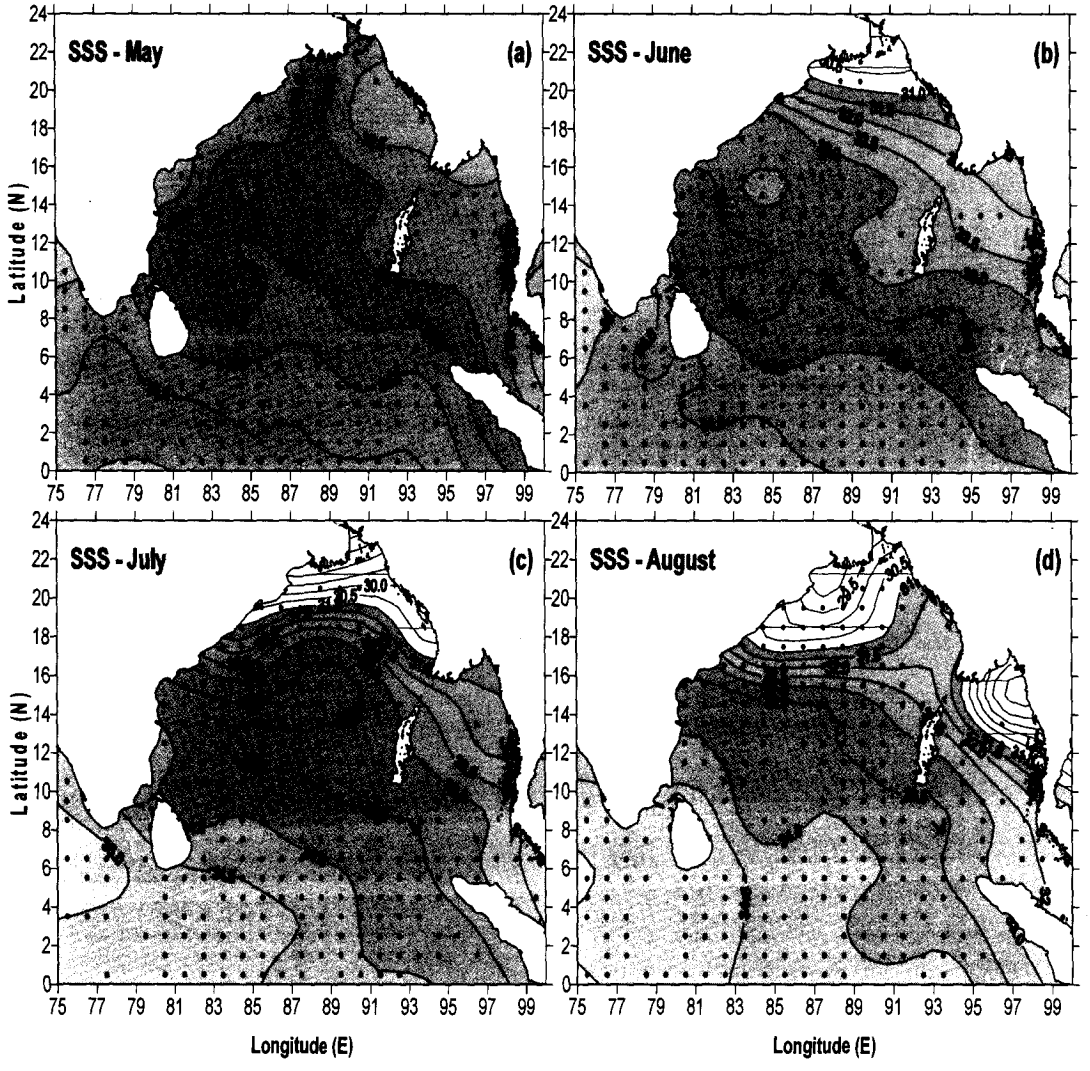

Fig.3.2.2 Monthly mean distribution of SSS (psu) in the Bay of Bengal during May to August.

southwestern part of peninsular India. The SSS during July showed fresher water near the head Bay with a minimum value of 29 psu. The region of low salinity expanded further away from the head Bay. The salinity front strengthened much more compared to June and the salinity variation across the front was about 4.5 psu, while the basin-wide north to south variation was 5.5 psu. The tongue of high salinity waters seen in June had spread

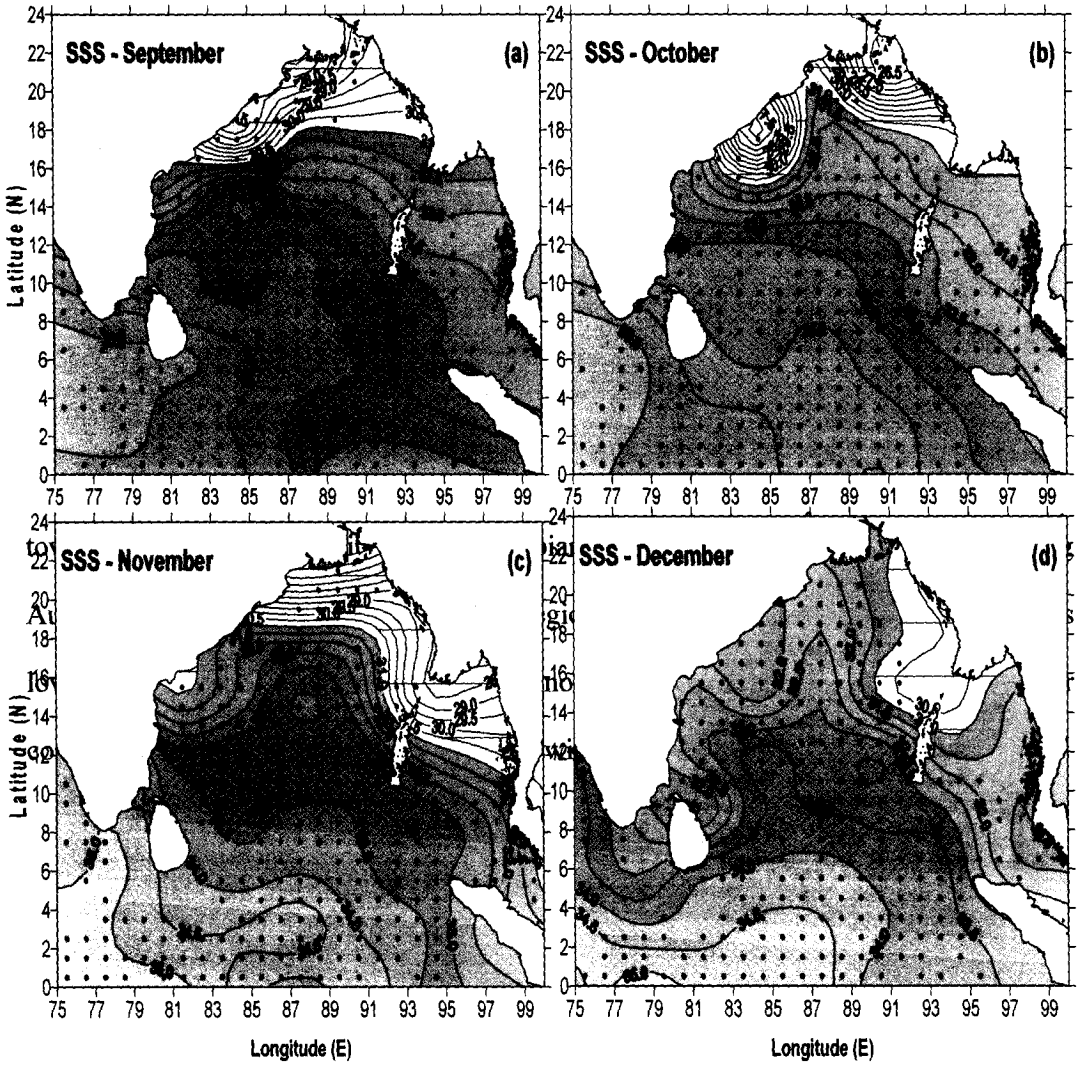

Fig.3.2.3 Monthly mean distribution of SSS in the Bay of Bengal during September to December.

The SSS during September showed further reduction in the salinity in the northern Bay with the lowest value of 27.5 psu (Fig.3.2.3a). The salinity front also showed much stronger gradient with variation of 6 psu salinity across the front. The tongue of a high salinity waters with salinity of 35 psu were seen intruding from the west further into the southern Bay south of Indian peninsula and Sri Lanka. Thus, SSS showed an increase of 7.5 psu from north to south. The lowest SSS in the Bay of Bengal was encountered during October with a salinity of 26.5 psu close to the head Bay (Fig.3.2.3b). In addition to the freshening near the head Bay, another region of freshening was seen located along the northern part of the western boundary with minimum salinity of 27 psu. Towards south, surface salinity showed an increasing trend reaching a maximum salinity of 35 psu near the equator. The spatial variation in salinity during this month was 8.5 psu, which was the highest compared with other months. The low salinity region close to the northern part of the western boundary seen in the previous month disappeared in November (Fig.3.2.3c). The band of low salinity was seen extending from northwestern Bay along the head Bay to the northeastern Bay. The lowest salinity was 26.5 psu close to head Bay. In the south the high salinity water was pushed further towards the equator. The variation in SSS from north to south was about 8 psu. In December the lowest salinity was 30.5 psu seen close to the Myanmar coast (Fig.3.2.3d). The low salinity waters, ~32 psu, were seen along the eastern as well as the western boundaries and also around Sri Lanka and into the southern part of the west coast of India. The waters with highest salinity were confined to the equator. The spatial variation in surface salinity was about 4 psu in December.

In summary, the SSS showed a strong annual cycle. The amplitude of the annual cycle was about 8.5 psu with lowest salinity of 26.5 psu in the north during October and highest SSS of about 35 psu in the southern Bay during September to November. The highest spatial variability occurred during October when SSS varied by 8.5 psu from north to south while the least spatial variability occurred during May, which was about 2 psu. The annual cycle of SSS was driven by the freshening that occurred in the northern Bay of Bengal during June to October and the seasonal circulation that redistributed the fresher water influencing the ambient salinity. In the southern Bay salinity remained almost same except during June to October when the high salinity waters (35 psu) of the Arabian Sea origin is advected into the Bay of Bengal. Since the freshwater input was from the peninsular rivers, which are located in the northern part of the Bay along the eastern and western boundaries, it is important to decipher the variability of the northern and southern Bay separately. In the northern Bay, north of 15°N, the amplitude of the annual cycle was about 6.5 psu with the highest salinity in May (~33 psu) and lowest (~26.5 psu) in October. In the southern Bay the amplitude of the annual signal is about 0.5 psu and this was associated with the intrusion of the high salinity waters from the Arabian Sea.

3.3 Mixed Layer Depth

The spatial distribution of mixed layer depth (MLD) during January showed deep MLD in excess of 30 m in a large area encompassing southwestern Bay including the western and central equatorial region, central Bay, and the northeastern region (Fig.3.3.1a). The deepest MLD of 40 m was noticed at two locations between 84° and 89°E centered at 15°N and 10°N respectively. The MLD close to the western boundary and the head Bay

was about 25 m. The southeastern Bay including the eastern equatorial region showed shallow MLD and the minimum value was 10 m. Thus, the spatial variation in MLD within the basin was about 30 m. In February, the region of deep MLD remained the same as that of January except that a low patch of shallow MLD (~20-25 m) appeared

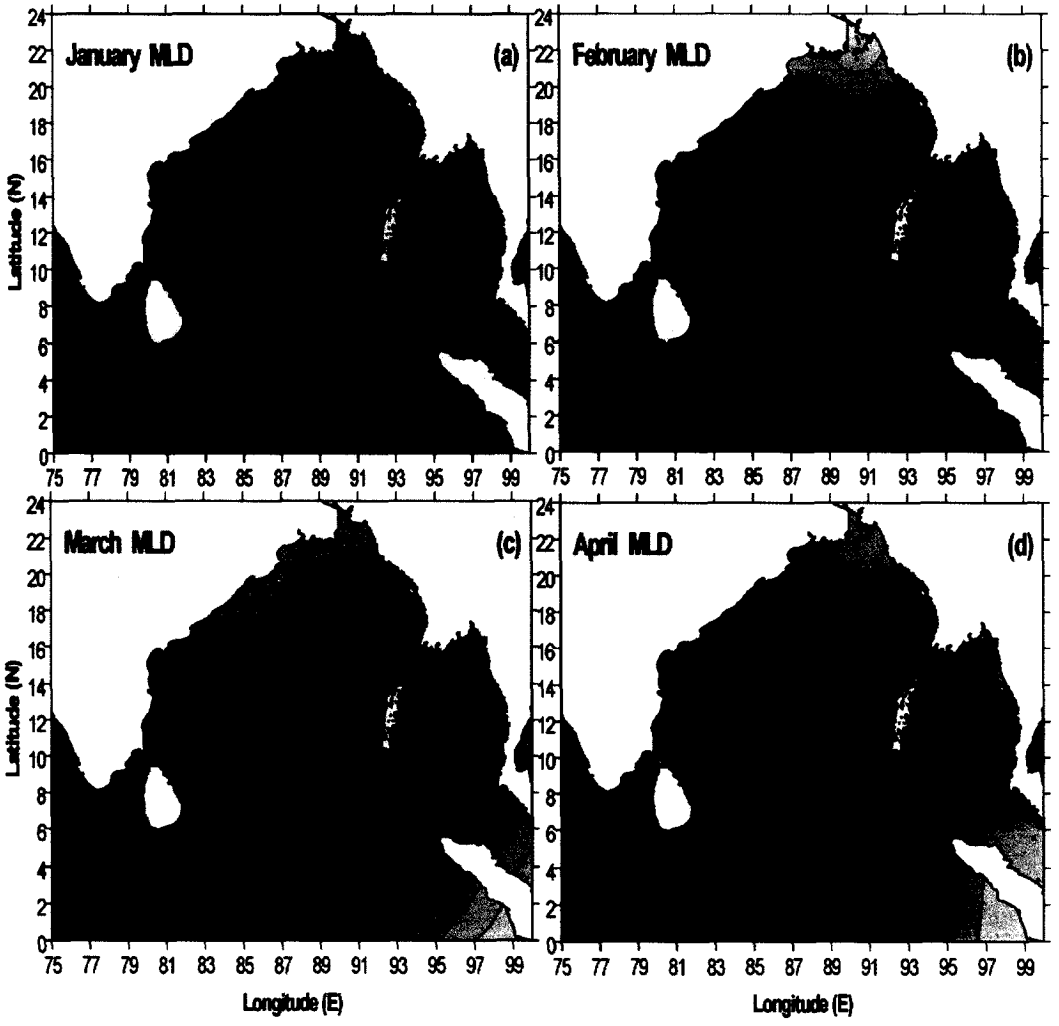

Fig.3.3.1 Monthly mean distribution of MLD (m) in the Bay of Bengal during January to April.

close to the Sri Lanka (Fig.3.3.1b). The region of the deepest MLD moved from the central Bay to the western boundary and was located between 12° and 14°N. Along the

western boundary north of 15°N and in the northern Bay the MLD shoaled to less than 15 m. The region of low MLD seen in the southeastern Bay in the previous month was also seen in February at the same location, but the depth showed a marginal deepening. During March most part of the Bay showed shallow MLD shallower than 25 m, except at two locations one around Sri Lanka and the other in the western equatorial region (Fig.3.3.1c). The shallowest MLD occurred close to the northwestern boundary including the head Bay and also in the southeastern part close to the equator. In April MLD in most part of the Bay was shallower than 20 m except two regions, one close to the equatorial region and the other region encompassing the western boundary between 12° and 18°N (Fig.3.3.1d).

During May two zonal bands of deep MLD (~30 m) was seen, one between 8°N and 16°N extending from western boundary towards the eastern boundary and the other between equator and 4°N (Fig.3.3.2a). However, east of 90°E the region of deep MLD tapered. These two zonal bands of high MLD were separated by a narrow band of comparatively shallow MLD of about less than 25 m. In the northern Bay, north of 16°N, MLD showed a rapid decrease with a minimum value of 15 m. Another patch of shallow MLD (~15-20 m) was observed near the southeastern Bay. In June the region of deep MLD in the southwestern Bay joined the deep MLD region in the central and western Bay (Fig.3.3.2b). Thus, most part of the Bay had deep MLD, deeper than 30 m and the deepest was 45 m in the southern Bay. Along the western and eastern boundary the MLD was shallow (~15-20 m). The MLD decreased rapidly north of 16°N and the shallowest MLD of 10 m was encountered close to the head Bay. Similarly, around Sri Lanka also the MLD decreased rapidly from 40 m to 20 m. The spatial distribution of MLD during

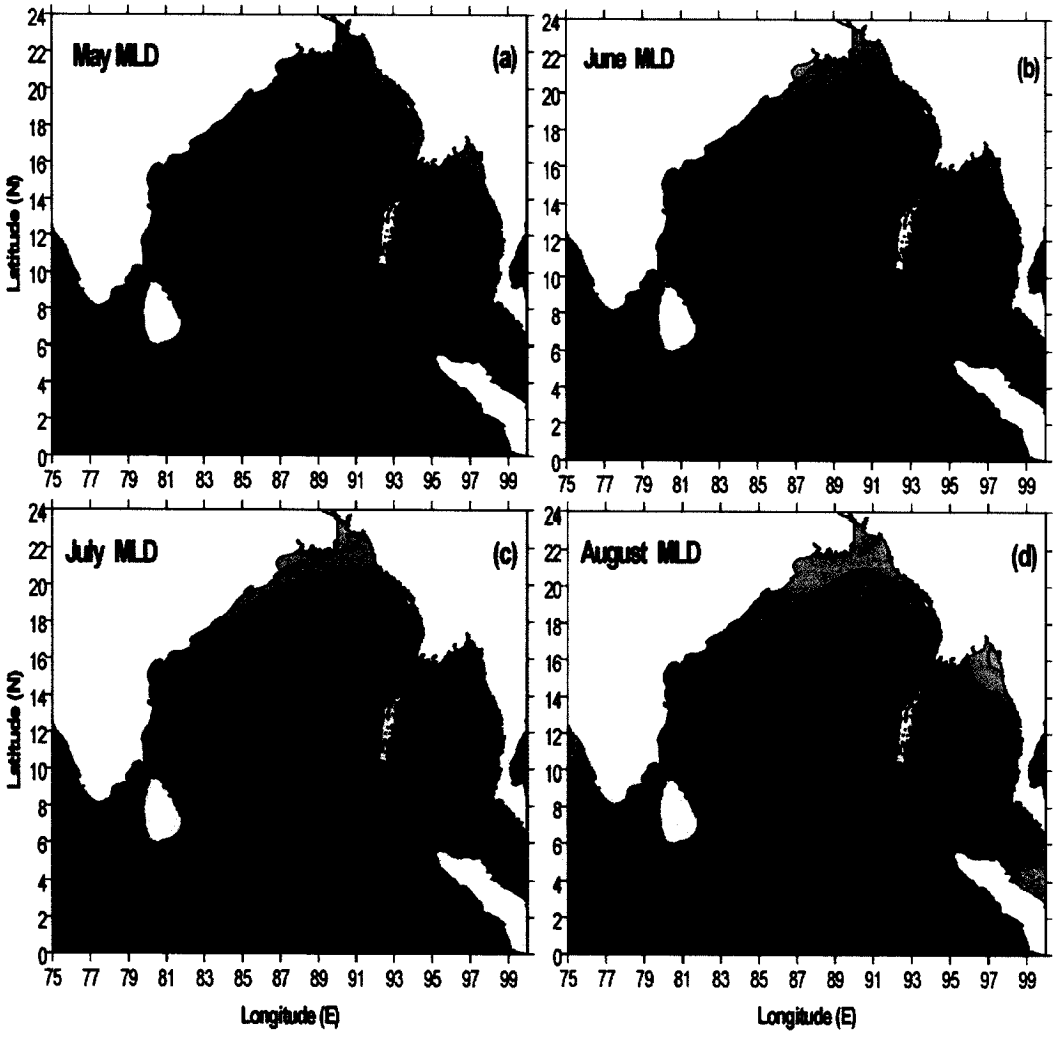

Fig.3.3.2 Monthly mean distribution of MLD (m) in the Bay of Bengal during May to August.

July was similar to that of June with most part of the Bay showing MLD deeper than 35 m (Fig.3.3.2c). The deepest MLD of 50 m was located close to the western equatorial region. The rapid shoaling of MLD seen in the north in June intensified further with shallowest MLD of 5 m close to the head Bay. Around Sri Lanka and southern tip of peninsular India MLD was shallow. In August also the spatial distribution of MLD was similar to that of July, except that shallower MLD was noticed in the central part of the

eastern boundary (Fig.3.3.2d). The MLD near the southern tip of India and Sri Lanka showed further shoaling of MLD compared to July.

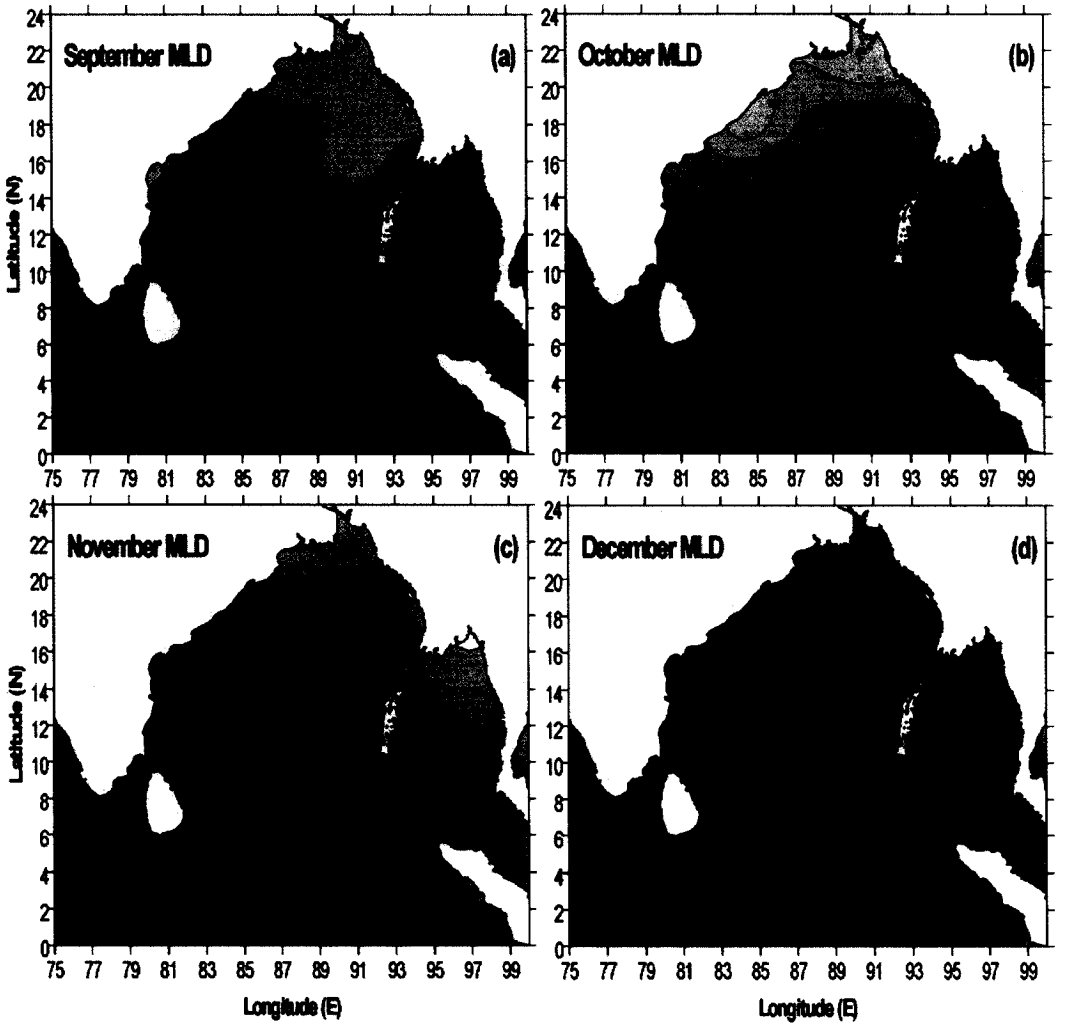

Fig.3.3.3 Monthly mean distribution of MLD (m) in the Bay of Bengal during September to December.

During September the region of low MLD (10-15 m) further expanded from head Bay towards south reaching up to 15°N (Fig.3.3.3a). Along the western boundary also the MLD decreased to 15 m. The deepest MLD (~40 m) occurred in the south central Bay

and equatorial region. In October the area of shallow MLD expanded further southward and reached up to 12°N (Fig.3.3.3b). Similarly, the shallow MLD region along the eastern boundary also expanded westward up to 92°E. Thus, the deep MLD region (~30 m) was mostly confined to south of 8°N and west of 92°E. The basin-wide MLD in November was shallower than 25 m except in two smaller regions – one in the central Bay and the other west of 83°E and south of 8°N (Fig.3.3.3c). The deepest MLD was 30 m in November. In December, the spatial pattern of MLD distribution was similar to that of November, except that a small patch of deep MLD appeared in the northwestern Bay, which was attached to the deep MLD of the central Bay (Fig.3.3.3d). The depth of MLD in the central and northwestern region increased to more than35 m.

In summary, the deepest MLD was about 50 m in the southern Bay during July and shallowest MLD was about 5 m in the northern Bay during October and November and along southeastern Bay during March. The period of shallow MLD was during March-April. The highest spatial variability occurred during July when MLD varied 40 m from south to north. The least spatial variability occurred during April-May, which was about 20 m. The deepest MLD in the north occurred during December-January, which was about 25-30 m. The seasonal cycle of MLD in the north (north of 15°N) showed semiannual variability with deep MLD during December-January and June-July while shallowest MLD during March and October. The amplitude of seasonal cycle in the north was about 15 m. The seasonal cycle of MLD in the south (south of 15°N) showed deep MLD during June-August and shallowest during April. The amplitude of seasonal cycle of MLD in the south was about 17 m.

3.4 Barrier Layer Thickness

The barrier layer thickness (BLT) showed large spatial variability during January, varying from 70 m in the northern Bay and eastern equatorial region to less than 30 m in the central and southern Bay (Fig.3.4.1a). The region around Sri Lanka and peninsular

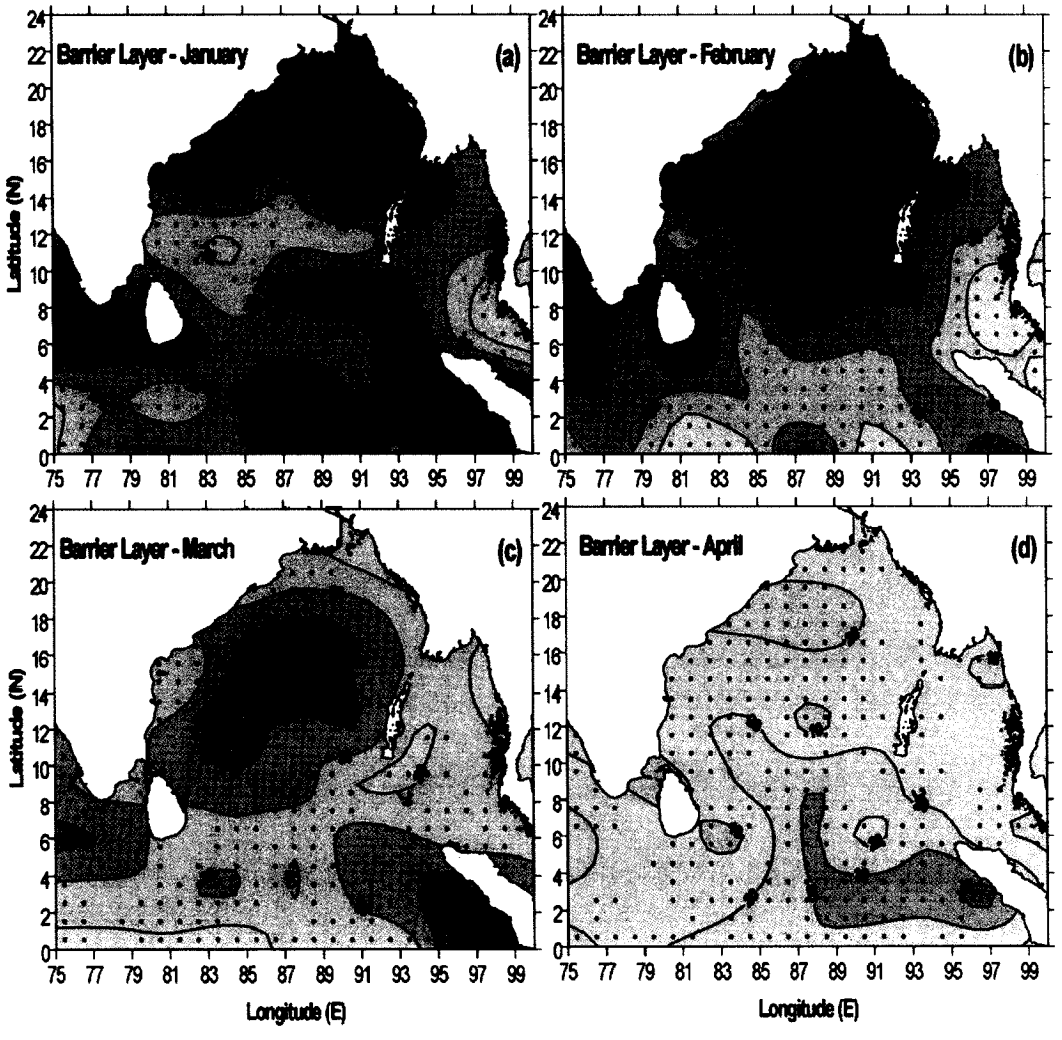

Fig.3.4.1 Monthly mean distribution of BLT (m) in the Bay of Bengal during January to April

India had a deep BLT. In February, the region of deep barrier layer expanded and occupied almost the entire basin (Fig.3.4.1b). Along the eastern and equatorial region

BLT was about 30 m. During March the basin was characterized by two regions of thick barrier layer, one in the central Bay of Bengal encompassing the western boundary and another region of high BLT near the Sumatra coast (Fig.3.4.1c). In the rest of the Bay BLT was low (20 m). The basin-wide BLT was the least in April, which was about 20 m, except close to the eastern part of the equator where it was about 30 m (Fig.3.4.1d). This

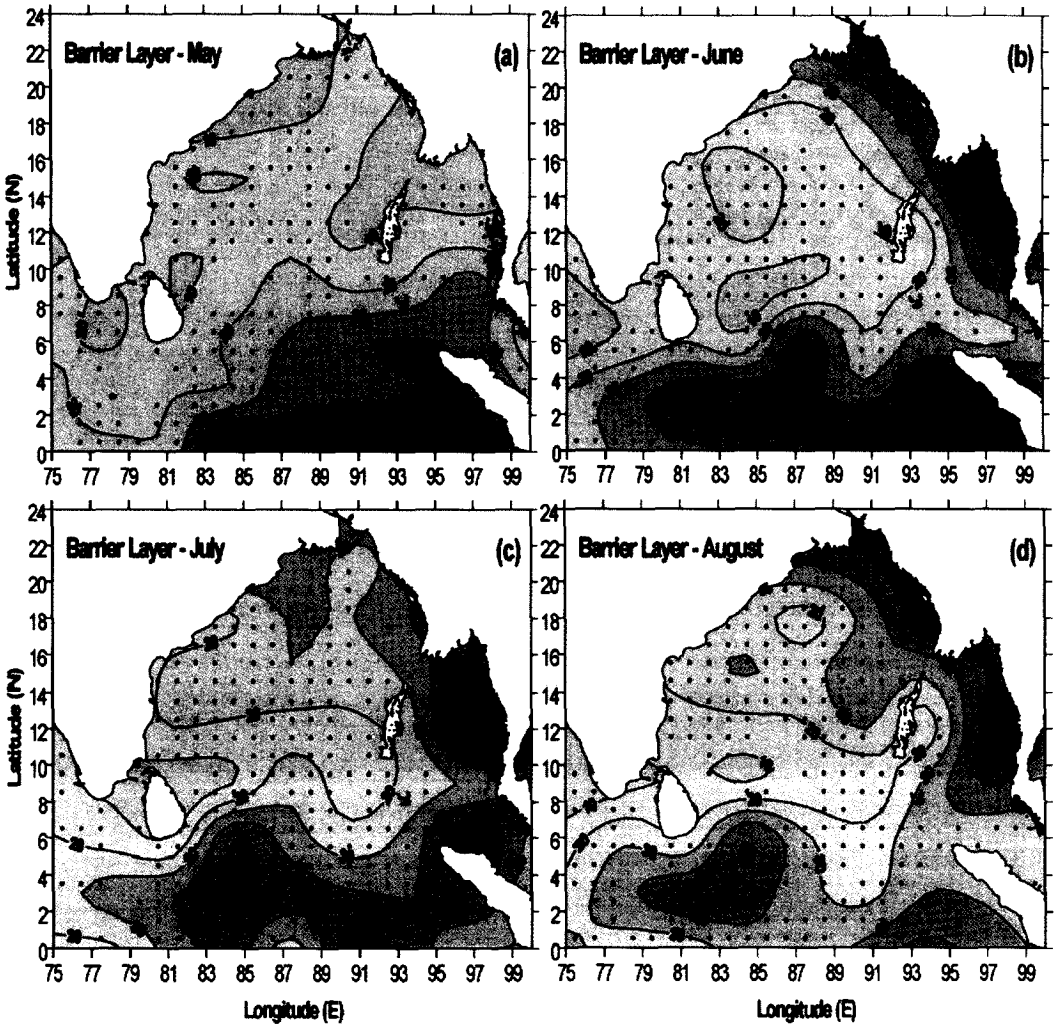

Fig.3.4.2 Monthly mean distribution of BLT in the Bay of Bengal during May to August.

patch of thick barrier layer near equator further increased its thickness in May, while in the rest of the Bay the BLT was between 10-20 m (Fig.3.4.2a). In June the region of high BLT expanded northward along the equator and along the eastern boundary (Fig.3.4.2b). The spatial distribution pattern of BLT remained similar in July (Fig.3.4.2c) and August (Fig.3.4.2d) with the exception that along the eastern boundary BLT increased westward.

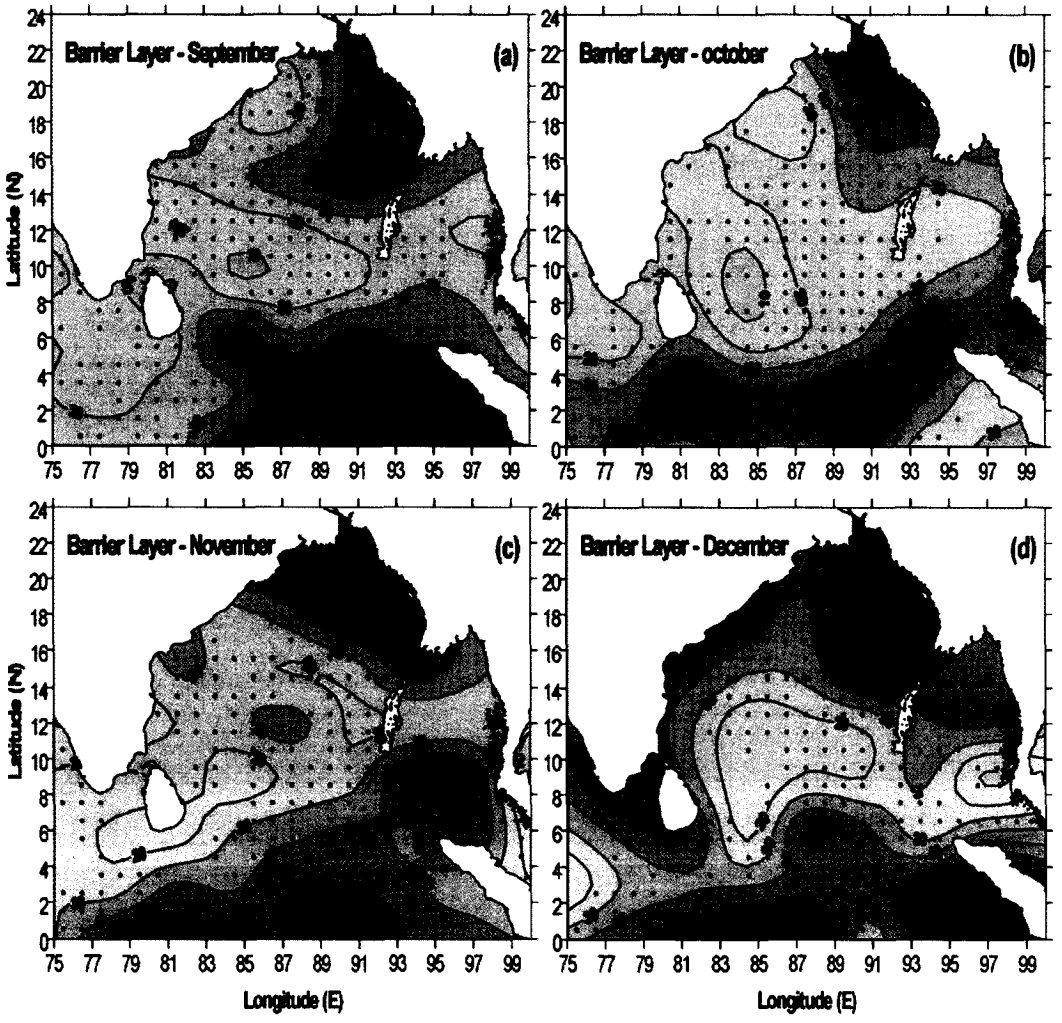

Fig.3.4.3 Monthly mean distribution of BLT (m) in the Bay of Bengal during September to December.

During September the barrier layer showed an increasing trend towards southeast Bay, south of 8°N with maximum barrier layer thickness of about 60 m very near to the equator (Fig.3.4.3a). In the central Bay of Bengal BLT varied between 20 and 30 m. The BLT in the northeastern Bay was 40 m. In October along the equatorial region, eastern boundary and the head Bay BLT deepened with maximum thickness of about 50 m (Fig.3.4.3b). Along central and western Bay BLT was thin and varied between 20 and 30 m. In November the BLT near the equator showed an increase with a maximum value of 60 m (Fig.3.4.3c). Similarly, in the northern Bay also BLT increased with maximum value of 50 m. During December BLT along the equator and the eastern and western boundary was high (Fig.3.4.3d). A zonal band of low BLT was seen between 6° to 14°N where the thickness was between 20-30 m.

In summary, the amplitude of the seasonal cycle of Barrier layer was about 70 m with thickest barrier layer of about 80 m in the south during December-January and thinnest barrier layer of 10 m in the central Bay during April-May and around Sri Lankan dome during June-July. The period of thick barrier layer was during January-February. The highest spatial variability occurred during June when Barrier layer varied 70 m within the basin. The least spatial variability occurred during April, which was about 20 m. The thickest barrier layer in the south occurred during June and December-January, which was 50 m deeper then the rest of the southern Bay. The deepest barrier layer in north occurred during December-January and February, which was about 70 m.

Chapter 4 – Atmospheric Forcing and Remote Forcing

In order to understand physical forcing that is responsible for the basin-wide variability of mixed layer depth and barrier-layer thickness, atmospheric forcing as well as the remote forcing were examined. Towards this the atmospheric forcing such as incoming short wave radiation, net heat flux, wind speed, wind-stress curl and evaporation minus precipitation, and remote forcing such as advection of high salinity waters from the Arabian Sea and propagation of Rossby waves in the Bay of Bengal were analyzed and presented in this chapter.

4.1 Incoming short wave radiation

The incoming short wave radiation (SWR) in the Bay of Bengal during January was low and showed a spatial variation of about 25 W/m^2 within the basin, which was lowest compared with other months (Fig.4.1.1a). North of 15°N, SWR showed decreasing trend with a minimum value of 190 W/m^2 very near to the head Bay. In the central Bay SWR varied marginally between 195 and 200 W/m^2. Highest value of SWR was seen in the Andaman Sea (~210 W/m^2) and west of Sri Lanka. In February SWR showed a general increase and varied from 210 W/m^2 in the head Bay to 240 W/m^2 in the southern Bay (Fig.4.1.1b). The highest SWR was in the Andaman Sea region (~250 W/m^2) and east of Sri Lanka (255 W/m^2) as in the case of January. The overall spatial variation in February was about 45 W/m^2. The SWR showed a further increase in March with highest value of 280 W/m^2 occurring in the western Bay and also in the Andaman Sea (Fig.4.1.1c). The high SWR was seen within a zonal band between 8° and 18°N. Away from this region the

SWR decreased rapidly towards north as well as south with the lowest value of about 230 W/m^2. Thus, the spatial variability of SWR in March was about 50 W/m^2. The incoming solar radiation was the highest in the Bay in April with the highest value of 290 W/m^2 occurring in the Andaman Sea (Fig.4.1.1d). In fact the entire Bay north of 10°N was having SWR higher than 250 W/m^2. The SWR decreased rapidly south of 15°N from 280 to 230 W/m^2. In the head Bay SWR was about 270 W/m^2. The spatial variation in SWR

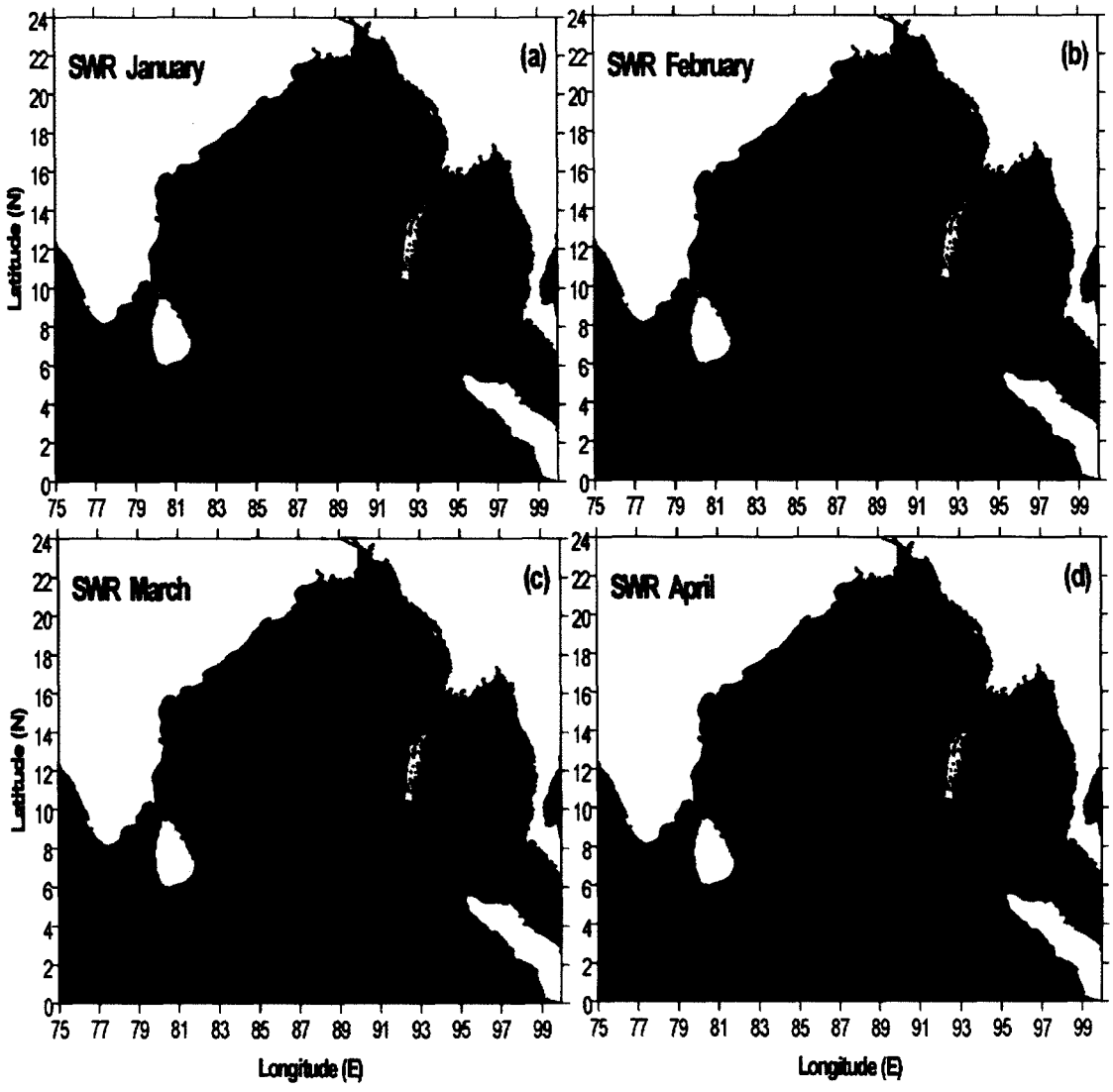

Fig.4.1.1 Monthly mean distribution of SWR (W/m^2) in the Bay of Bengal during January to April.

was about 65 W/m^2.

During May the SWR showed a decreasing trend from north to south with highest value of 280 W/m^2 close to the northeastern boundary (Fig.4.1.2a). North of about 15°N SWR was higher than 250 W/m^2. In the south SWR decreased rapidly and the lowest value of 195 W/m^2 was seen near the eastern equatorial region off Sumatra. The spatial variation

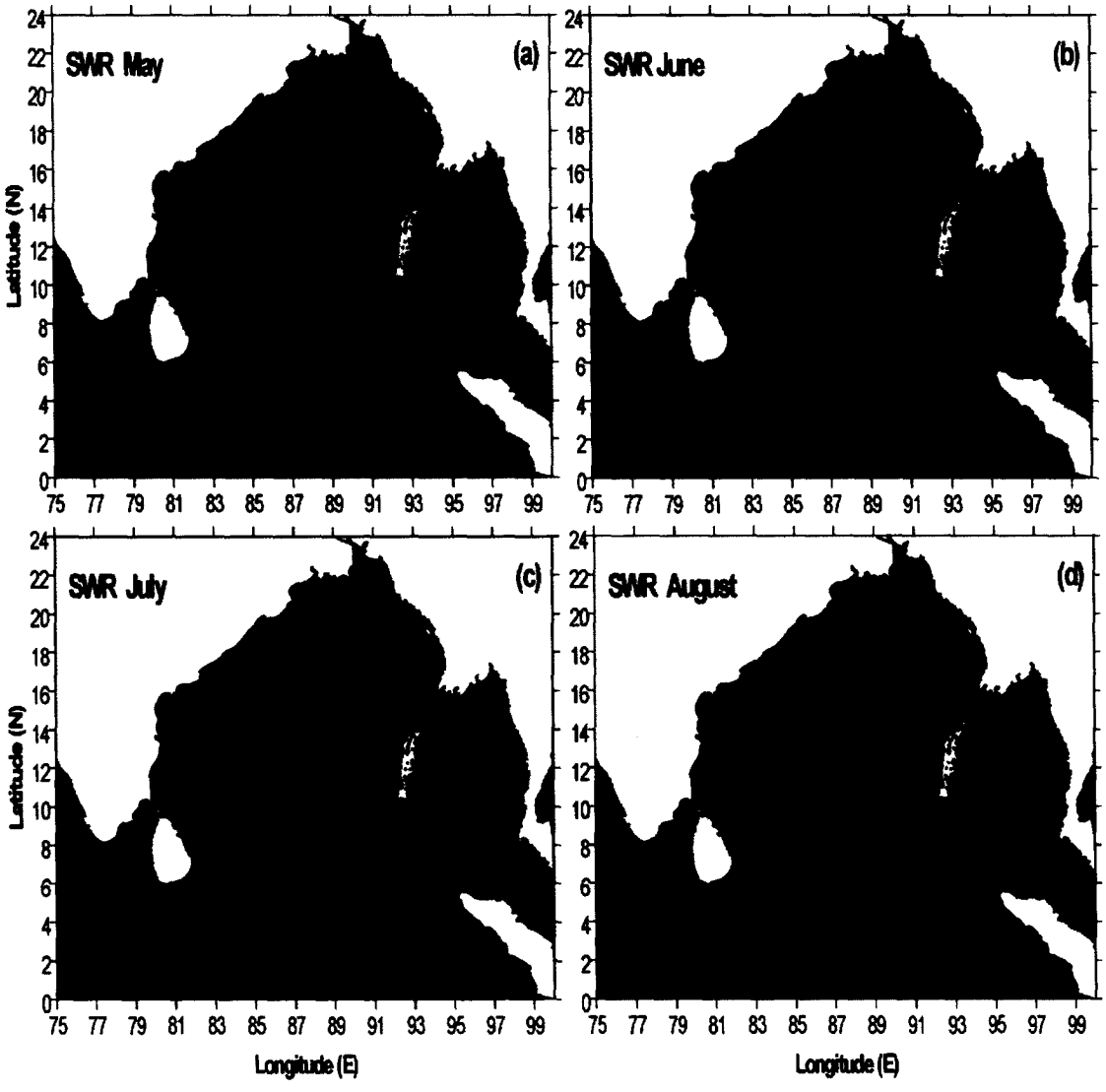

Fig.4.1.2 Monthly mean distribution of SWR (W/m^2) in the Bay of Bengal during May to August.

in SWR from south to north was about 85 W/m^2, which was highest compared with other months. During June SWR showed a further decrease in the northern Bay with highest value of 230 W/m^2 close to the head Bay (Fig.4.1.2b). Along the western boundary SWR was about 220 W/m^2, which decreased towards the central Bay reaching a minimum value of 195 W/m^2. From the central Bay towards the eastern boundary the SWR showed a weak increase. The variation in the SWR from south to north was about 40 W/m^2. In July the spatial distribution of SWR was similar to that of June except that the central and eastern Bay showed a warming of about 10 W/m^2 (Fig.4.1.2c). During August the region encompassing southern part of the western boundary and Sri Lanka showed high incoming short wave radiation with maximum value of 235 W/m^2 (Fig.4.1.2d). In the central and eastern Bay SWR were low and varied between 205 and 215 W/m^2. The lowest SWR was 195 W/m^2, which occurred near the Sumatra coast.

In September SWR further increased around Sri Lanka and southern part of the western boundary with maximum value of 240 W/m^2 (Fig.4.1.3a). The remaining Bay showed a distribution pattern very similar to that of August and SWR varied between 205 and 220 W/m^2. The SWR showed least spatial variability of about 20 W/m^2 in October with highest value of 220 W/m^2 towards the west of Sri Lanka as well as close to the central part of the eastern boundary (Fig.4.1.3b). In November SWR showed a decrease, especially north of 15°N, where the value changed form175 to 165 W/m^2 (Fig.4.1.3c). The highest value of about 230 W/m^2 occurred in the western part near the equator. In the central Bay the SWR varied between 175 W/m^2 to 195 W/m^2. The variation in SWR from north to south was about 55 W/m^2. A further decrease of SWR was noticed in December (Fig.4.1.3d), though the spatial distribution pattern remained similar to that of November.

The highest SWR of about 210 W/m^2 was observed very near to the equator in the western region while the lowest value of 170 W/m^2 was towards the northern Bay.

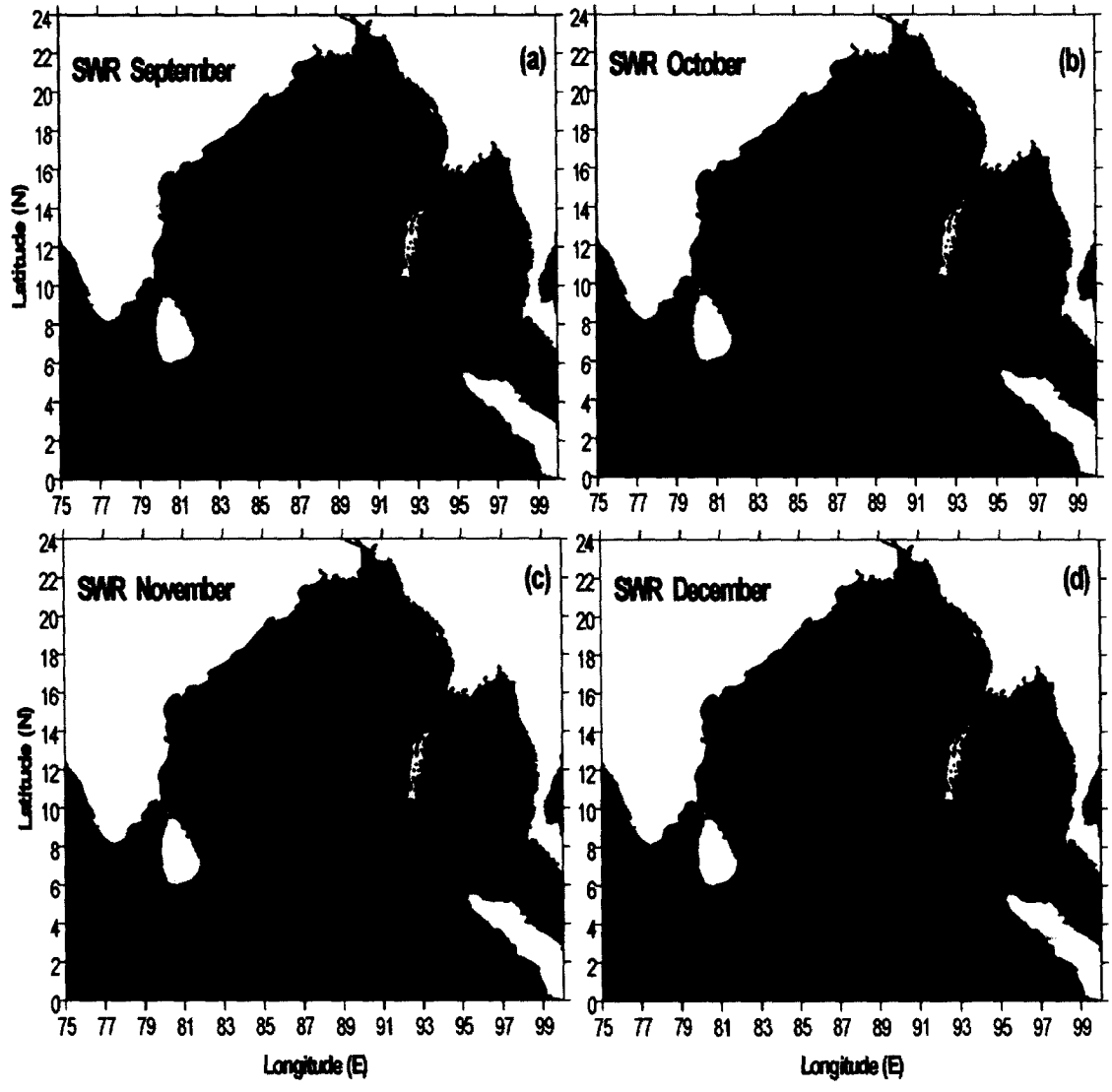

Fig.4.1.3 Monthly mean distribution of SWR (W/m^2) in the Bay of Bengal during September to December.

In summary, the amplitude of the seasonal cycle of incoming short wave radiation within the basin was about 120 W/m^2 with lowest SWR during November – December and highest during March-April. The lowest incoming short wave radiation was about 165 W/m^2 during November while highest SWR was about 285 W/m^2, which was during

April. The seasonal cycle of SWR showed two warming period with high incoming short wave radiation during March-April and September. The period of low incoming short wave radiation was during November-February and June-August. The highest spatial variability occurred during May when SWR varied 80 W/m^2 from south to north. The least spatial variability occurred in January and October which was about 20 W/m^2.

4.2 Net Heat Flux

Spatial distribution of the net heat flux (NHF) in the Bay of Bengal showed heat gain by the ocean in January (Fig.4.2.1a). The net heat gain was highest in the Andaman Sea, which was about 70 W/m^2. In most part of the Bay the NHF showed very small variation, from 0 to 20 W/m^2. Along the northern part of the western boundary NHF was 30 W/m^2. Towards the south, south of 4°N, NHF increased to 50 W/m^2. In February NHF showed a basin-wide increase, with highest value of 120 W/m^2 in the Andaman Sea (Fig.4.2.1b). In the northern Bay, north of 18°N, NHF showed a sharp decrease from 70 to 0 W/m^2 very near to the head Bay. The central Bay gained about 70 W/m^2 over its January value. The variation in the NHF was about 100 W/m^2. During March entire Bay gained more heat compared to February and in the central Bay the gain was almost twice with the highest value of 150 W/m^2 (Fig.4.2.1c). The highest net heat gain in the head Bay was about 100 W/m^2. The highest NHF was in April, which showed a spatial variation of about 90 W/m^2 (Fig.4.2.1d). The high NHF was seen as a zonal band between 11° and 13°N with highest value of 160 W/m^2 located west of 90°E. Away from this zonal band of high NHF, the values reduced towards both north and south. The lowest NHF was 70 W/m^2 and was

seen close to head Bay in the north and equator in the south. The spatial variation in net heat flux was about 90 W/m^2.

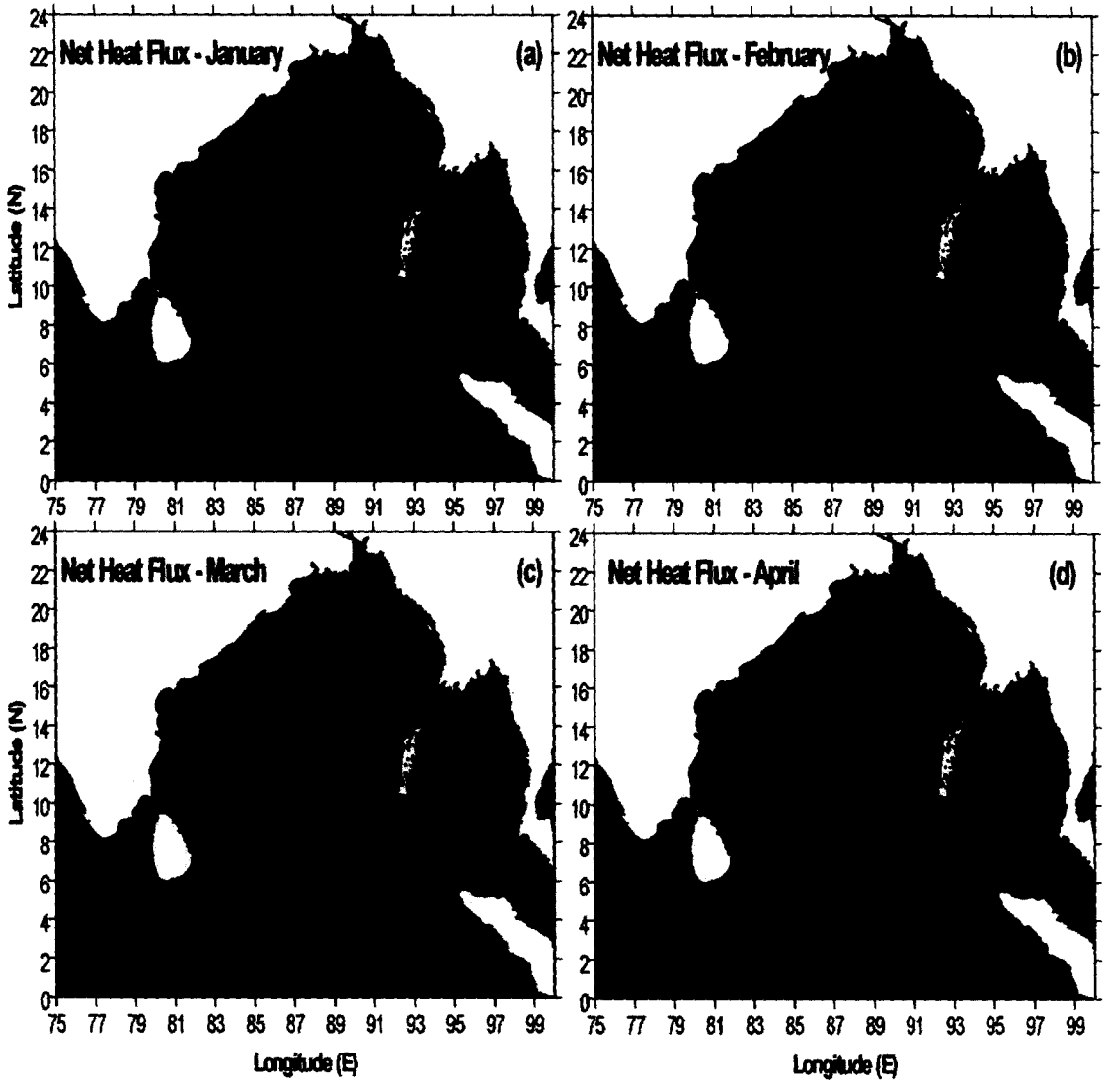

Fig.4.2.1 Monthly mean distribution of NHF (W/m^2) in the Bay of Bengal during January to April.

In May, the neat heat gain showed an increase towards the western boundary with maximum value of 170 W/m^2 located near the central part of the western boundary (Fig.4.2.2a). The minimum net heat gain was in the south near equator with value of about 30 W/m^2. The spatial variation of NHF was 140 W/m^2.

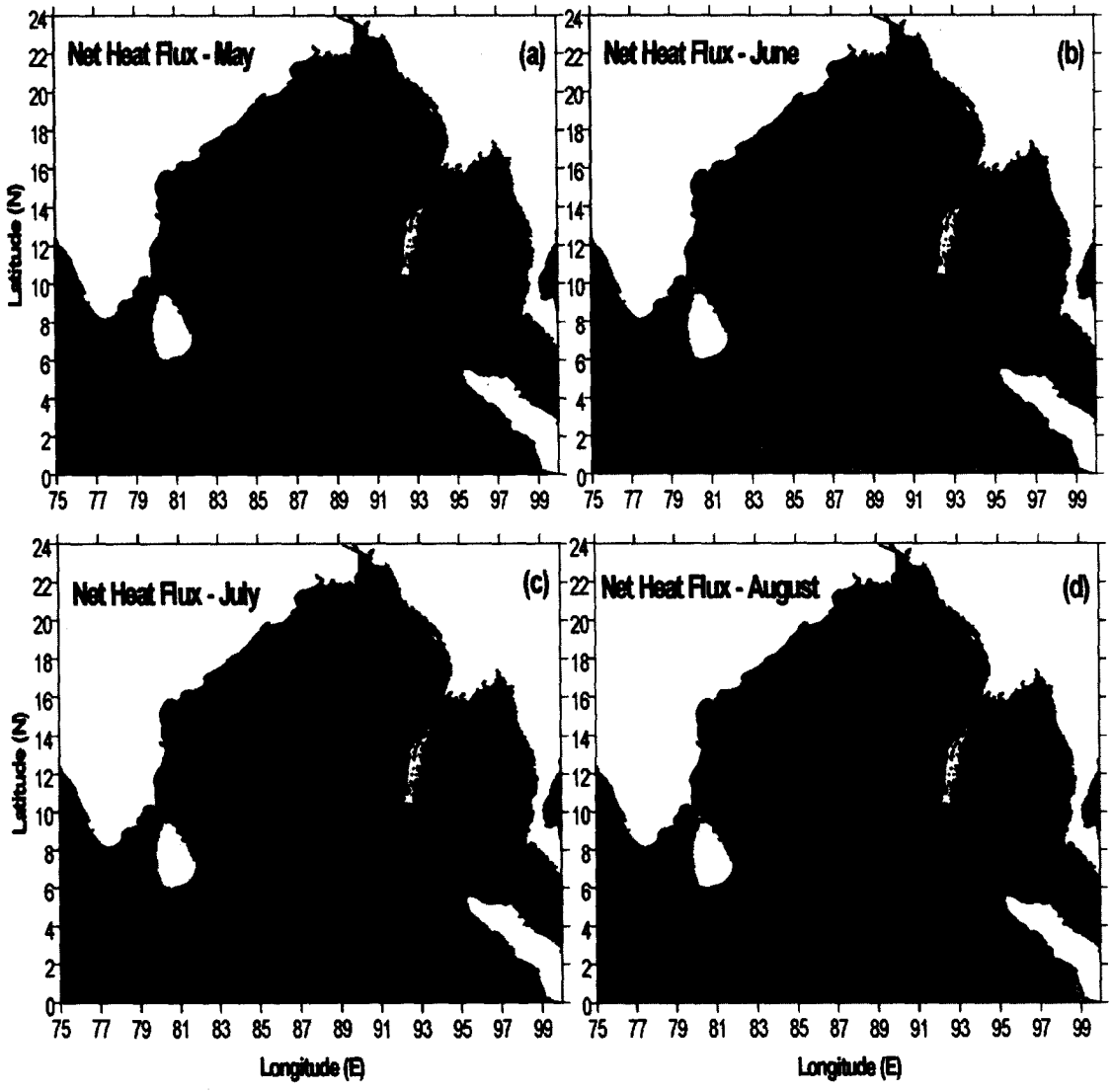

Fig.4.2.2 Monthly mean distribution of NHF (W/m^2) in the Bay of Bengal during May to August.

The NHF during June showed a basin-wide decrease with high values along the boundaries such as off peninsular India, central part of the western boundary, northeastern Bay and Sumatra coast (Fig.4.2.2b). Along the western boundary the maximum net heat gain was about 70 W/m^2, while that along the northeastern Bay was 90 W/m^2. The lowest NHF was observed in the southern part of the central Bay. The spatial variation in net heat flux was about 90 W/m^2.

The spatial distribution pattern of NHF during July was similar to that of June, except that the northern Bay showed a general increase (Fig.4.2.2c). In August the entire region from the southern peninsular India, along the western boundary of the Bay, and the northeastern Bay showed high NHF (Fig.4.2.2d). In the central Bay NHF varied between 70-80 W/m^2 while the highest NHF of 120W/m^2 occurred close to the central part of the western boundary. The lowest NHF values were seen towards south and east.

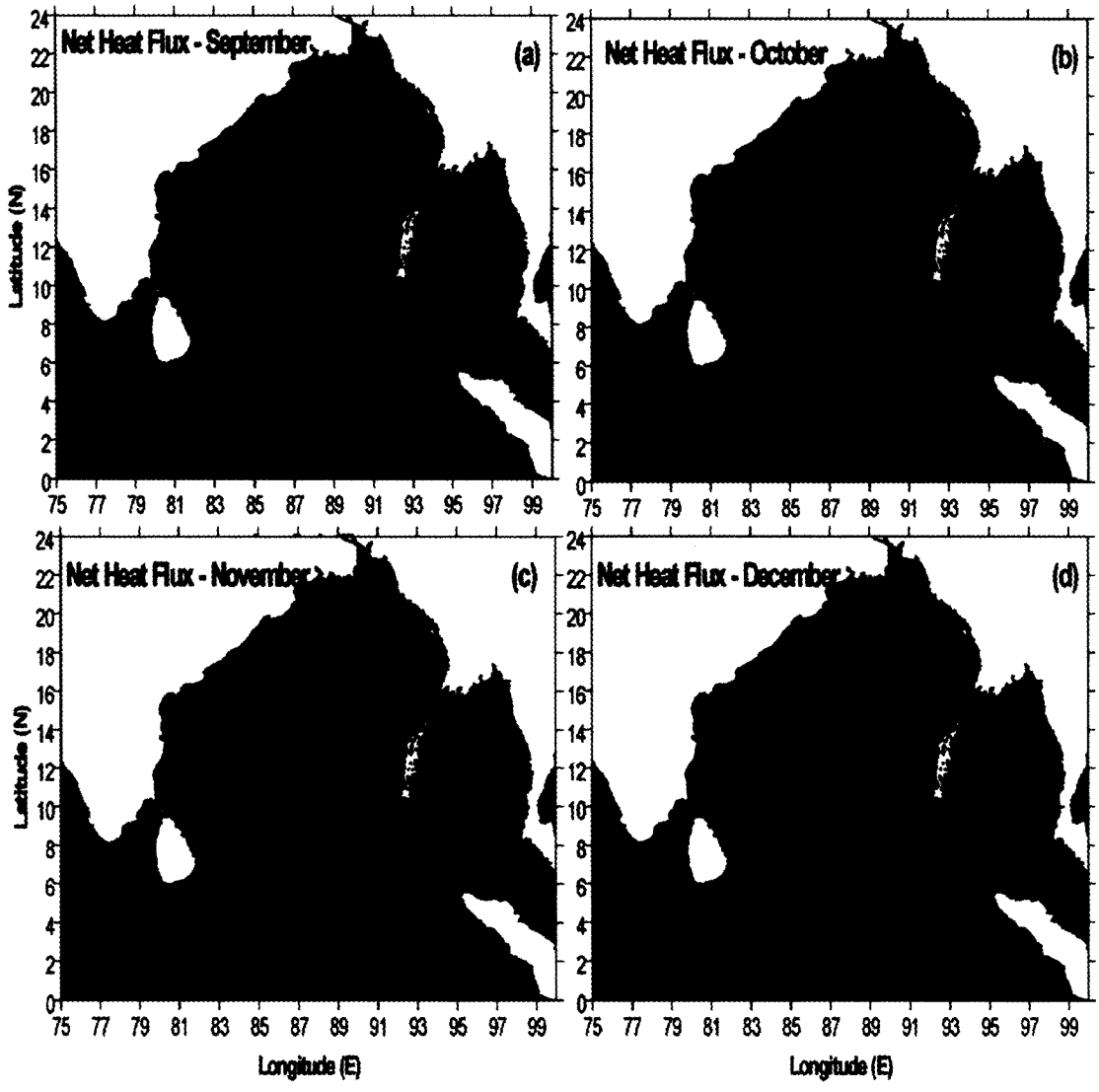

Fig.4.2.3 Monthly mean distribution of NHF (W/m^2) in the Bay of Bengal during September to December.

The NHF during September also showed the net gained by the northern Bay was higher than the southern part (Fig.4.2.3a). In the northern Bay the NHF increased from 70 to 110 W/m^2, while in the southern part it decrease from 60 to 40 W/m^2. The spatial variation of NHF was about 60 W/m^2, which was lowest compared with the other months. In October a general basin-wide increase in the NHF was observed (Fig.4.2.3b). A prominent feature in the northern Bay was a region where the net heat gain was about 30 W/m^2 lower than the ambient waters. The highest NHF of 100 W/m^2 was seen close to the central part of the western as well as the eastern boundary. The lowest NHF of 40 W/m^2 was close to the Sumatra coast.

During November the NHF showed a basin-wide decrease with the northern Bay north of 15°N showing a net heat loss by about 10-20 W/m^2 (Fig.4.2.3c). Along the western boundary this loss of heat extended up to 12°N. In the southern Bay south of 10°N, the net heat gain showed an increase towards the western part and close to the equator NHF was 90 W/m^2. In December NHF showed a further heat loss from northern Bay with a highest value of 70 W/m^2 close to the head Bay (Fig.4.2.3d). In the eastern Bay, east of 90°E and south of 20°N, NHF showed a net gain, which increased towards east with the highest value of 40 W/m^2. South of 10°N NHF showed an increase with a maximum value of 50 W/m^2 near the equator.

In summary, the maximum net heat loss was 60 W/m^2 in the north during December and the highest net heat gain was 160 W/m^2 in the central Bay during April. The period of low Net heat flux was during December. The highest spatial variability occurred during May when Net heat flux varied by 130 W/m^2 from south to north. The least spatial

variability occurred during September, which was about 50 W/m^2. The seasonal cycle of net heat flux in the northern Bay (north of 15°N) showed two warming period with High positive net heat flux during March-May and August-October, while low (negative) net heat flux during November-January and June. The seasonal cycle of net heat flux in the southern Bay (south of 15°N) showed semiannual variability with high net heat gain during March-April and October while low net heat during December-January and June.

4.3 Wind Speed

The spatial distribution of wind speed during January showed a zonal band of high wind speed of about 7 m/s between 6° and 12°N (Fig.4.3.1a). Within this high wind speed there were two core of highest wind speed one west of Sri Lanka with a speed of 8 m/s and the other in the central part of the Bay with a speed of 7.5 m/s. Away from this region the wind speed showed a steady decrease towards north as well as south. The lowest wind speed of 4 m/s was observed close to the head Bay as well as eastern part of the equatorial region off Sumatra. In February though the spatial pattern of wind speed distribution remained same, the strength of wind showed a decrease of about 1.5 to 2 m/s (Fig.4.3.1b). The maximum wind speed was 6 m/s and the minimum wind speed of 4 m/s was noticed close to the eastern equatorial region. The basin-wide distribution of wind speed showed the least variability in March with highest value of 5 m/s close to the northwestern boundary and the lowest value of 4 m/s in the northeastern boundary as well as in the northern part of the central Bay (Fig.4.3.1c). The wind speed showed strengthening in the northern Bay in April with highest value of 8 m/s (Fig.4.3.1d). Wind

speed decreased rapidly away from this wind speed maxima and the lowest speed of 4 m/s was noticed over a large region in southern part of the Bay.

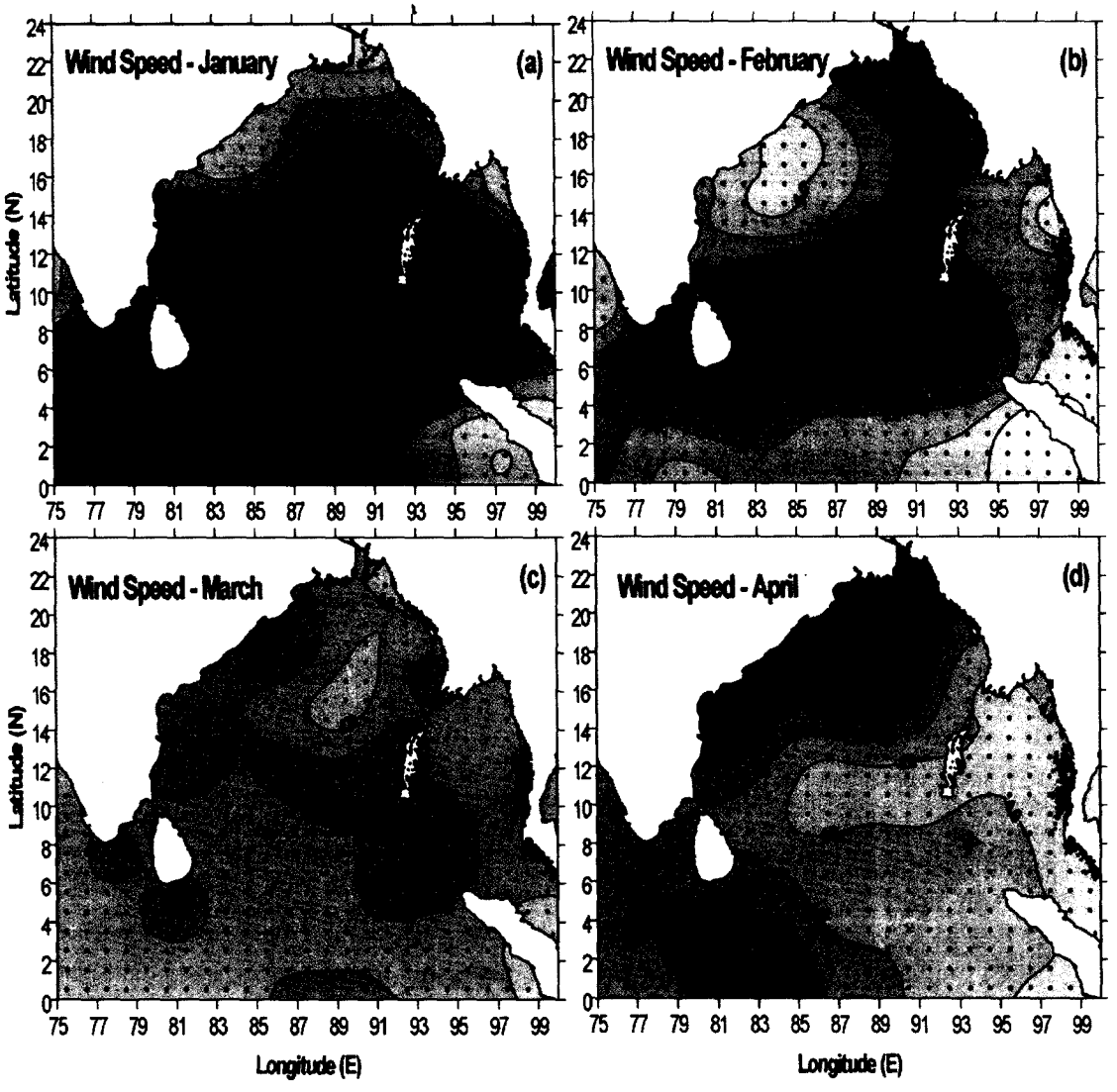

Fig.4.3.1 Monthly mean distribution of wind speed (m/s) in the Bay of Bengal during January to April.

During May two regions of high wind speed were noticed, a band along the western boundary and the other a band encompassing Sri Lanka into the central Bay in a southwest-northeast direction (Fig.4.3.2a). The highest wind speed in both the regions was 8 m/s.

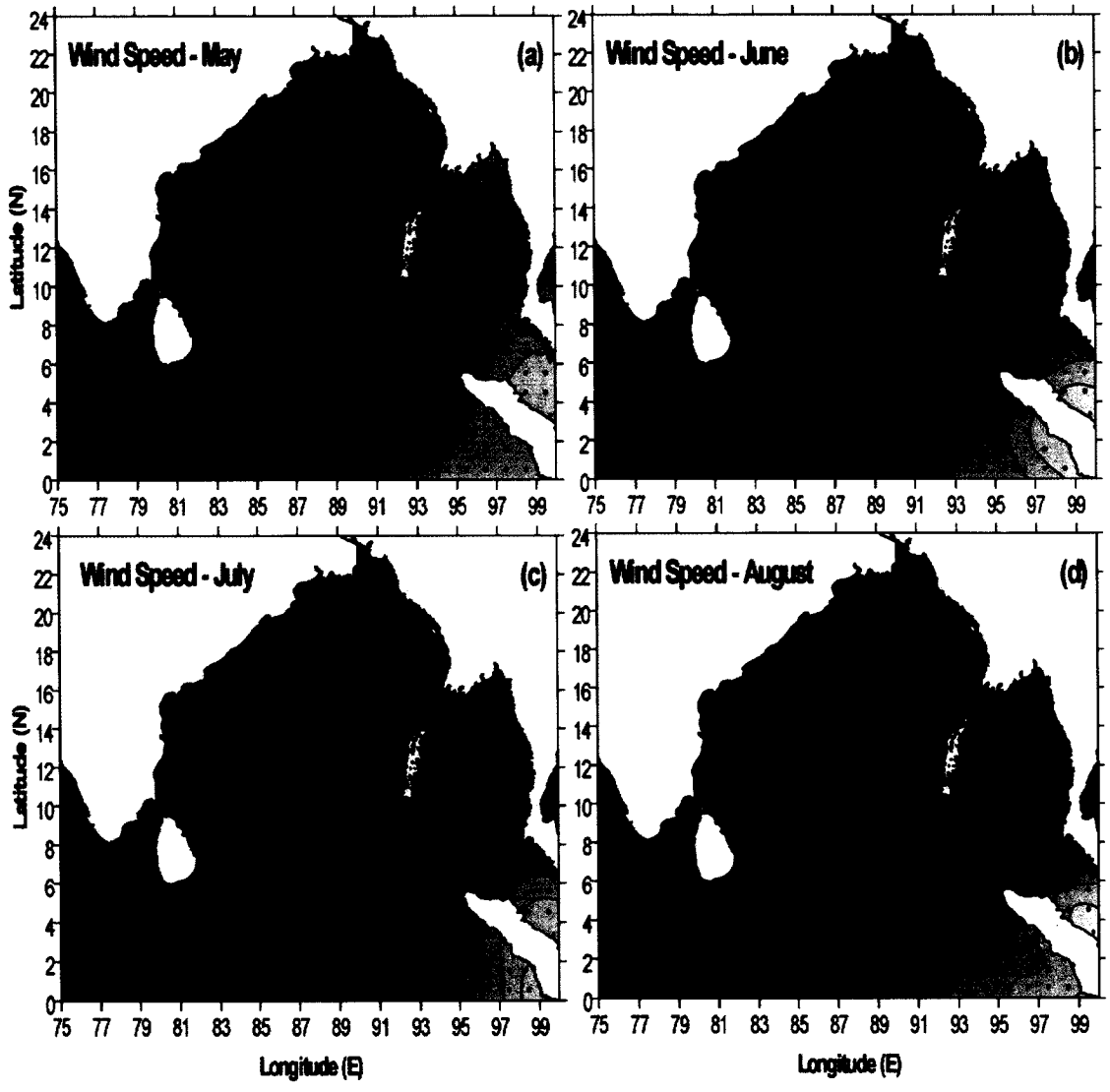

Fig.4.3.2 Monthly mean distribution of wind speed (m/s) in the Bay of Bengal during May to August.

The wind speed showed a sudden increase in June with most part of the Bay with high winds (Fig.4.3.2b). The maximum wind speed was about 10 m/s, which was the highest of all the months. In most part of the basin wind speed was between 9 and 10 m/s. The wind speed decreased towards the boundary and south of 4°N. The lowest wind speed of 6 m/s was noticed near the equator. Another region of low wind speed was observed near the southeastern Bay with minimum value of 4 m/s. Both during July (Fig.4.3.2c) and

August (Fig.4.3.2d) the spatial distribution pattern of wind remained similar. However, during July the highest wind speed in the central Bay showed a reduction of 1 m/s compared to June. In contrast, during August the speed increased by 0.5 m/s in the central Bay compared to July.

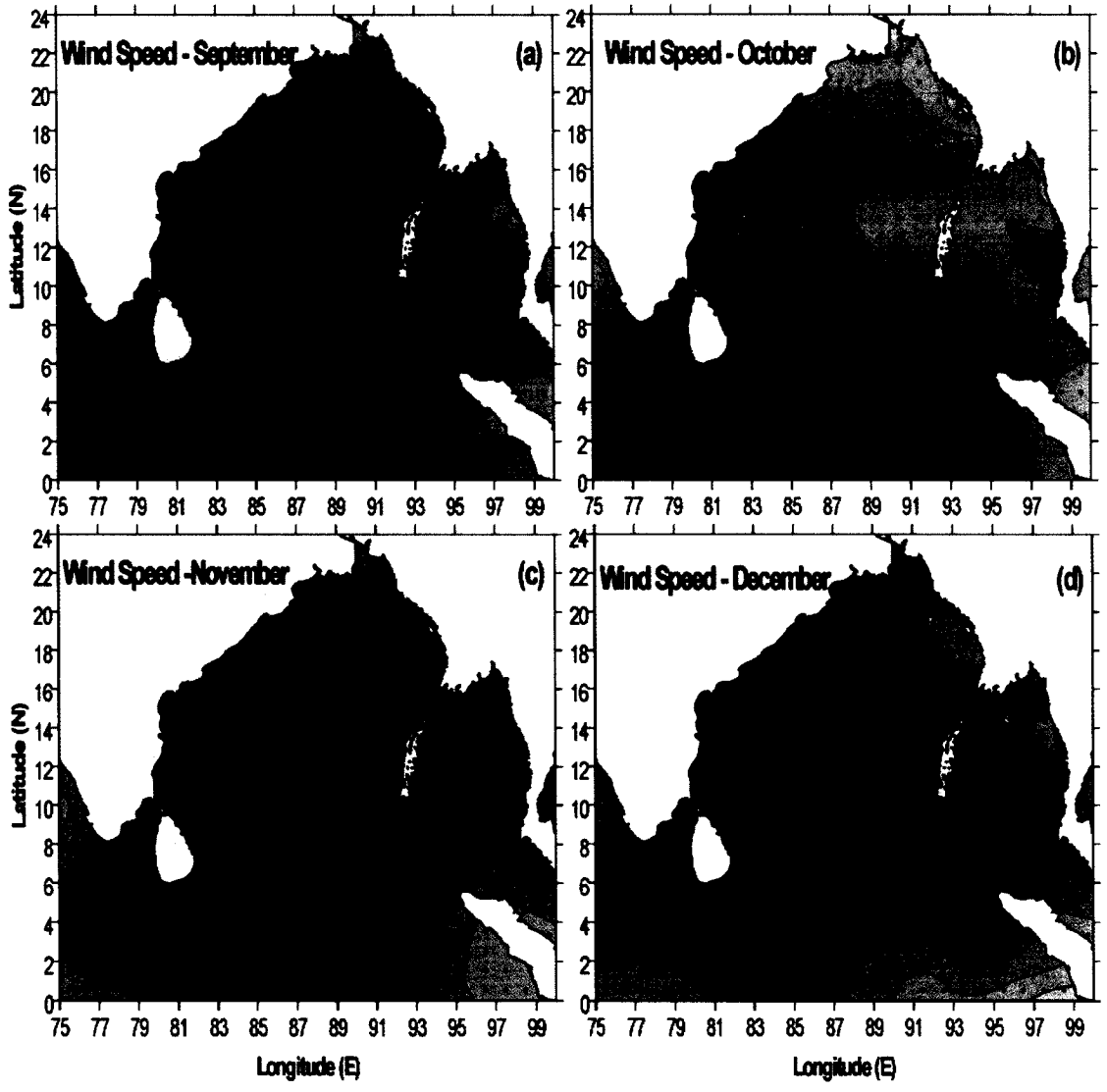

Fig.4.3.3 Monthly mean distribution of wind speed (m/s) in the Bay of Bengal during September to December.

During September the wind speed over the Bay decreased and the core of the high wind speed was located in a southwest-northeast direction off Sri Lanka (Fig.4.3.3a). The

highest wind speed was 8.5 m/s and the speed showed a steady decrease towards the north with lowest value of 4 m/s close to the head Bay. The wind speed further reduced in October and the core of the high wind speed was located in a small region south of Sri Lanka (Fig.4.3.3b). The highest wind speed was 6.5 m/s, while the lowest value was 4.5 m/s in the northern Bay. The spatial variation of the wind speed was about 2 m/s. In November a region of high wind speed of 8 m/s was noticed in the central part of the western boundary (Fig.4.3.3c). Away from the western boundary the wind speed decreased rapidly towards north as well as south. In the head Bay the lowest wind speed was 5 m/s, while in the eastern part of the equator it was 4.5 m/s. During December the region of high wind speed expanded into the central Bay, but the strength reduced to 7 m/s. Again towards north and south of this high wind speed band the value decreased.

In summary, the amplitude of the seasonal cycle of wind speed within the basin was about 6 m/s with lowest wind speed of about 4 m/s and highest wind speed of about 10 m/s. The highest wind speed occurred during June while lowest wind speed occurred during February-April. The highest spatial variability occurred during June when wind speed varied by 6 m/s from south to north. The least spatial variability occurred during March, which was about 1 m/s. The seasonal cycle of wind speed in the northern Bay (north of 15°N) showed semiannual cycle with high wind speed during June-August and November-December, while low wind speed was during January-March and October. The seasonal cycle of wind speed in the southern Bay (south of 15°N) showed semiannual variability with high wind speed during June-August and January while low wind speed during March-April and October-November.

4.4 Wind stress curl

The wind-stress curl during January showed negative curl in the northern Bay, north of 12°N, while towards the south the curl was positive (Fig.4.4.1a). The negative curl showed an increase towards the north. The highest positive curl was noticed in the southeastern region. The negative wind stress curl in the north would lead to downward

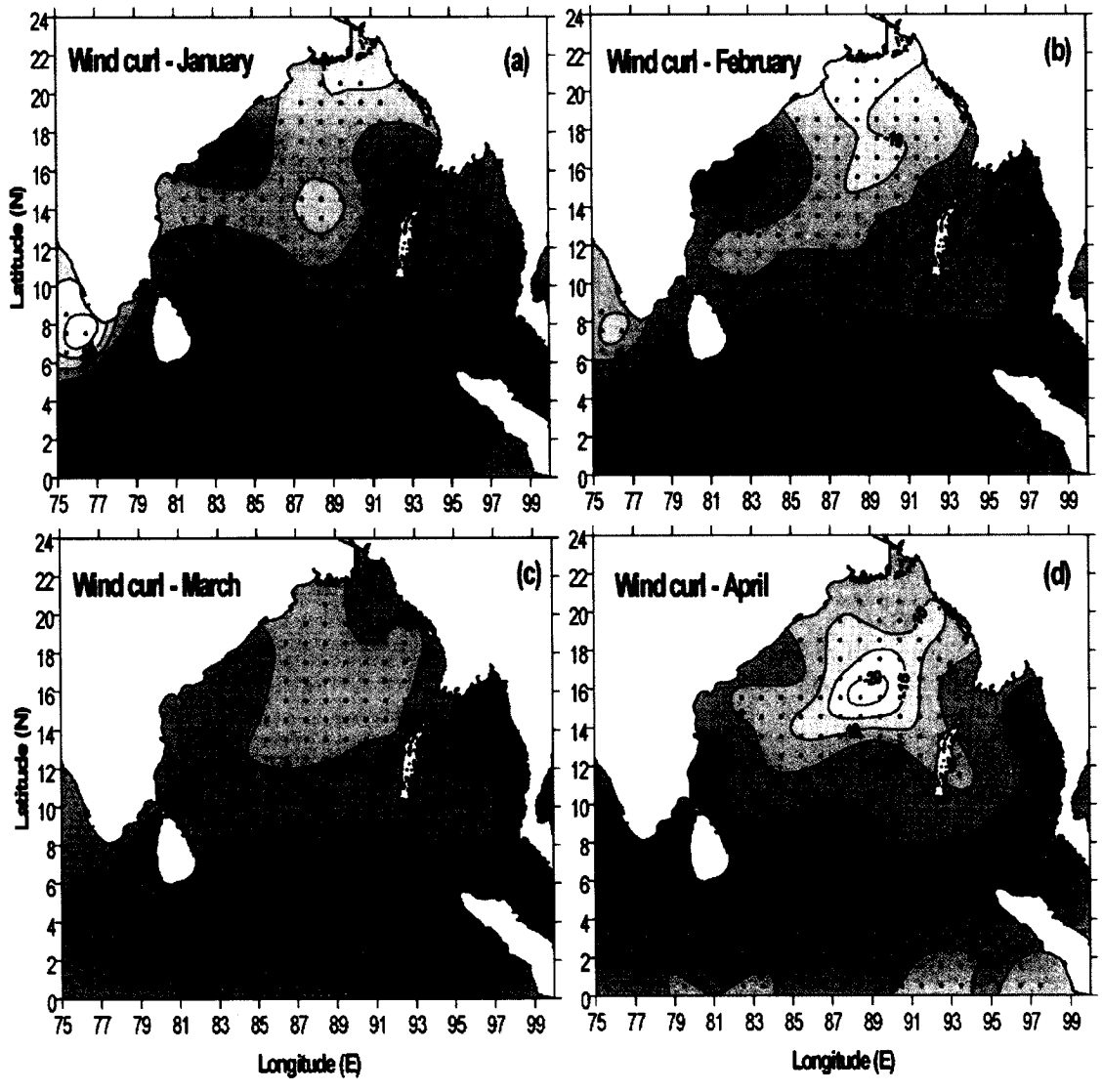

Fig.4.4.1 Monthly mean distribution of wind stress curl ($x10^{-8}$ Pascal/m) in the Bay of Bengal during January to April.

Ekman pumping and downwelling, while the positive curl would lead to upward Ekman pumping and upwelling. The region around southern tip of Indian Peninsula also showed a negative wind stress curl. In February the wind stress curl showed a weakening in the south, south of 12°N, and mild strengthening in the northern Bay (Fig.4.4.1b). The region of negative wind stress curl expanded further south in March but its strength in the northern Bay weakened slightly (Fig.4.4.1c). In April the region north of 8°N showed negative wind stress curl and a very strong curl region was noticed with its core located between 14°and 18°N (Fig.4.4.1d). This indicated strong downward Ekman pumping and downwelling.

During May the spatial distribution of the wind stress curl showed two regions of negative values, one a band oriented parallel to the western boundary encompassing the head Bay and part of northeastern Bay, and the other south of 4°N (Fig.4.4.2a). A strong positive wind stress curl was noticed in the region encompassing the tip of peninsular India. The positive wind stress curl would drive an upward Ekman pumping and upwelling. In the north the negative wind stress curl would lead to downward Ekman pumping. In June the entire Bay approximately north of 5°N, except towards the southeastern region, showed positive wind stress curl (Fig.4.4.2b). The region of strong positive curl east of Sri Lanka and along the western boundary would lead to strong upward Ekman pumping. South of 5°N the wind stress curl was negative. In July the distribution pattern remained the same as that of June, except an intensification of positive wind stress curl seen close to the northeastern Bay (Fig.4.4.2c). During August, the positive wind stress curl east of Sri Lanka intensified much more than June indicating stronger upward Ekman pumping (Fig.4.4.2d). The region of positive wind stress curl

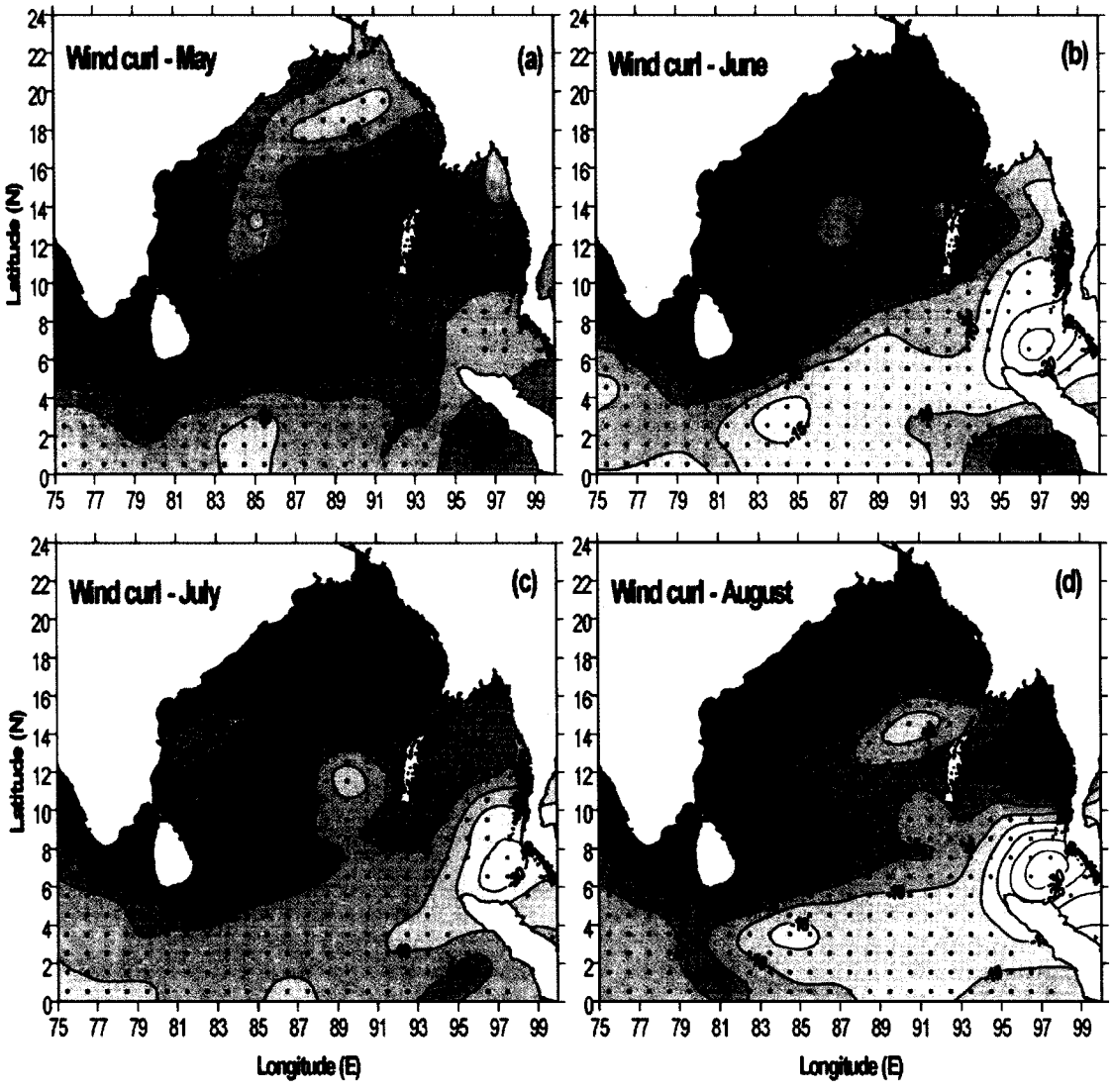

Fig.4.4.2 Monthly mean distribution of wind stress curl ($x10^{-8}$ Pascal/m) in the Bay of Bengal during May to August.

seen off the northeastern boundary in June extends further offshore in the southwest direction making the entire western boundary a region of upward Ekman pumping.

In September there was a general reduction in the value of wind stress curl both positive as well as negative (Fig.4.4.3a). The wind stress curl showed further reduction in October when the values over the Bay was the least (Fig.4.4.3b). In November the wind stress curl

showed an increase and almost the entire Bay showed positive values (Fig.4.4.3c). In addition, these positive wind stress curl showed a strengthening towards the western boundary. During December the wind stress curl once again showed a weakening in the northern Bay and the values were negative, while the southern Bay showed a strengthening of positive wind stress curl.

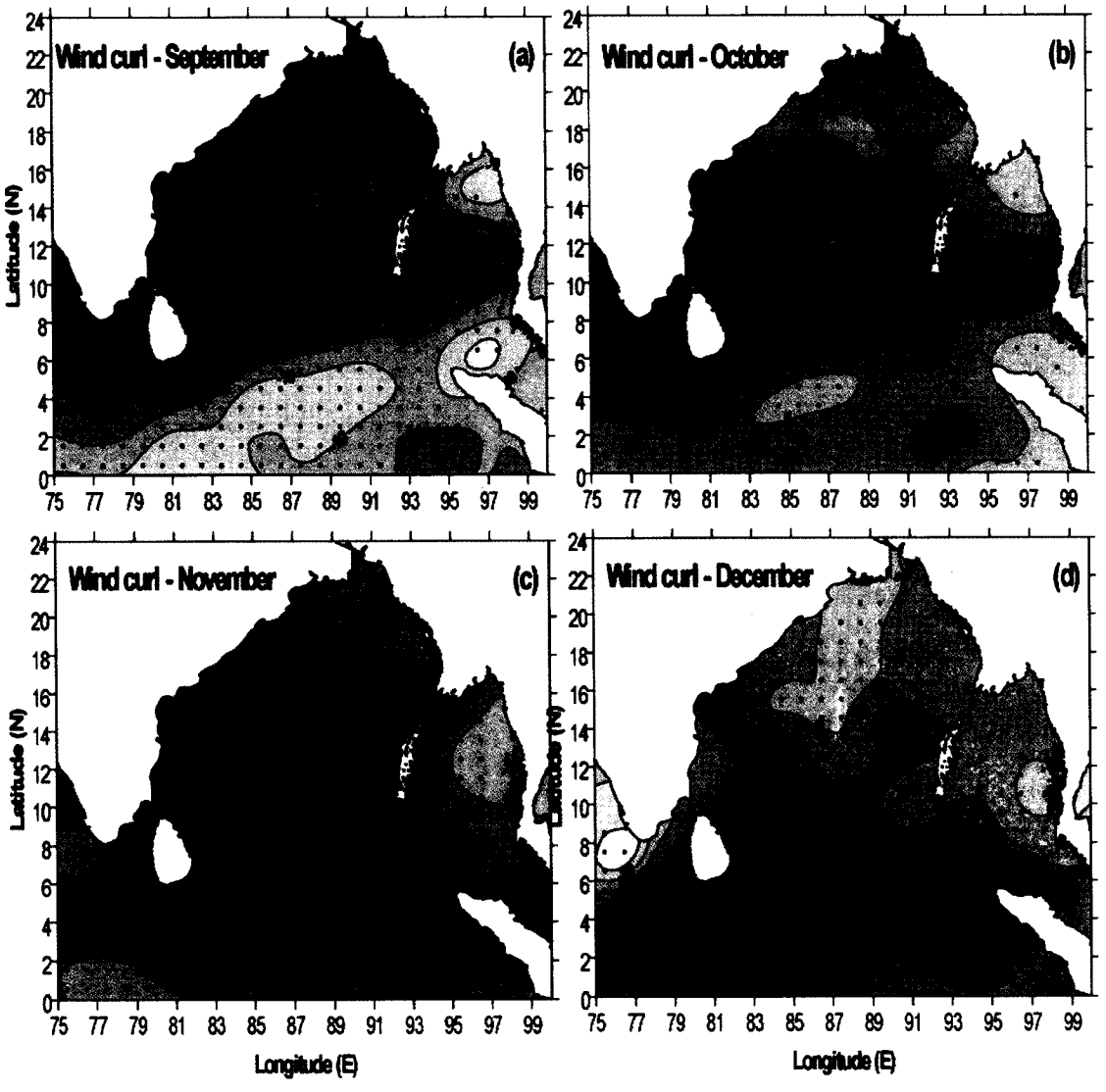

Fig.4.4.3 Monthly mean distribution of wind stress curl ($x10^{-8}$ Pascal/m) in the Bay of Bengal during September to December.

In summary, the maximum negative wind stress curl was about 30 x 10^{-8} Pascal/m which occurred during August along the southeastern boundary of Bay of Bengal while highest positive wind stress curl was about 20 x 10^{-8} Pascal/m which occurred during January along the south eastern Bay and also during June to August along the eastern part of Sri Lanka. The highest spatial variability occurred during August when wind stress curl varied from –30 to 20 x 10^{-8} Pascal/m. The least spatial variability occurred during March, when wind stress curl varied between –5 to 5 x 10^{-8} Pascal/m. The seasonal cycle of wind stress curl in the northern Bay (north of 15°N) showed annual cycle with positive wind stress curl from June-November and negative during December-May. The seasonal cycle of wind stress curl in the southern Bay (south of 15°N) showed annual variability with positive wind stress curl from November-March and negative wind stress curl from June-September.

4.5 Evaporation – Precipitation

The spatial distribution of evaporation minus precipitation (E-P) in January showed a net evaporation in the region north of 8°N, while south of it, there was a net precipitation (Fig.4.5.1a). The maximum evaporation of 120 mm/month was observed in the northeastern region and the maximum net precipitation of 240 mm/month was near equator. In February most part of the Bay showed net evaporation, though the magnitude of it was lower than the previous month by about 20 mm/month (Fig.4.5.1b). The region of net precipitation shifted to south of 4°N and the maximum value was 80 mm/month. During March the entire Bay showed a net evaporation of about 70-80 mm/month (Fig.4.5.1c). The region near the eastern part of the equator was the only place where E-P

showed a net precipitation with a maximum value of 80 mm/month. The spatial distribution of E-P showed a change in April with the highest net evaporation shifting from head Bay to the central part of the western boundary, which was 80 mm/month (Fig.4.5.1d). The head Bay showed a decreasing net evaporation from 40 to 10 mm/month. South of 4°N E-P showed net precipitation with the maximum value of 110 mm/month close to Sumatra coast.

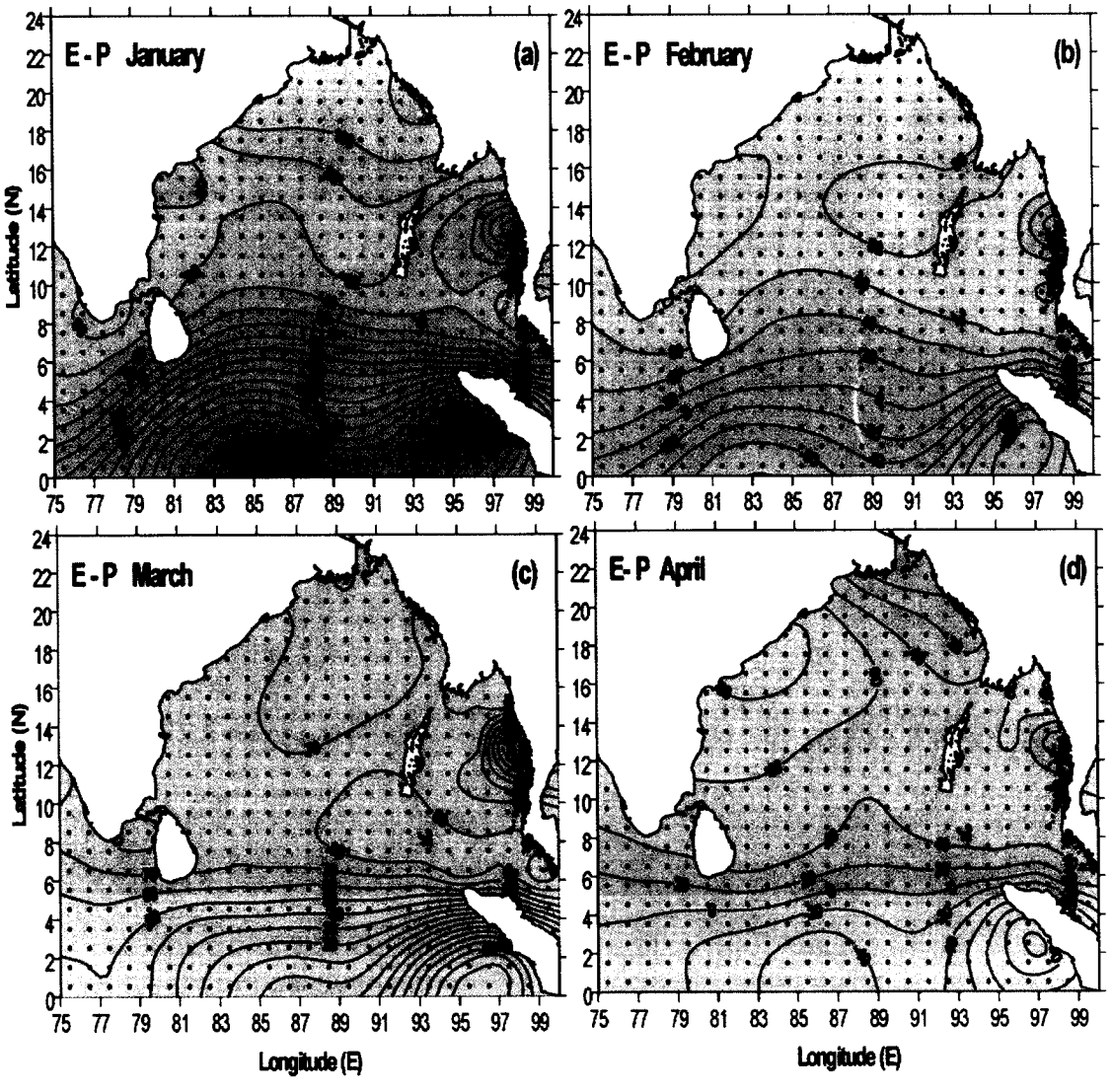

Fig.4.5.1 Monthly mean distribution of E-P (mm/month) in the Bay of Bengal during January to April.

In May the head Bay showed a net precipitation of about 80 mm/month in addition to a region in the southeastern part of the Bay with a value of 20 mm/month (Fig.4.5.2a). The rest of the Bay showed a net evaporation increasing towards west with the highest value of 80 mm/month around Sri Lanka. The E-P showed a dramatic change in its distribution pattern in June with a net precipitation in the entire Bay of Bengal except in region close to Sri Lanka, which showed a net evaporation (Fig.4.5.2b). The huge net precipitation

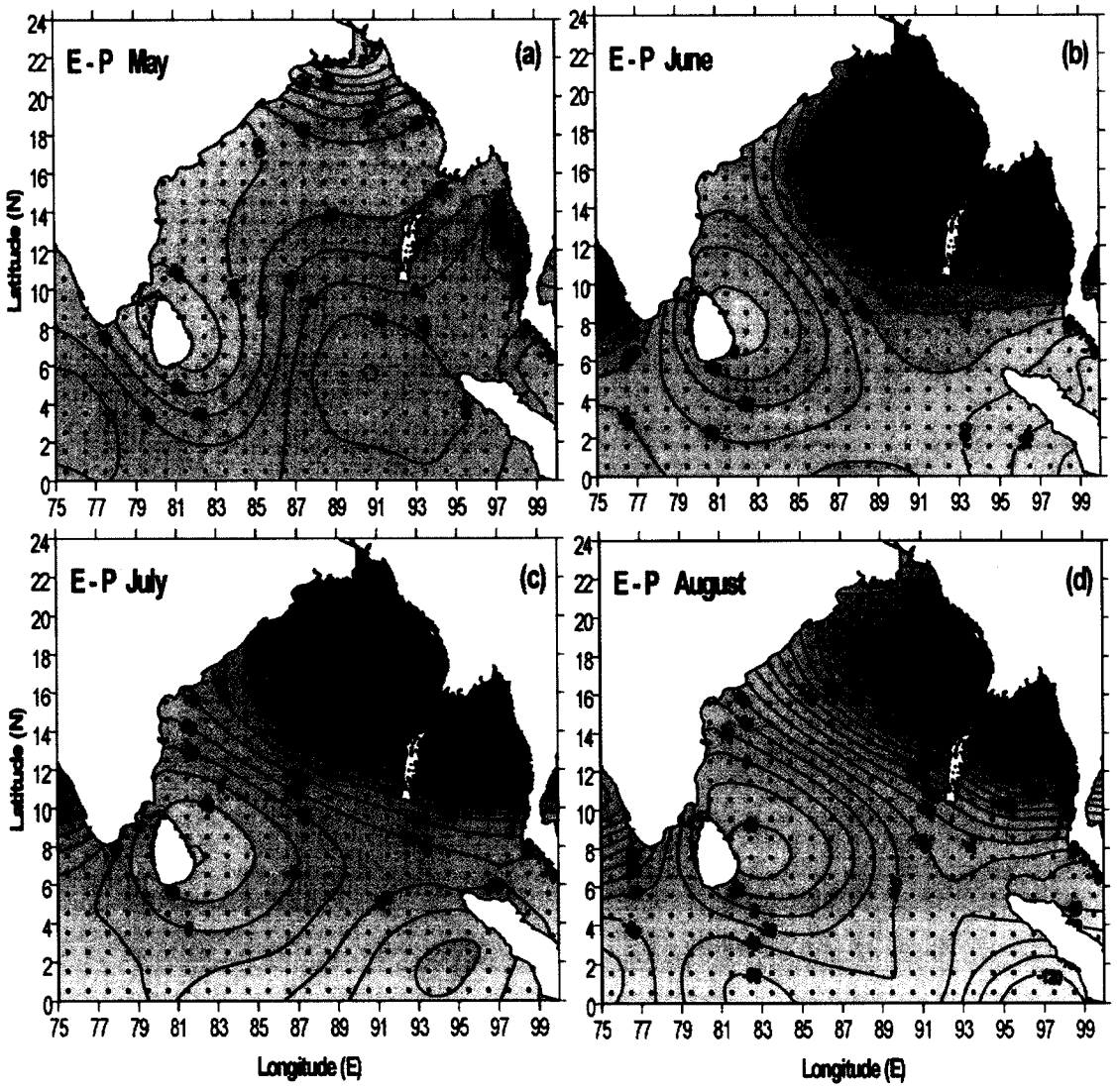

Fig.4.5.2 Monthly mean distribution of E-P (mm/month) in the Bay of Bengal during May to August.

was concentrated in a region encompassing the northwestern Bay, central Bay and the eastern boundary with the maximum value of 380 mm/month. The peninsular India showed a maximum net precipitation of 260 mm/month. The highest net evaporation around Sri Lanka was 60 mm/month. In July the pattern of E-P distribution remained similar, but the values showed an increase (Fig.4.5.2c). The highest net precipitation was 480 mm/month and was in the head Bay. The highest net evaporation around Sri Lanka showed a reduction and was 40 mm/month. During August also, the distribution pattern was similar to that of July but the net precipitation showed the maximum value of 440 mm/month in the northeastern Bay (Fig.4.5.2d). This was the highest net precipitation compared to all the months. Near the Indian Peninsula the highest net precipitation was 180 mm/month.

During September the entire Bay showed net precipitation except the region north of Sri Lanka but the values reduced drastically (Fig.4.5.3a). The highest precipitation in the northern Bay was 220 mm/month while that in the southeastern region was 280 mm/month. In October the E-P showed further reduction in their values with the entire Bay showing a net precipitation (Fig.4.5.3b). The highest net precipitation in the northern Bay was 140 mm/month near the northeastern boundary, while in the southern region it was about 220 mm/month. The region of net evaporation around Sri Lanka in September changed to net precipitation. In November, the region close to central part of both western and eastern boundary showed net evaporation while the rest of the Bay showed net precipitation (Fig.4.5.3c). The maximum precipitation was near southern Bay, which was about 180 mm/month while the maximum evaporation was about 60 mm/month. During December E-P showed net evaporation north of 12°N with highest value of 120

mm/month close to the northeastern Bay (Fig.4.5.3d). In the south the net precipitation showed an increasing trend with maximum value of 180 mm/month near equator.

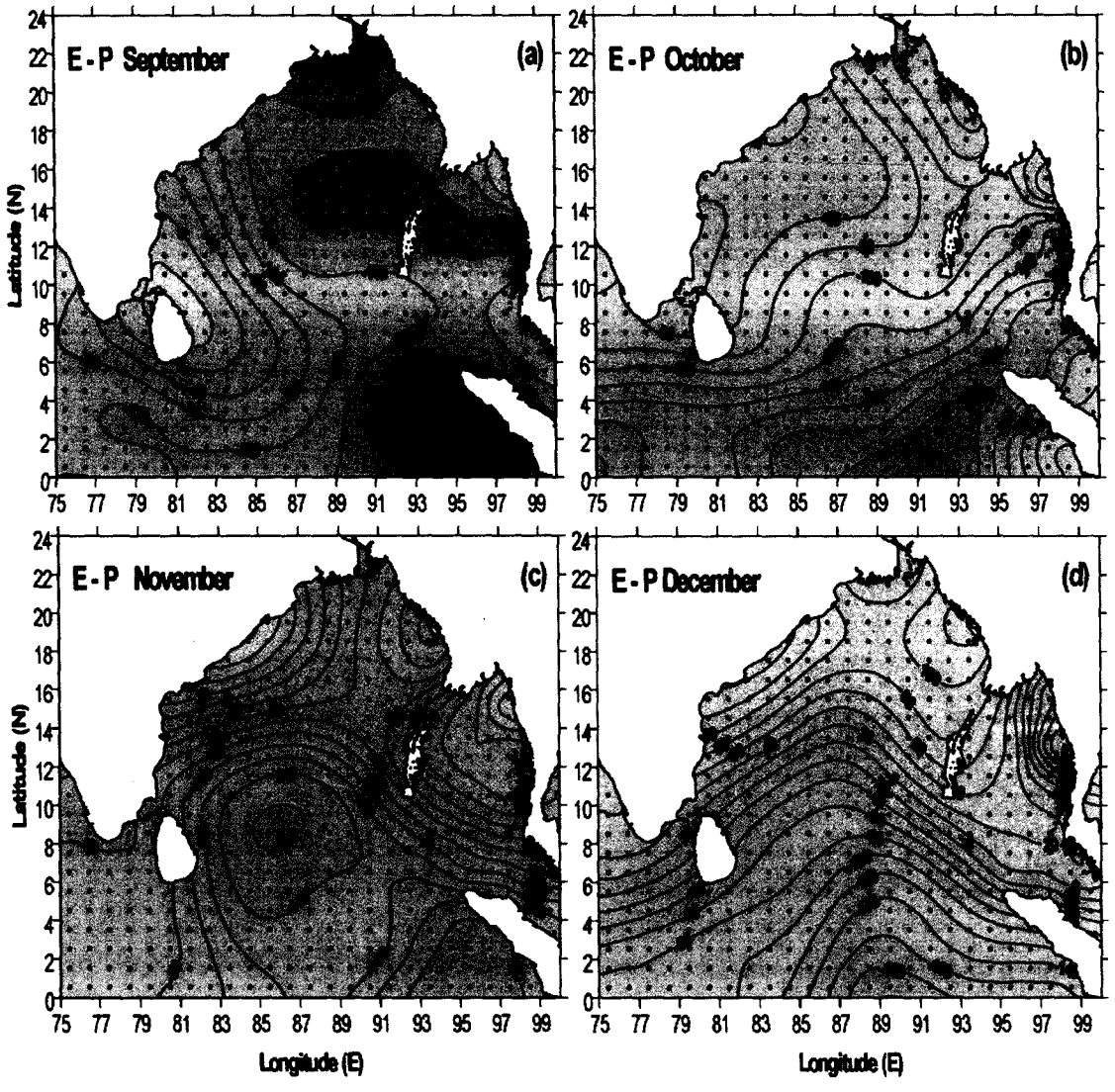

Fig.4.5.3 Monthly mean distribution of E-P (mm/month) in the Bay of Bengal during September to December.

Thus, the amplitude of the seasonal cycle of E-P within the basin was from –440 mm/month to 120 mm/month. The lowest evaporation was about 40 mm/month, which occurred during July-September while highest evaporation was about 120 mm/month

which occurred during December. The lowest precipitation occurred during May, which was about 60 mm/month while highest precipitation was about 440 mm/month which occurred during July. The highest spatial variability occurred during July when E-P varied from 40 mm/month to –440 mm/month. The least spatial variability occurred during May, when E-P varied from 80 mm/month to –60 mm/month. The seasonal cycle of evaporation minus precipitation (E-P) in the northern Bay (north of 15°N) showed annual cycle with positive E-P from December-April and negative E-P during June-September. The seasonal cycle of E-P in the southern Bay (south of 15°N) showed annual variability with net evaporation from February-May and net precipitation from June-December.

4.6 Factors controlling the mixed layer variability

In order to decipher the factors that are responsible for the observed variability in the mixed layer and barrier layer, these were examined in the light of heat flux, momentum flux (wind-stress curl) and fresh water flux (evaporation-precipitation).

4.6.1 Spring intermonsoon

The mixed layer depth during the spring intermonsoon (March-April-May) was the shallowest in the Bay of Bengal compared to the rest of the months, particularly during March and April. It varied between 10 and 25 m except in the southwestern region in March and April and near the western boundary in April (Fig.4.6.1.1a). In May, however, the shallow MLD was confined to the region north of 16°N. Another region of comparatively shallow MLD (~ 25 m) was seen in a band between 6° and 9°N (Fig.4.6.1.1c). The rest of the basin, however, showed deep MLD (30-35 m).

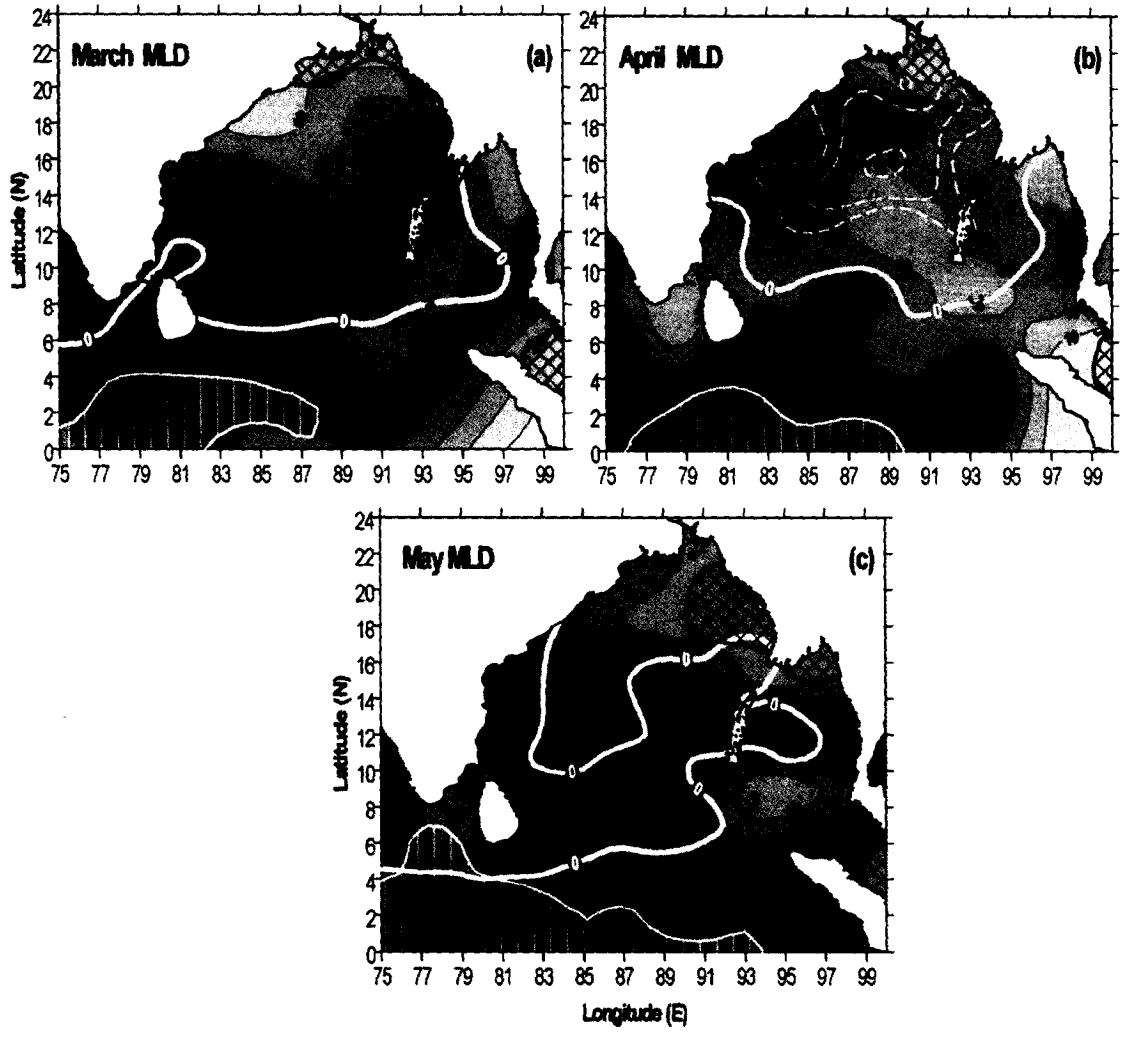

Fig.4.6.1.1 Spatial distribution of mixed layer depth in spring intermonsoon. The blue cross-hatch represents the region where salinity is less than 32 psu while vertical lines within the thin yellow solid line represent the region where the salinity is greater than 34.5 psu. The thick broad white line indicates the zero wind stress curl. The yellow broken lines in (b) indicate the negative wind stress curl (-10 to -20 x 10^{-8} Pascal/m) with increasing magnitude towards the centre.

The observed MLD variability could be understood in the light of the prevailing ocean-atmospheric conditions. The incoming solar radiation peaked during March-April with a value of 280-290 W/m^2 (Fig.4.1.1) and the net heat flux also was the highest 150-160 W/m^2 (4.2.1). The basin-wide winds were the weakest during this period (~4 – 5 m/s), except near the western boundary in April where a core of high wind speed was noticed

(Fig.4.3.1) and a strong negative wind stress curl (Fig.4.4.1). The shallow MLD in March-April was driven by the strong stratification induced by peak solar heating and subsequent highest net heat gain by the ocean. Note that the salinity in the northern Bay (north of 18°N) was less than 32.5 psu during March-April (Fig.3.2.1) which makes the waters highly stratified (Fig.4.6.1.2). The weak winds during this period were unable to drive deep wind-mixing due to strong stratification and hence led to the formation of shallow mixed layer.

In the south, the comparatively deeper mixed layer (~ 35 m) seen west of 90°E was due to the presence of high salinity waters (>34.5 psu) which made the water column less stable (Fig.4.6.1.2) and the moderate winds were able to initiate greater mixing leading to the

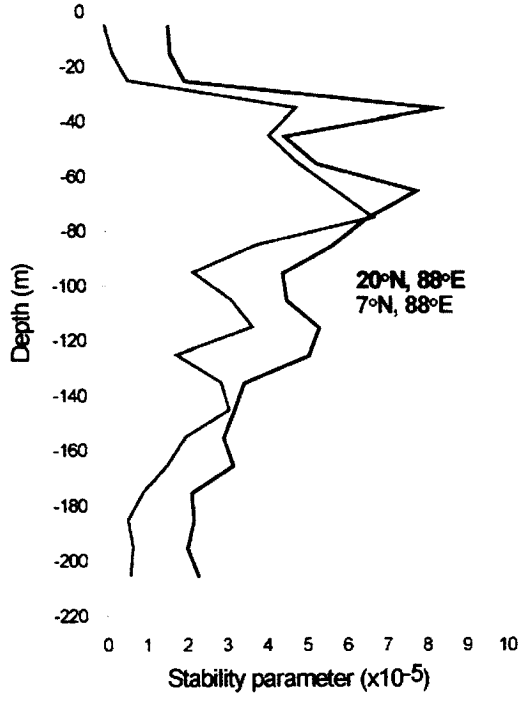

Fig.4.6.1.2 Profiles of upper ocean static stability parameter (E, m^{-1}) at 20°N, 88° E (blue line) and 7°N, 88°E (red line) in the Bay of Bengal during April.

observed deep MLD. However, the deep MLD east of Sri Lanka during March was linked to the development of anti-cyclonic circulation associated with the formation of subtropical gyre which begins in May (Fig.1.2.1). This anti-cyclonic circulation drives down-welling and deepens the mixed layer. The deep MLD along the western boundary (>25 m) in April was driven by the strong negative wind stress curl (~ -20 x 10^{-8} Pascal/m, Fig.4.4.1) as could be inferred from the location of the deep MLD and wind stress curl (Fig.4.6.1.1). Note that the subtropical gyre was well developed in April in the central and western Bay of Bengal (Fig.1.2.1), which also leads to down-welling and augments the deepening of the mixed layer. The shallow MLD in the northeastern Bay in May was due to the presence of low salinity waters (~ 32.5 psu, Fig.3.2.2) along with the high incoming solar radiation (270-280 W/m^2, Fig.4.1.2) which gives rise to strong stratification. The comparatively weaker winds (5 – 5.5 m/s) in the northeastern region were unable to drive strong wind-mixing and hence the MLD was shallow. Comparatively shallow MLD in a band between 6° and 10°N east of Sri Lanka and southern tip of India was due to the presence of positive wind stress curl in this region (Fig.4.4.2). The deep MLD in the central and western Bay was due to the presence of anti-cyclonic circulation and downwelling associated with the subtropical gyre which occupies the region between western boundary and 90°E (Fig.1.2.1). Again the deep MLD in May in the south, south of 4°N was related to the presence of high salinity waters (>34.5 psu, Fig.3.2.2) and negative wind stress curl (Fig. 4.4.2).

4.6.2 Summer monsoon

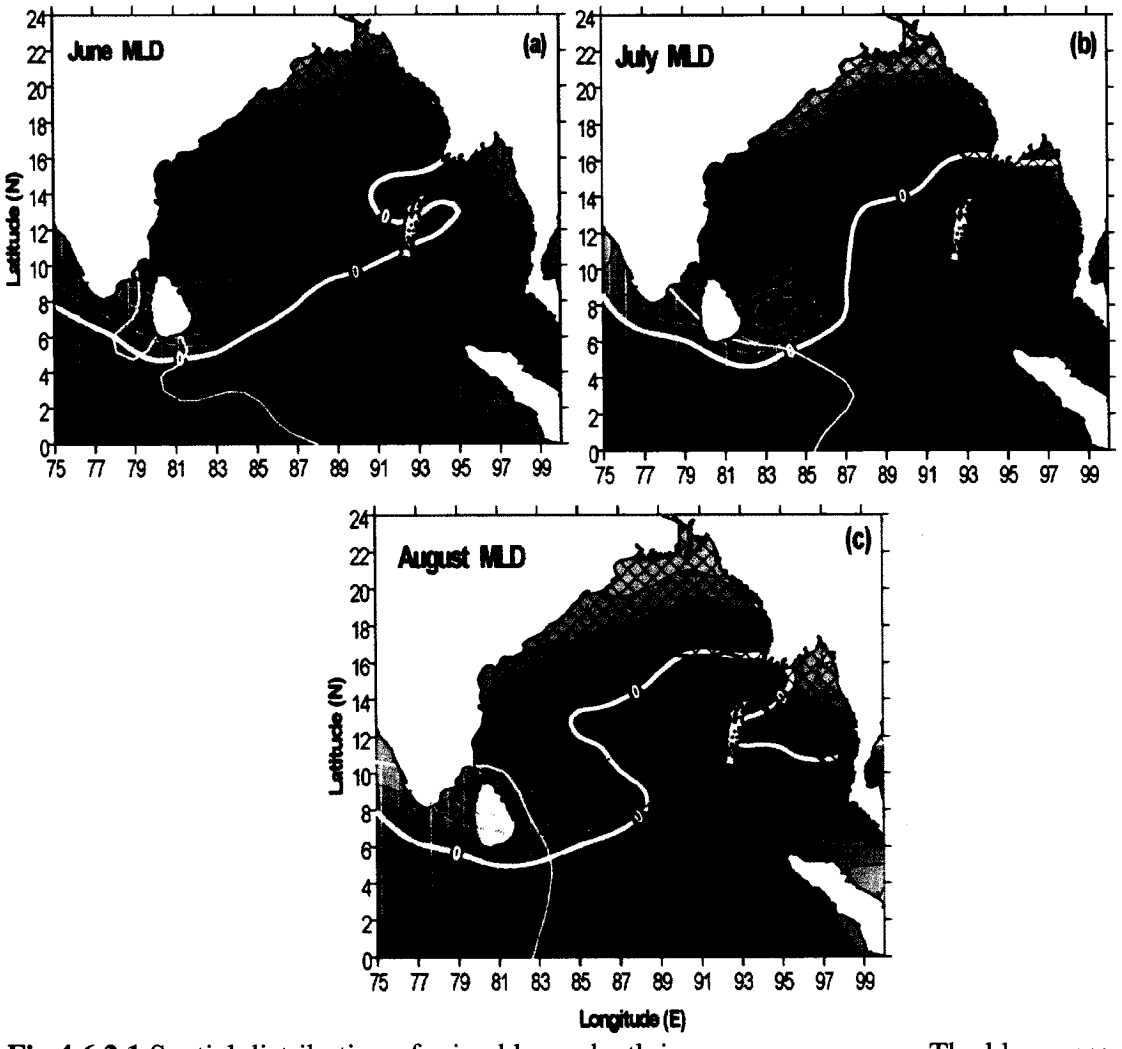

Fig.4.6.2.1 Spatial distribution of mixed layer depth in summer monsoon. The blue cross-hatch represents the region where salinity is less than 32 psu while vertical lines within the thin yellow solid line represent the region where the salinity is greater than 34.5 psu. The thick broad white line indicates the zero wind stress curl. The yellow broken lines in indicate the positive wind stress curl (5 to 20 x 10^{-8} Pascal/m) with increasing magnitude towards the centre.

Mixed layer during summer monsoon was deep in a band between equator and 6°N (Fig.4.6.2.1), which joined the deep MLD region seen closer to the western boundary towards the end of spring intermonsoon. The northern and eastern part of the Bay had shallow MLD (Fig. 4.6.2.1). With the progress of summer monsoon, the region of deep

MLD expands towards the central and northern Bay. The region around Sri Lanka showed a progressively shallow mixed layer which expanded eastward with time, during summer monsoon. The observed pattern of MLD variation could be explained in the following manner. Though the wind speeds were the highest during summer monsoon in the entire basin (Fig.4.3.2), the MLD were the shallowest in the northern Bay (~ 5m). An examination of E-P showed that it was negative and the highest of all the season, implying excess precipitation, in excess of 440 mm/month, in the northern Bay (Fig.4.5.2). In addition to the oceanic precipitation, the influx of freshwaters from the rivers adjoing the Bay of Bengal also contributed towards freshening of the surface waters of the Bay. An examination of the monthly mean climatology of river discharge of 5 major rivers Ganges, Brahmaputra, Irrawady, Godavari, and Krishna showed that the freshwater discharge dominated during July to October (Fig.4.6.2.2). The spreading of low salinity waters (<32 psu) were seen from the northern Bay towards the south and east (Fig.4.6.2.1) with the progress of summer monsoon. These low salinity waters strongly stratified the upper ocean as could be inferred from the stability parameter (Fig.4.6.2.3). Note that the upper ocean was very warm with SST in excess of 28.5°C (Fig.3.1.2) which also contributed towards strengthening the stratification. Hence, the winds though were the strongest of all the season, it was unable to break the stratification to initiate wind-driven mixing and deepen the mixed layer. The shallow MLD seen around Sri Lanka, irrespective of the low E-P implying excess evaporation (Fig.4.5.2), was driven by the positive wind stress curl (Fig.4.6.2.1). The positive wind stress curl was seen developing in May (Fig.4.4.2) which peaks in June (Fig.4.4.2) and collapses by September (Fig.4.4.3). The positive wind stress curl drives an upward Ekman pumping and this led

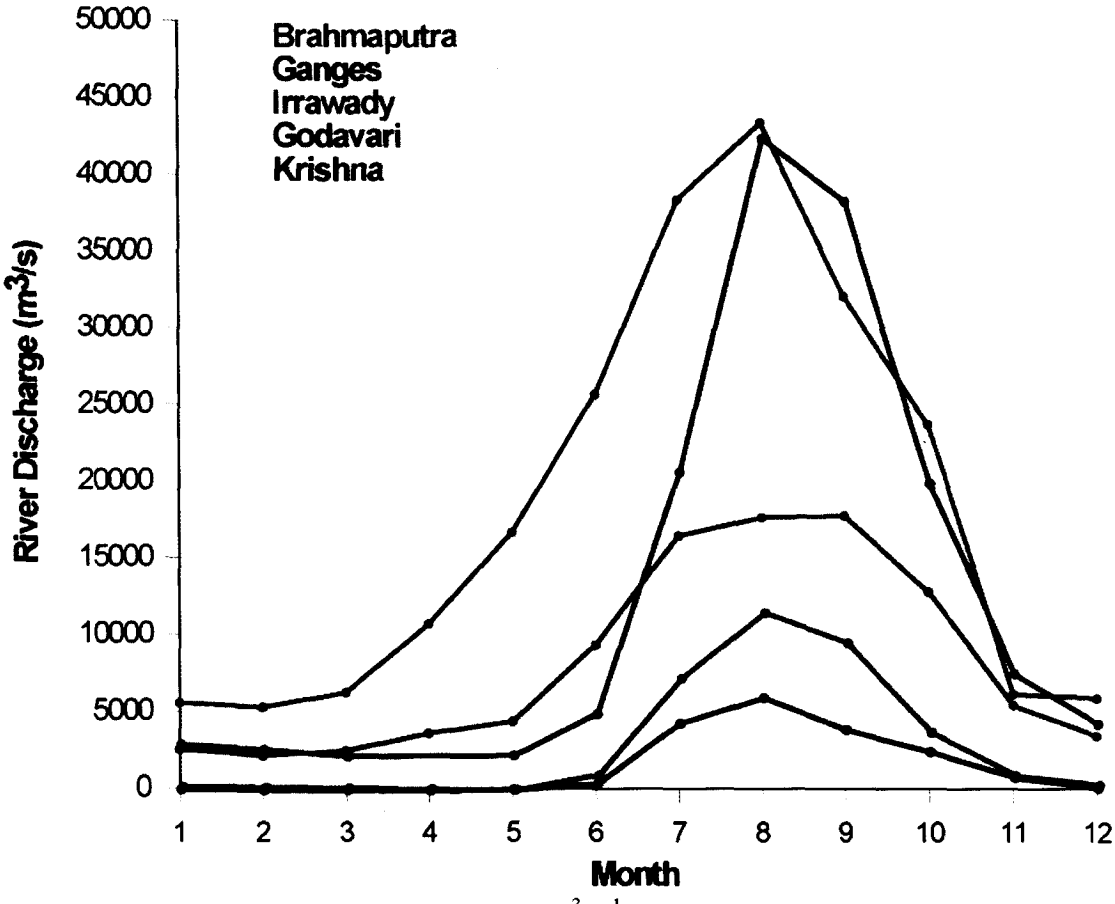

Fig.4.6.2.2 Monthly mean river discharge (m^3 s^{-1}) climatology of Ganges, Brahmaputra Irrawady, Godavari and Krishna

to the observed shallow mixed layer during summer monsoon. The band of deep mixed layer seen extending from the southwestern region into the central Bay was linked to the advection of high salinity waters from the Arabian Sea. An examination of SSS showed that the high salinity waters from the Arabian Sea was progressively advecting into the central Bay around Sri Lanka during summer monsoon (Fig.3.2.3). This high salinity waters reduced the stratification of the upper ocean as could be inferred from the stability parameter (Fig. 4.6.2.3). Thus, the high winds of the summer monsoon combined with

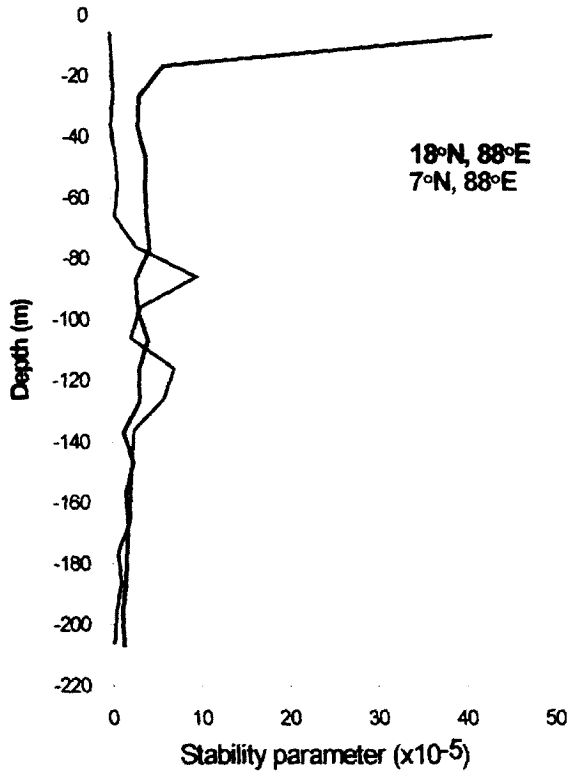

Fig.4.6.2.3 Profiles of upper ocean static stability parameter (E, m^{-1}) at 18°N, 88° E (blue line) and 7°N, 88°E (red line) in the Bay of Bengal during July.

the less stratified upper ocean due to the intrusion of high salinity waters from the Arabian Sea were able to drive strong wind-driven mixing. This was the mechanism which led to the formation of deep MLD in summer. In addition to this, the negative wind stress curl in the central and western Bay also contributed to the observed deep MLD there.

4.6.3 Fall intermonsoon

As the summer monsson tapers off and the fall intermonsoon sets in, the shallow MLD which was confined to northern Bay, north of 18°N, was seen extending southward to 15°N in October (Fig.4.6.3.1). This could be explained in the context of changing

atmospheric forcing from summer monsoon to fall intermonsoon. The short wave

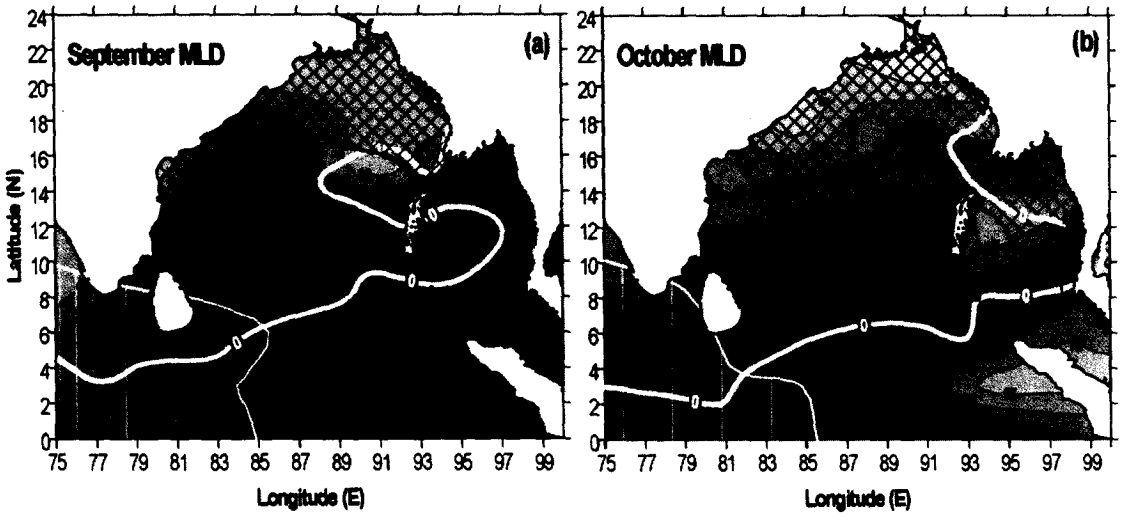

Fig.4.6.3.1 Spatial distribution of mixed layer depth in fall intermonsoon. The blue cross-hatch represents the region where salinity is less than 32 psu while vertical lines within the thin yellow solid line represent the region where the salinity is greater than 34.5 psu. The thick broad white line indicates the zero wind stress curl.

radiation as well as net heat flux showed a secondary heating of the upper ocean during fall intermonsoon (Fig.4.1.3 & Fig.4.2.3) and accordingly the SST was in excess of 29°C in October (Fig. 3.1.3). Though the E-P showed a rapidly decreasing precipitation (Fig.4.5.3), the surface salinity showed a progressive decrease from that of summer monsoon and also a further southward extension of the low salinity waters (Fig.3.2.3). This indicated that the shallow MLD in the northern Bay and its further southward extension was linked to the presence of low salinity waters and its advection southward. As seen from the data, the river discharge was dominant during July to October (4.6.2.2) and hence the low salinity of the surface water was the manifestation of the influence. With the fall intermonsoon the winds over the Bay showed a drastic reduction in their speed in the north (Fig.4.3.3). The high wind speed was confined to the southern Bay. Thus, the deep MLD in the southern Bay was driven by a combination of comparatively

high wind speed and the presence of high salinity waters (Fig.3.2.3) both of which destabilized the water column.

4.6.4 Winter monsoon

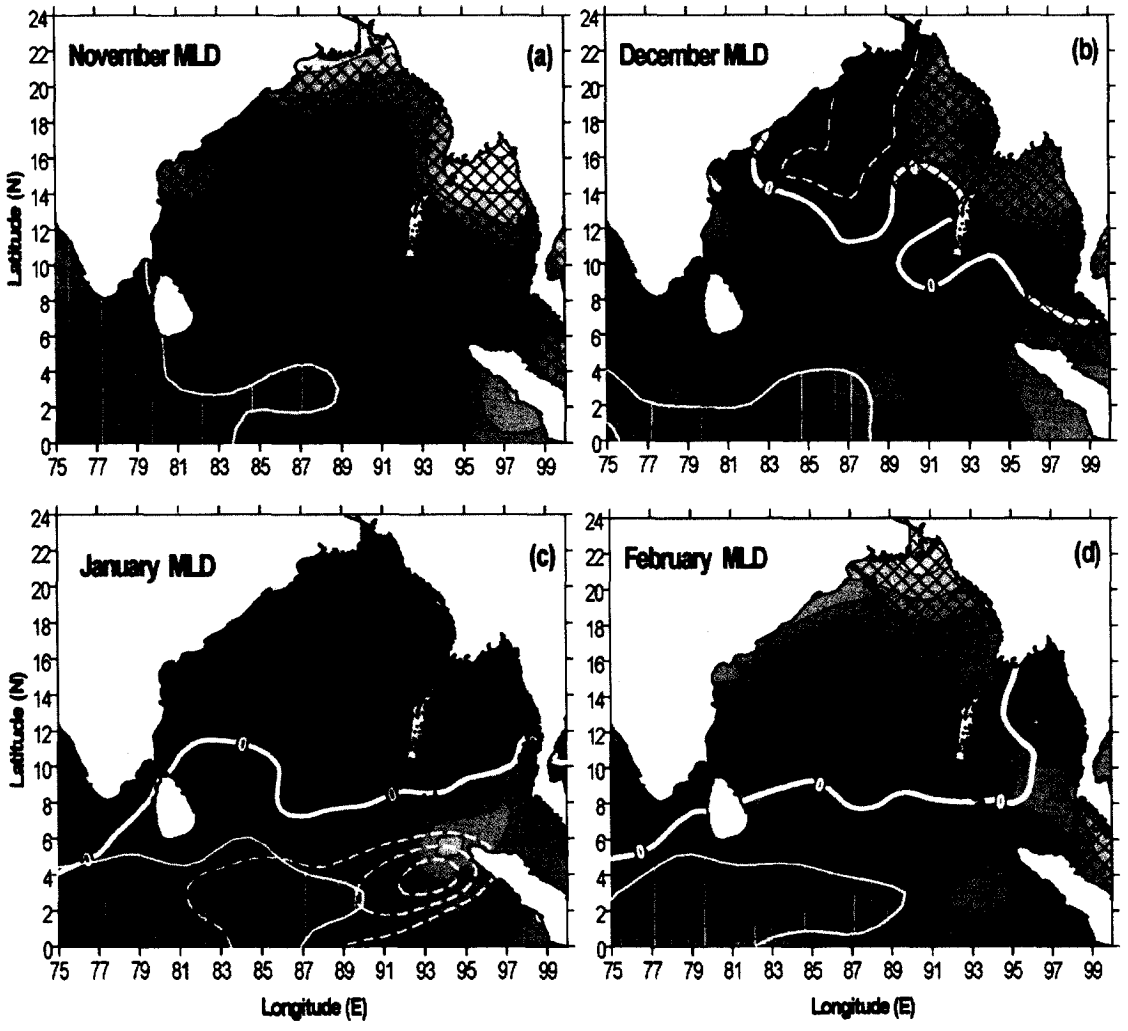

Fig.4.6.4.1 Spatial distribution of mixed layer depth in winter monsoon. The blue cross-hatch represents the region where salinity is less than 32 psu while vertical lines within the thin yellow solid line represent the region where the salinity is greater than 34.5 psu. The thick broad white line indicates the zero wind stress curl. The yellow broken lines in (b) indicate the negative wind stress curl (-5 x 10^{-8} Pascal/m) while that in (c) indicates the positive wind stress curl (10 to 20 x 10^{-8} Pascal/m) with increasing magnitude towards the centre.

The winter monsoon in general showed comparatively deep MLD (~30-40 m) all over the Bay except in the north and eastern Bay (Fig.4.6.4.1). The shallow MLD (~5-15 m) in the north and eastern Bay could be explained in the context of the presence of low salinity waters (<32 psu) during November-December (Fig.3.2.3) and associated strong stratification. As the winter progress with E-P showing a net evaporation (Fig.4.5.3) and

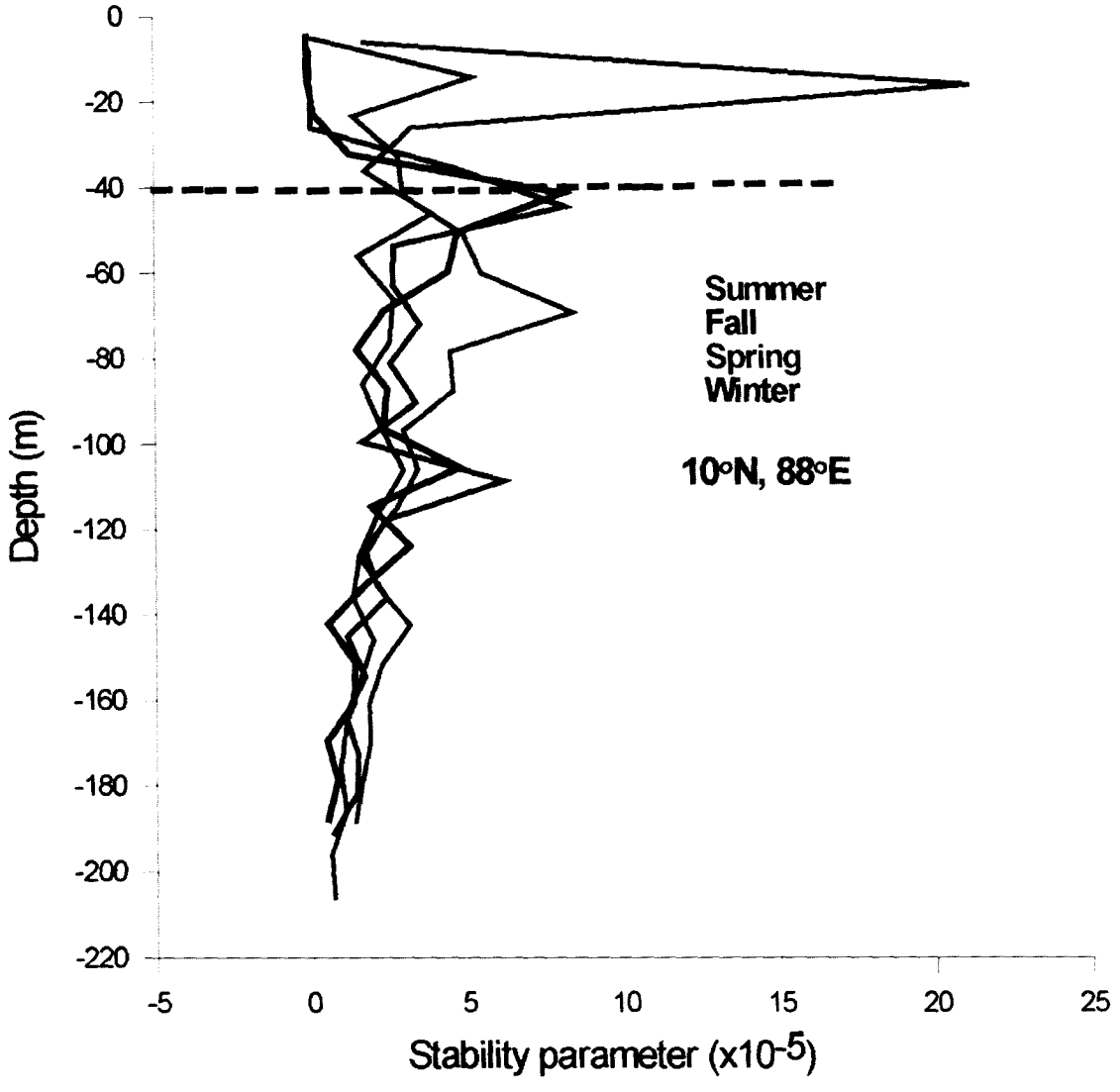

Fig.4.6.4.2 Profiles of upper ocean static stability parameter (E, m^{-1}) at 10°N, 88° E during summer monsoon (red), fall intermonsoon (blue), winter monsoon (green) and spring intermonsoon (pink) in the Bay of Bengal.

retreat to the northern part during January-February (Fig.3.2.1). As a result the area of deeper mixed layer expands further towards eastern boundary. The shallow MLD observed near the Sumatra coast in January was driven by the strengthened positive wind stress curl (Fig.4.4.1) and the associated upward Ekman pumping. The deep MLD in the rest of the Bay was related to the weak stratification that occurred in the Bay during winter monsoon compared to all other seasons, except fall intermonsoon in the upper 40 m (Fig.4.6.4.2). The wind speed, which showed a secondary peak in winter (Fig.4.3.3) were able to initiate deeper wind-mixing as the stratification of the water column was the weakest and this gave rise to the deep mixed layer.

4.6.5 Role of Rossby waves

In order to understand the role of Rossbay waves in regulating the MLD the time-longitude plots of sea-level anomaly along latitudes 4°and 16°N were analyzed. For this purpose the sea-level anomaly for the period 1992 to 2006 were used to compute the monthly mean climatology.

The time-longitude plot along 4°N showed bands of alternate positive and negative sea-level anomaly (Fig.4.6.5.1a). These are the signature of westward propagating Rossby waves with positive sea-level anomaly during summer and negative during winter. In summer the central and eastern region showed the highest positive sea-level height anomaly (Fig.4.6.5.1a) and this again contributed to the observed deep MLD in the southern Bay in addition to the reduction in stratification due to the intrusion of high salinity waters from the Arabian Sea.

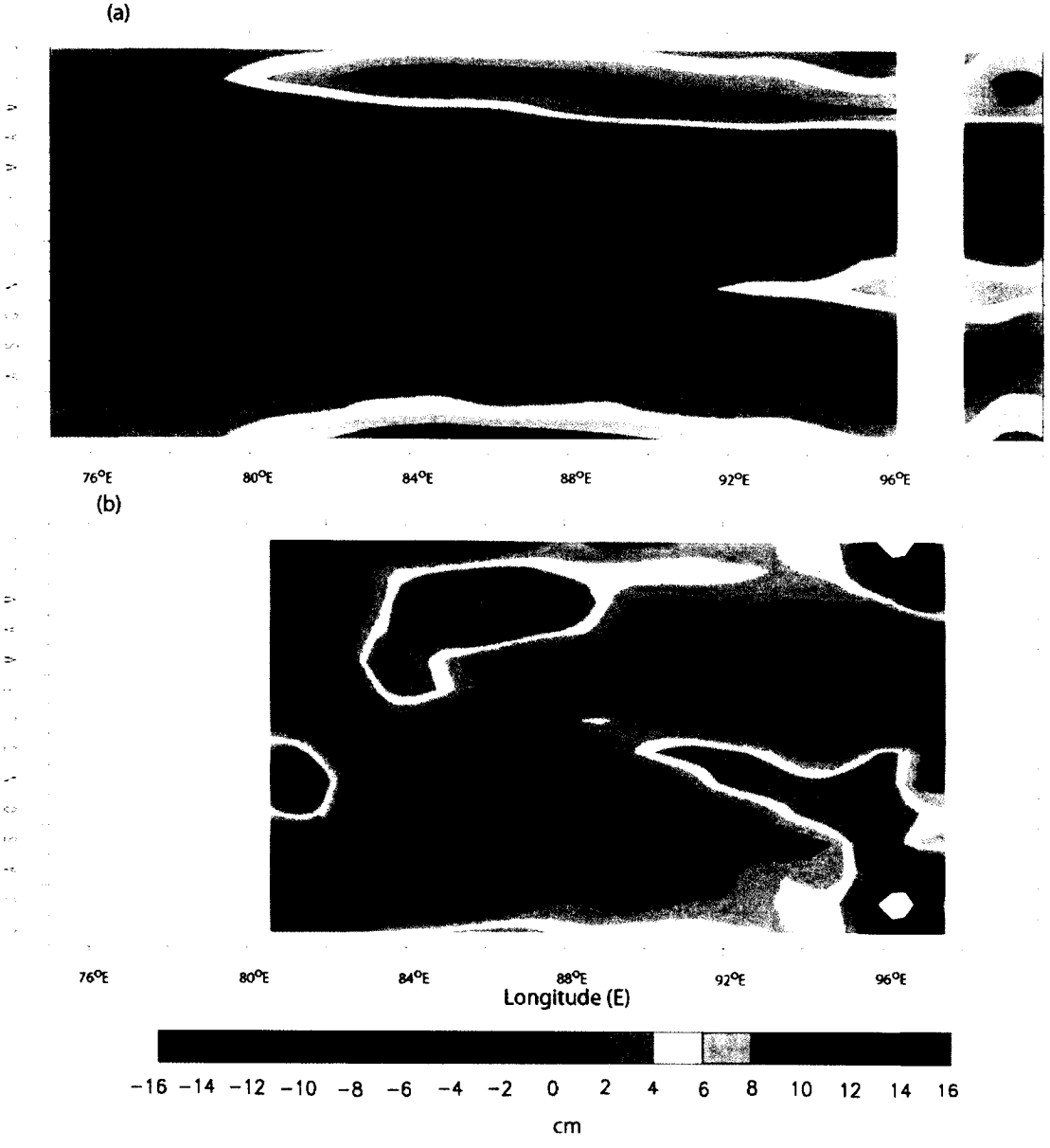

Fig.4.6.5.1 Time-longitude plot of monthly mean sea-level anomaly climatology derived from merged sea-level anomalies of Topex/Poseidon and ERS 1/2 satellites along (a) 4°N and (b)16°N.

The sloping contours in Fig.4.6.5.1b indicated the signatures of the westward propagating Rossby waves. Close to the eastern boundary the SSH anomaly was negative only during January to April while the rest of the time it was positive. The negative SSH anomaly indicated a shallow MLD, while positive anomaly indicated deep MLD. A patch of

positive SSH anomaly close to the western boundary towards the end of January indicated the development of the western boundary current which peaks in March-April. The region of positive SSH anomaly between western boundary and 90°E was associated with the subtropical gyre, which was the region of deep MLD.

4.7 Factors controlling the barrier layer thickness

The seasonal variability in the barrier layer thickness (BLT) was examined in the context of fresh water flux (E-P) and sea surface salinity (SSS) variability in order to decipher the factors that are responsible for the observed variability.

4.7.1 Spring intermonsoon

The basin-wide barrier layer (BL) thickness was the least in spring intermonsoon (March-April-May) compared to the rest of the seasons (Fig.4.7.1.1). This is due to the lack of freshwater from the river discharge as well as the precipitation during this season. As the occurrence of BL is closely linked to the freshwater flux and salinity distribution, the spatial variation of the barrier layer in the Bay could be understood in the context of freshwater flux, salinity distribution, wind stress curl and prevailing circulation. In March the comparatively thick BL in the northwestern Bay was seen within the region of negative wind stress curl (Fig.4.4.1). In addition, the northern part of the BL was within the low salinity region (<32.5 psu). During March the subtropical gyre with cyclonic circulation develops in the western and central Bay. The observed thick BL was driven by the negative wind stress curl and the prevailing cyclonic circulation. In May the co-location of thick BL in the equatorial regions with that of stronger negative wind stress

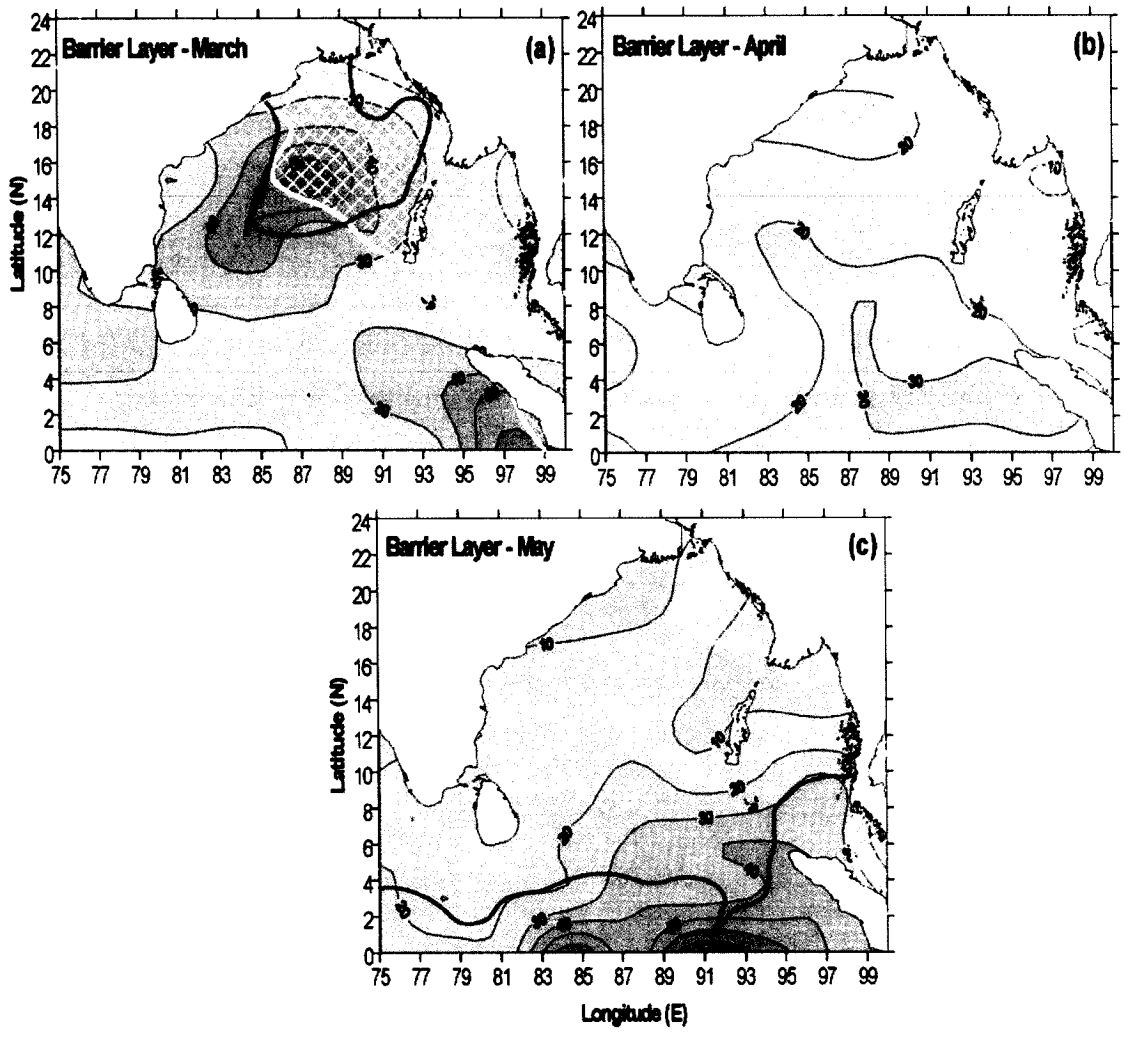

Fig.4.7.1.1 Barrier layer thickness overlaid with salinity less than 32.5 psu (white cross hatch) and negative wind stress curl (5 x 10^{-8} Pascal/m, solid blue line) during spring intermonsoon.

curl (5-10 x 10^{-8} Pascal/m) implied the role of wind. Thus, the basin-wide thin BL thickness in the spring intermonsoon was controlled by the strong stratification due to the peak heating and the lack of freshwater input either by the river discharge or through precipitation. The comparatively thick BL in the northwestern Bay was linked to the negative wind stress curl and proximity to the low salinity ambient waters, while that

near the equatorial region was controlled by the negative wind stress curl. The spring-time Wyrtki jet during April-May (Fig.1.2.1) also contributes to the deepening of BL.

4.7.2 Summer monsoon

During summer monsoon (June-July-August) thick BL was noticed along the equatorial region and the eastern boundary of the Bay (Fig.4.7.2.1). The thickest BL occurred near

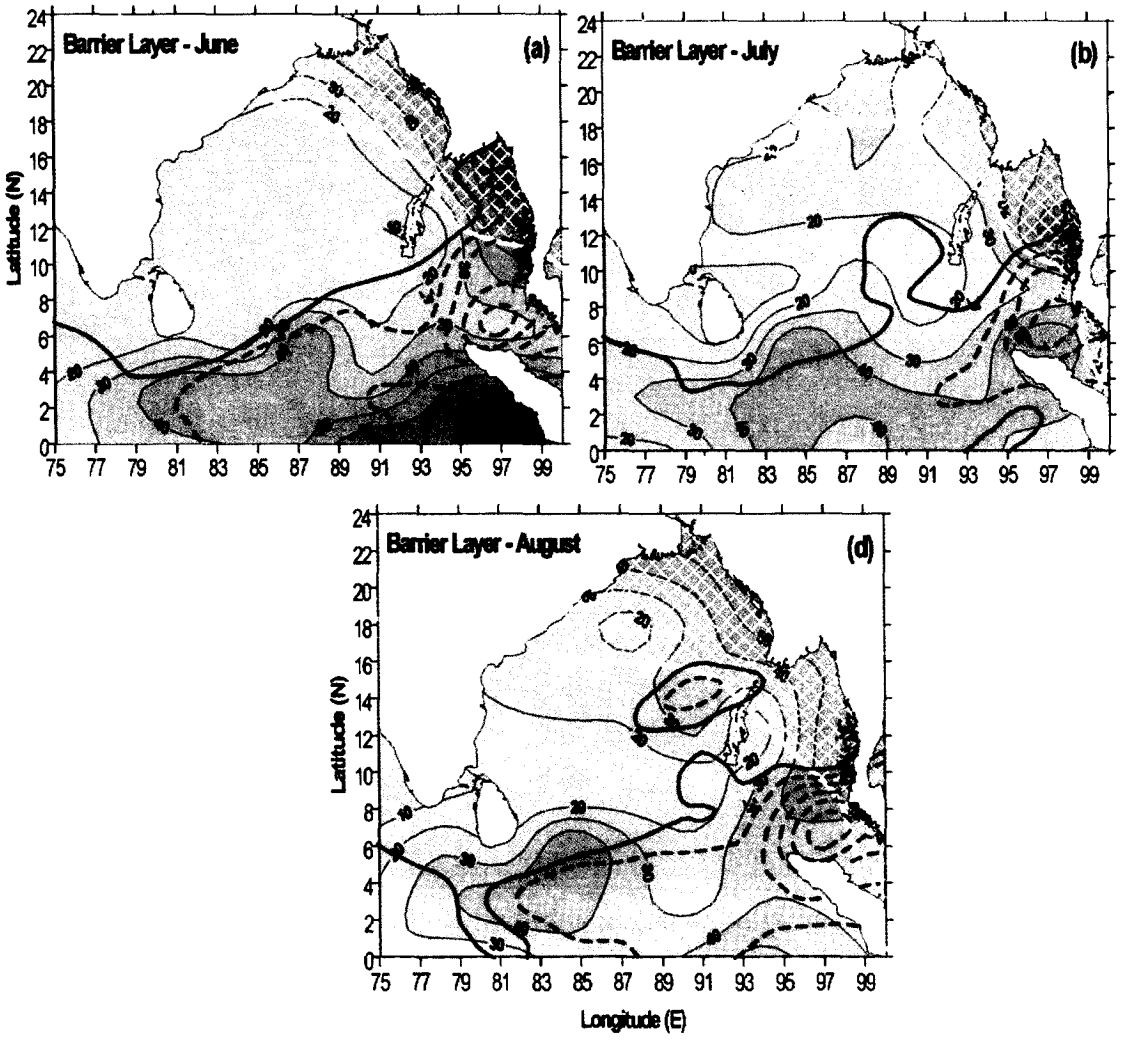

Fig.4.7.2.1 Barrier layer thickness overlaid with salinity less than 32.5 psu (white cross hatch) and negative wind stress curl (solid blue line indicates 5 x 10^{-8} Pascal/m, and broken blue line indicates values from 10 to 25 x 10^{-8} Pascal/m) during summer monsoon.

the equatorial region where the negative wind stress curl as well as negative E-P occurred. The negative wind stress curl was the highest in June (> 20 x 10^{-8} Pascal/m, Fig.4.4.2) near the equatorial region, especially in the eastern region, and showed a decrease in July and August. Accordingly, BL also showed highest thickness in June, followed by July and August. Along the eastern boundary the region of thick BL was located in the region of high precipitation (Fig.4.5.2) and low salinity (Fig.3.2.2) which indicated the role of freshwater flux. In addition, along the southern part of the eastern boundary strong negative wind stress curl occurred. Thus, during summer the thick BL near the equatorial region was driven by wind stress curl, while that along the eastern boundary was due to a combination of large negative wind stress curl as well as the excess precipitation.

4.7.3 Fall intermonsoon

With the tapering of summer monsoon and beginning of fall intermonsoon the BL thickness showed an increase in the eastern equatorial region (Fig.4.7.3.1) which was located within the negative wind stress curl region (Fig.4.4.3). This also was the region of negative fresh water flux (Fig.4.5.3) indicating the contribution of precipitation in the thickness of the BL. In the north, the thick BL was within the region of low salinity (Fig.4.7.3.1). In September the northern Bay in addition to having low salinity also showed excess precipitation. The thick BL in the equatorial region in October was not driven by the negative wind stress curl but by the eastward moving Wyrtki jet (Fig.1.2.1). Note that the fresh water flux was negative in the equatorial region in October (Fig.4.5.3) and the eastward moving Wyrtki jet drives a downwelling.

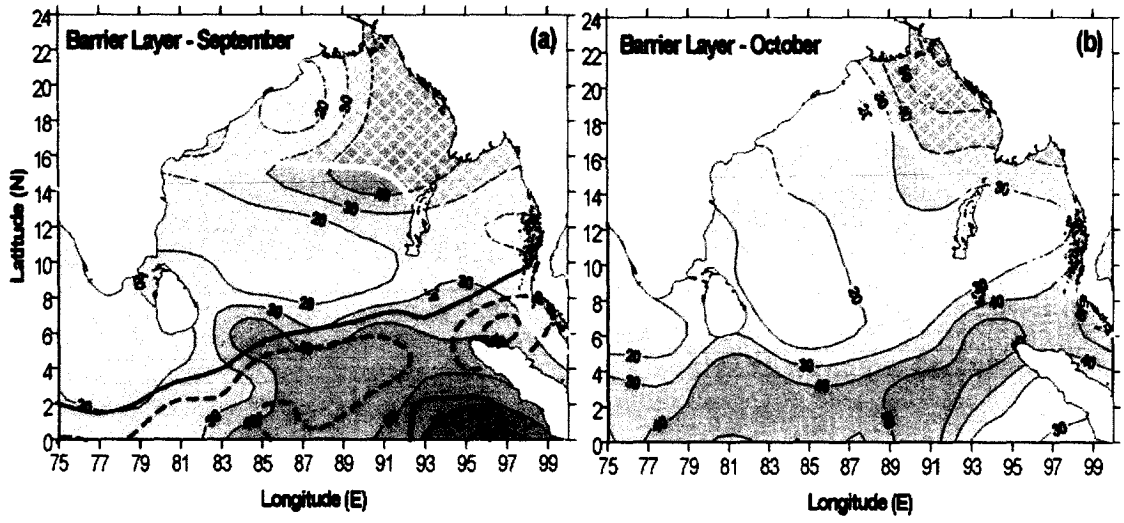

Fig.4.7.3.1 Barrier layer thickness overlaid with salinity less than 32.5 psu (white cross hatch) and negative wind stress curl (solid blue line indicates 5 x 10^{-8} Pascal/m, and broken blue line indicates values from 10 to 20 x 10^{-8} Pascal/m) during fall intermonsoon.

4.7.4 Winter monsoon

During winter thick BL was seen along the equator as well as along the eastern and western boundary of the Bay, while the rest of the basin showed comparatively thin BL (Fig.4.7.4.1). Along the equator the BL thickness in November was ~ 40 m which increased during December-January and in February BL thickness reduced considerably in the equatorial region. This could be understood in the context of freshwater flux and prevailing circulation. The fall-time Wyrtki jet flows from west to east was present during November also (Fig.1.2.1). The freshwater flux showed excess precipitation near the equatorial region which peaked during December-January (Fig.4.5.3 & Fig.4.5.1). Thus, the eastward flowing Wyrtki jet will cause down-welling and sinking of surface water which was fresher in winter and gives rise to the observed thick BL along the equatorial region. The thick BL seen in the northeastern and northern region in November

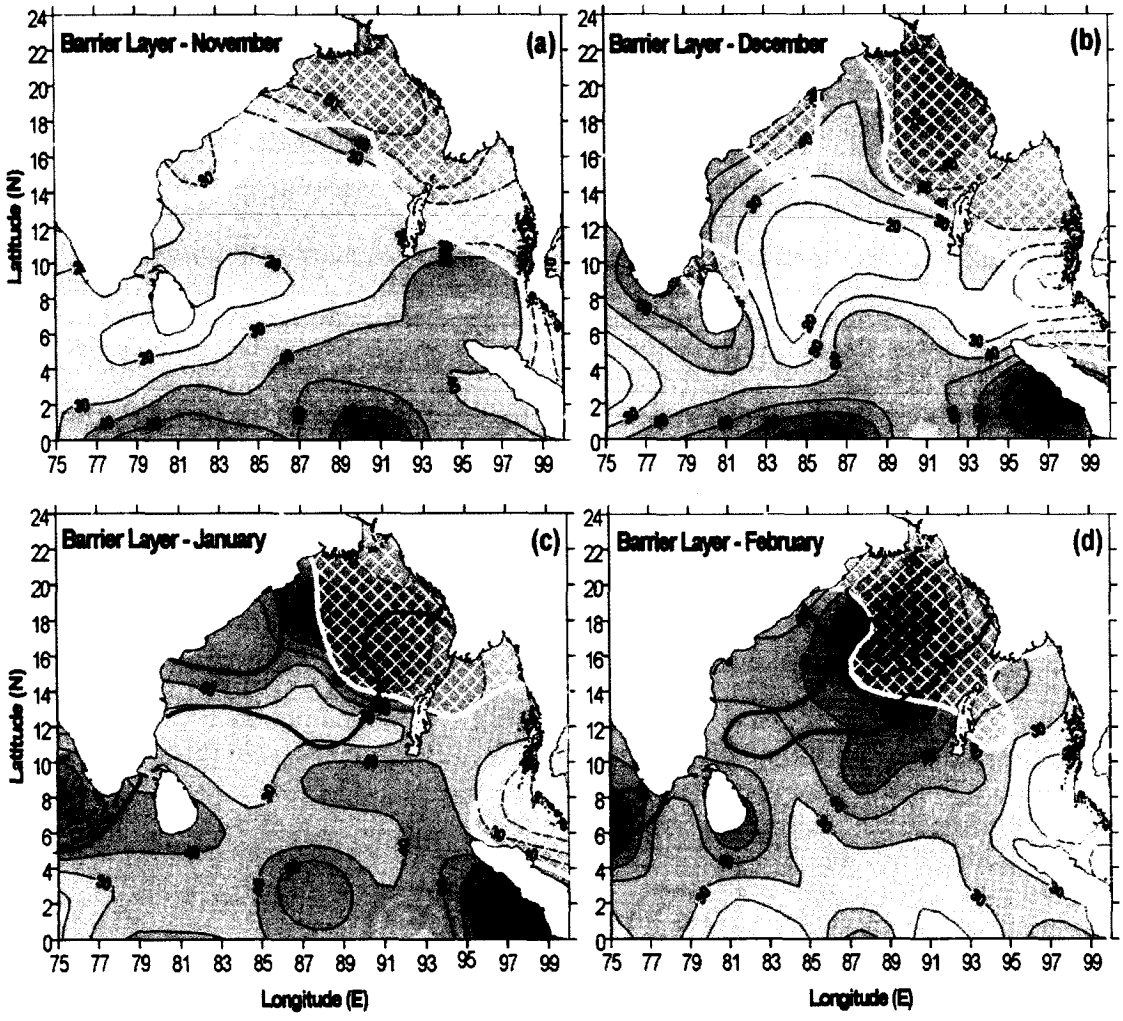

Fig.4.7.4.1 Barrier layer thickness overlaid with salinity less than 32.5 psu (white cross hatch) and negative wind stress curl (solid blue line indicates 5 x 10^{-8} Pascal/m, and broken blue line indicates values from 10 to 20 x 10^{-8} Pascal/m) during winter monsoon.

showed a gradual spreading along the western boundary of the Bay during December-January and in February the region of thick BL occupied the northern and central Bay. Note that the region of thick BL occurred within low salinity (< 32.5 psu) region (Fig.4.7.4.1) and the southward spreading of thick BL was associated with the development of East India Coastal Current (EICC). During the mature phase of EICC in December-January it flows southward along the western Bay carrying with it the low

salinity waters from the northern Bay. Thus, the observed spreading of thick BL from the northern-northeastern Bay towards the south along the western boundary and into the west coast of India was driven by the EICC.

Chapter 5 – Eddies and mixed layer variability

In the previous chapter the basin-scale variability of the mixed layer and barrier layer were analyzed in the context of large-scale atmospheric forcing and remote forcing. In addition to these large-scale forcing, mixed layer can also be influenced by the meso-scale features such as eddies, both cyclonic (cold-core) and anti-cyclonic (warm-core). To decipher the role of meso-scale eddies in affecting the mixed layer variability, the high resolution *in situ* CTD (Conductivity-Temperature-Depth) data collected during four different seasons, spring intermonsoon, summer monsoon, fall intermonsoon and winter monsoon, along the central Bay (88°E) and western boundary were analyzed and presented in this chapter.

5.1 Spring intermonsoon (12 April to 7 May, 2003)

During the spring intermonsoon MLD along the central Bay was, in general, shallow specially in the south (Fig.5.1.1a). The MLD was about 32 m at 7°N, increased to 42 m at 8°N, and then decreased rapidly to 15 m at 9°N. From 9° to 14°N MLD remained at 15m. North of 14°N MLD showed an increasing trend up to 17°N and again a decrease was seen north of 17°N. The vertical distribution of temperature showed oscillation of isotherms, especially within the thermocline, all along the section. Two regions with large thermocline oscillations were noticed, one between 17° and 18°N and the other centered at 19°N. At 18°N the isotherms showed a large deepening, while that at 19°N showed a steep shoaling. Along the western boundary MLD varied from 35 at 12°N to 45 m at 15°N and north of 15°N it showed a decreasing trend reaching a minimum value of

15 m at 18°N. North of 18°N mixed layer showed a deepening trend (Fig.5.1.1b). The vertical thermal structure along the western boundary also showed thermocline oscillations and the most prominent one was centered between 17° and 18°N.

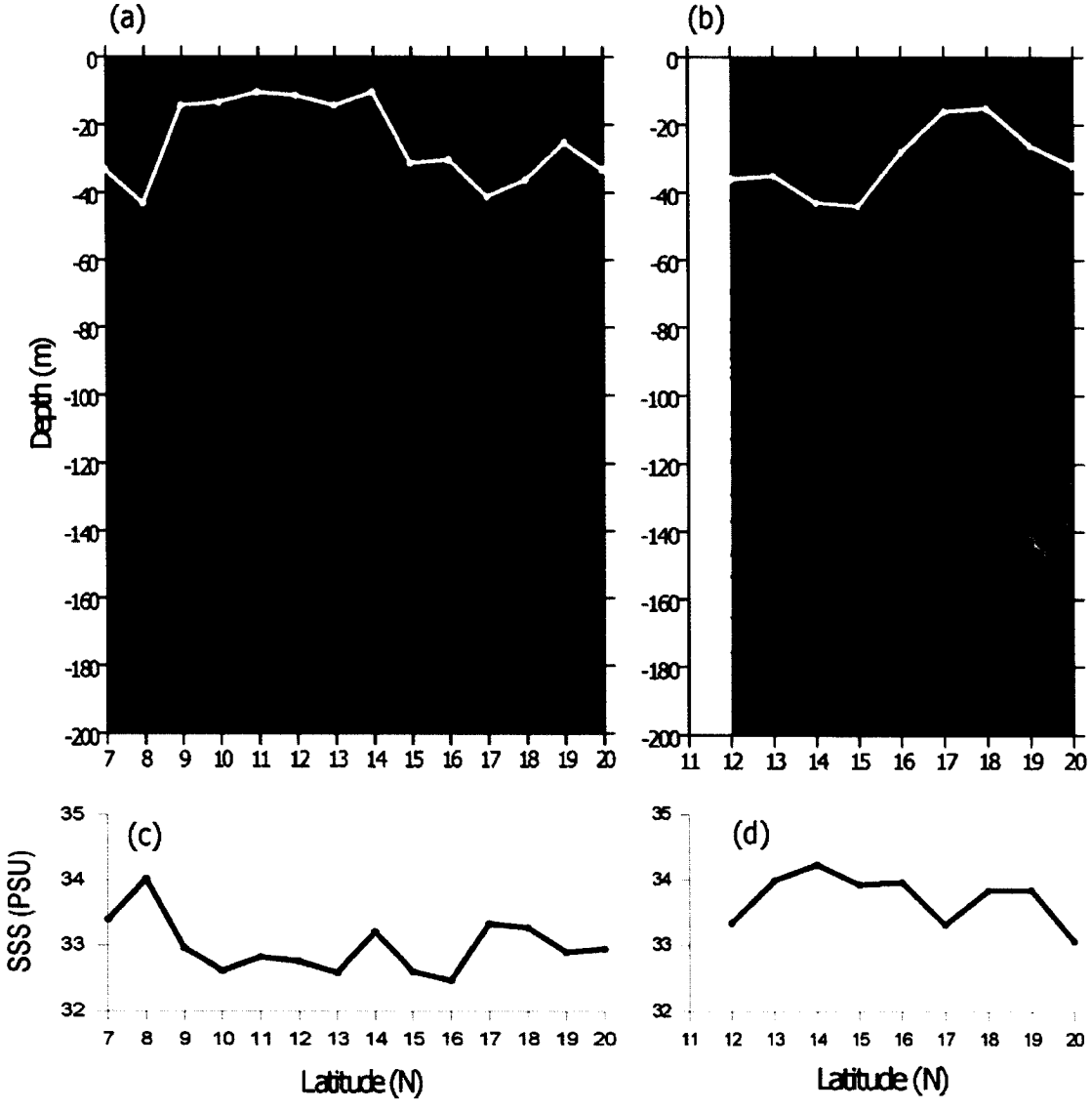

Fig.5.1.1 Vertical distribution of temperature (°C) in the upper 200 m along the (a) central Bay of Bengal (88°E) and (b) western boundary during spring intermonsoon (12 April-7 May 2003). The white line indicates the MLD (m). Distribution of surface salinity (psu) along the (c) central Bay and (d) western boundary during the same period.

Along the central Bay, the shallow mixed layer in the south between 9° and 15°N was due to the presence of low salinity water of about 32.5 psu (Fig. 5.1.1c) along with the increased solar radiation in spring intermonsoon which peaked in April as could be seen from Fig.4.1.1d. Accordingly, the net heat gain by the ocean was the highest in April (see Fig.4.2.1d), which was located between 10° and 15°N. Note that the SST in the south (30°C) was about 1°C warmer than that of the north (29°C, Fig.5.1.1a). The low salinity surface waters as well as the peak heating made the water column highly stratified. The weak winds during this period were unable to break the stratification to initiate strong wind-driven mixing and hence the MLD remained shallow. In the north the deep mixed layer at 17°N was driven by the presence of warm core eddy (positive sea-level anomaly) as inferred from the sea-level anomaly (Fig.5.1.2a) as well as depression in the thermal structure between 17° and 18°N (Fig.5.1.1a). The warm core eddy drives an anti-cyclonic circulation and the associated downwelling deepens the MLD. Similarly, the shallow MLD at 19°N was the result of cyclonic eddy (negative sea-level anomaly) inferred from the sea-level anomaly (Fig.5.1.2a) as well as the shoaling in the thermal structure between 18° and 20°N (Fig.5.1.1a). The cold core eddy drives the cyclonic circulation and the associated upwelling shallows the MLD.

Along the western boundary also the SST in the southern part was warmer than the north and surface salinity varied from 33 to 34 psu (Fig.5.1.1d). The warm SST and comparatively low surface salinity should increase the stratification of the upper ocean and this in turn should lead to shallow mixed layer. However, in the southern part of the western boundary the CTD stations at 14° and 15°N were at the periphery of the warm core eddy (positive sea-level anomaly) as inferred from sea-level anomaly (Fig.5.1.2b),

while the stations at 17° and 18°N were within the cold core (negative sea-level anomaly) eddy. Thus, the observed deep and shallow MLD along the western boundary was associated with the prevailing meso-scale eddies.

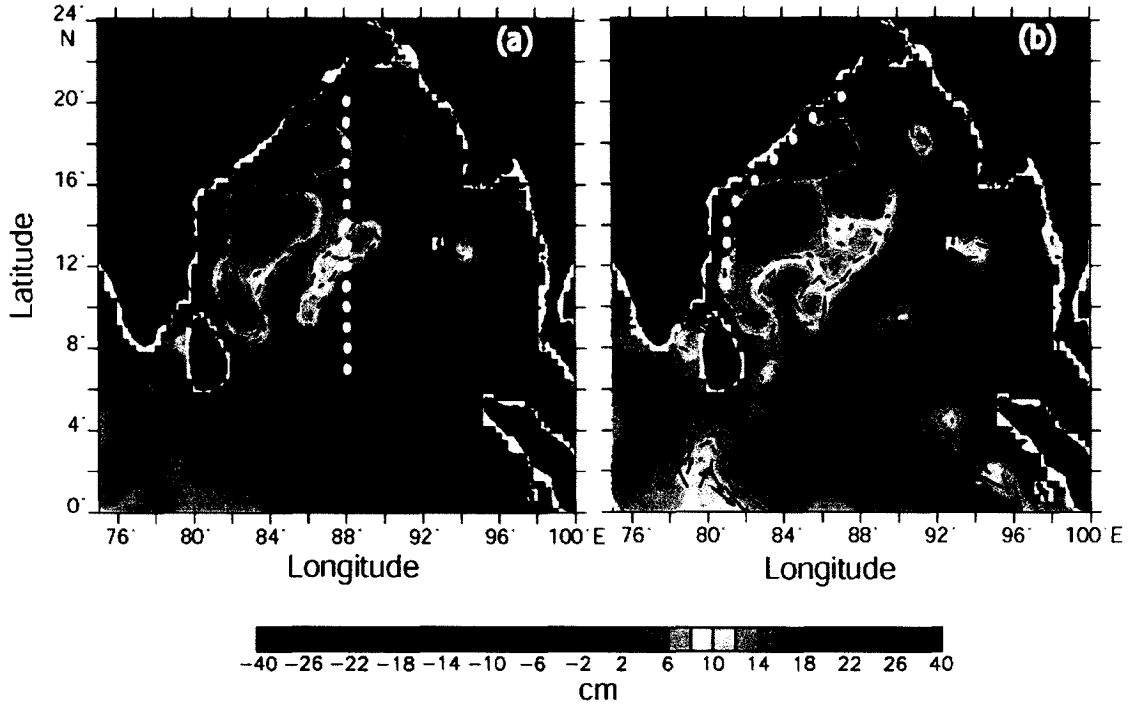

Fig.5.1.2 7-day snap-shots of Topex/Poseidon ERS1/2 merged sea-level anomalies overlaid with geostrophic velocities during (a) 23-27 April 2003 and (b) 30 April-5May 2003. The white filled circles denote the location of CTD stations. The CTD stations along the central Bay were occupied during 16-25 April 2003 and that along the western boundary was during 27 April-5 May 2003.

5.2 Summer monsoon (6 July to 2 August, 2001)

The MLD along central Bay during summer showed a large variation with deeper MLD in the south and a progressively shoaling MLD towards the north (Fig.5.2.1a). MLD was as deep as 60 m at 7°N, which showed a sharp decrease to 15 m at 8°N. MLD remained as shallow as 15 m between 8° and 10°N. From 10° to 12°N mixed layer deepened sharply to 50 m and from 12° to 20°N it showed a general shoaling reaching a value as

low as 5 m at 20°N. The vertical thermal structure showed thermocline oscillations, as in the case of spring intermonsoon, with maximum up-down sloping of isotherms between 8°-11°N, and 18°-20°N. Along the western boundary MLD deepened from 25 m at 11°N to 35 m at 15°N (Fig.5.2.1b). North of 15°N MLD showed a general shoaling, decreasing to a minimum value of 5 m at 20°N, as in the case of the central Bay.

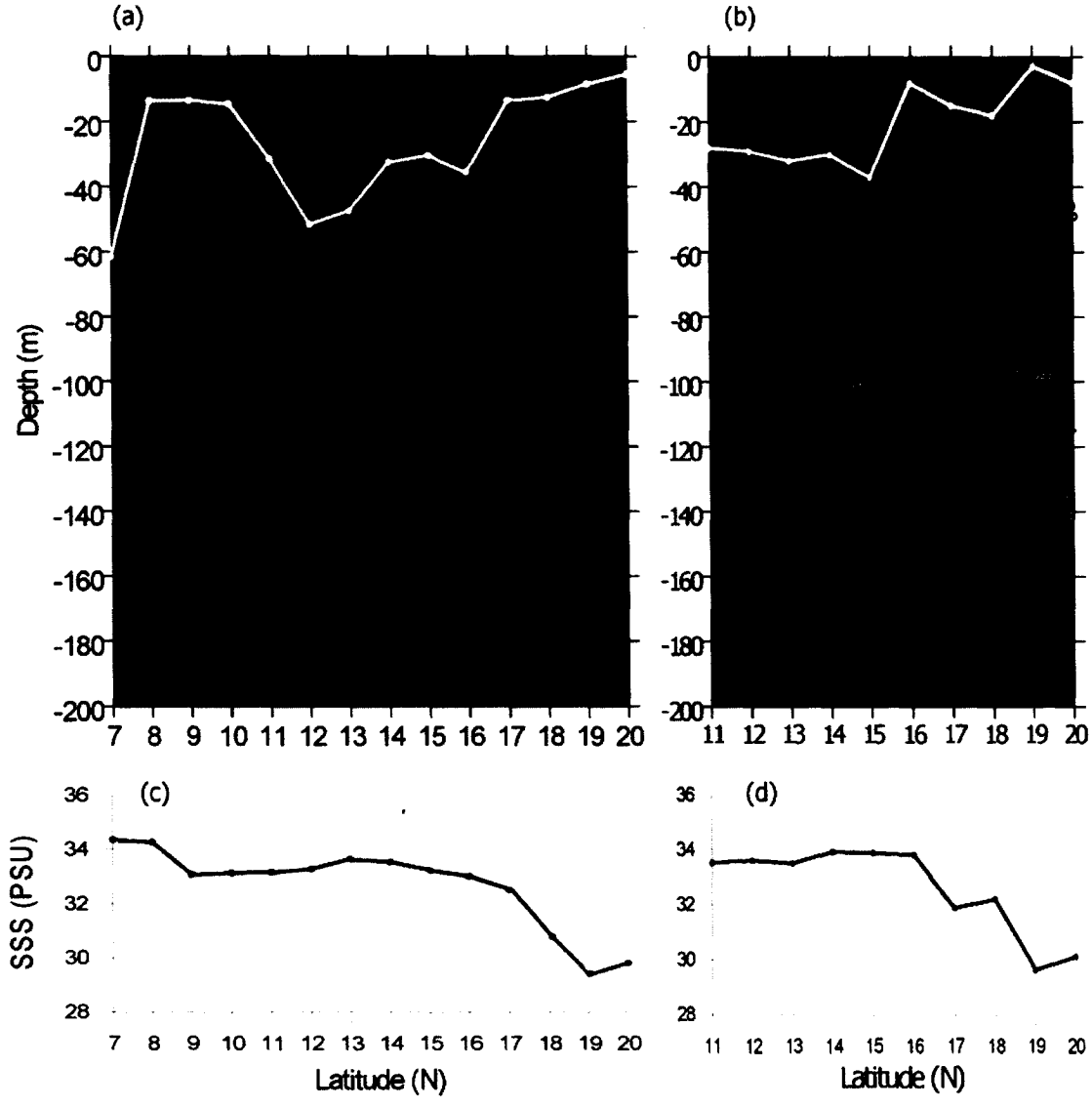

Fig.5.2.1 Vertical distribution of temperature (°C) in the upper 200 m along the (a) central Bay of Bengal (88°E) and (b) western boundary during summer monsoon (6 July to 2 August, 2001). The white line indicates the MLD (m). Distribution of surface salinity (psu) along the (c) central Bay and (d) western boundary during the same period.

This general decrease of MLD towards north could be explained in the context of salinity distribution. The surface salinity along both the central Bay (Fig.5.2.1c) as well as the western boundary (Fig.5.2.1d) showed a sharp decrease towards the north from 33 psu at 16°N to 29 psu at 20°N. Though the wind speed during summer was high (~8-9.5 m/s, Fig.4.3.2) in the northern Bay of Bengal, the increased stratification due to the presence of low salinity waters curtailed the strong wind-driven mixing leading to shallow mixed layer. But the deep MLD at 7°N (Fig 5.2.1a) was driven by the presence of warm core eddy as could be seen from the sea-level anomaly, which was positive (Fig.5.2.2a). As the 7°N station was located within the warm core eddy, the anti-cyclonic circulation and the associated downwelling deepened the mixed layer. The shallow MLD from 8 to 10°N

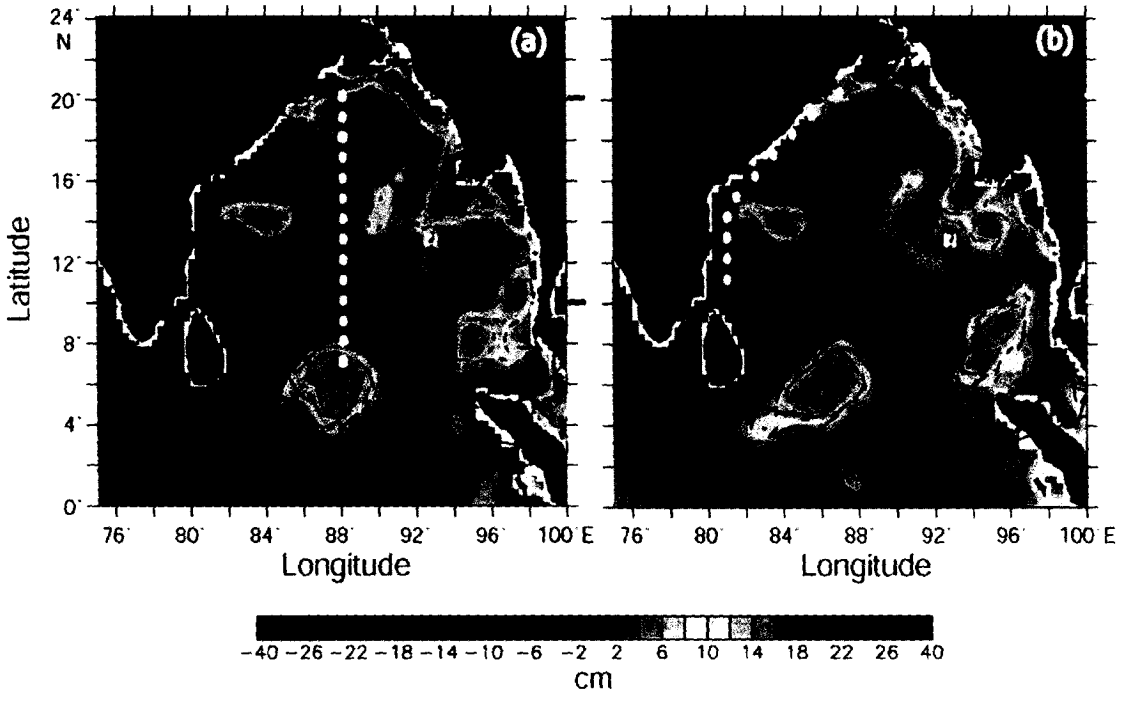

Fig.5.2.2 7-day snap-shots of Topex/Poseidon ERS1/2 merged sea-level anomalies overlaid with geostrophic velocities during (a) 11-17 July 2001 and (b) 18-24 July 2001. The white filled circles denote the location of CTD stations. The CTD stations along the central Bay were occupied during 10-21 July 2001 and that along the western boundary was during 23 July-1 August 2001.

was due to the presence of cold core eddy (negative sea-level anomaly). The cyclonic circulation associated with the cold core eddy drives the upwelling and the upheaval of isotherms between 8° and 10°N (Fig.5.2.1a) was the manifestation of this. Thus, the existence of warm core eddy adjacent to the cold core eddy leads to the sharp shoaling of MLD from 7° to 10°N. Again, the shallow MLD from 14° to 16°N was a result of cold core eddy located at this location as inferred from the sea-level anomaly map.

Along the western boundary the deep MLD in the south between 11° and 15°N was driven by the strong winds which are able to initiate deeper wind-driven mixing as the upper ocean was less stratified due to the presence of comparatively high surface salinity (~33.5 psu, Fig.5.2.1d) The shallow MLD at 16°N was driven by the presence of cold core eddy as could be inferred from the vertical thermal structure which shows the upheaval of isotherms at 16°N (Fig.5.2.1b) as well as from the sea-level anomaly map which was negative (Fig.5.2.2b).

5.3 Fall intermonsoon (14 September to 12 October, 2002)

In the central Bay of Bengal MLD showed a deepening from 25 m at 7°N to 65 m at 11°N during fall intermonsoon (Fig.5.3.1a). From 11°N onwards MLD showed a gradual decrease towards north with the lowest value of 5 m at 20°N. The vertical thermal structure showed thermocline oscillations the prominent ones were centered between 7° and 9°N, and between 17° and19°N within which the isotherms showed large up-down sloping. The largest isotherm depression was noticed between 11° and 13°N. Along the western margin also the MLD showed a shoaling trend (Fig.5.3.1b). The MLD was 20 m at 11°N, which shoaled to 5 m at 18° as well as 20°N. Thermal structure showed

prominent thermocline oscillation located at two regions, one between 11° and 13°N and the other between 17° and 19°N.

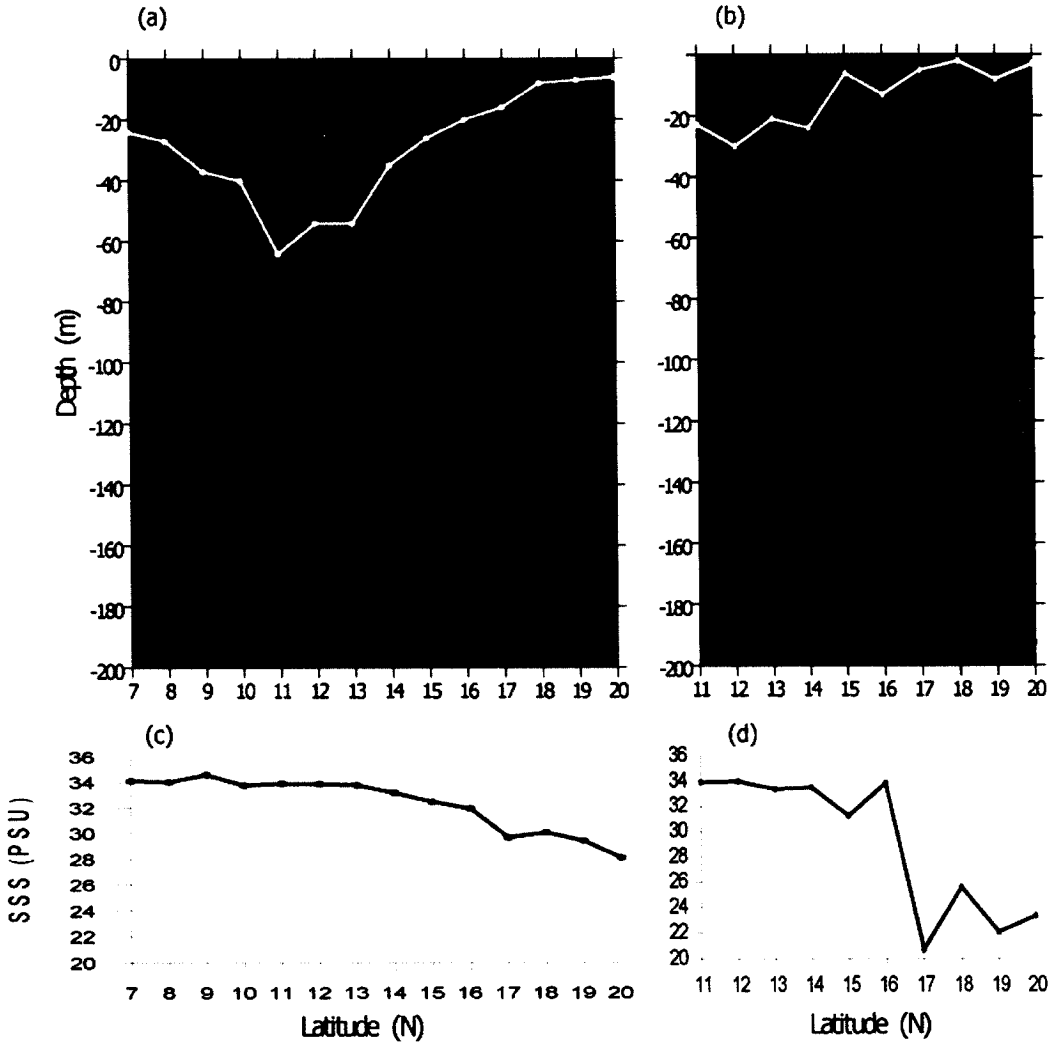

Fig.5.3.1 Vertical distribution of temperature (°C) in the upper 200 m along the (a) central Bay of Bengal (88°E) and (b) western boundary during fall intermonsoon (14 September to 12 October, 2002). The white line indicates the MLD (m). Distribution of surface salinity (psu) along the (c) central Bay and (d) western boundary during the same period.

An examination of the sea-level anomaly map showed the presence of a weak cold core eddy (negative sea-level anomaly) between 7° and 9°N (Fig.5.3.2a) within which shallow MLD was noticed and the thermal structure also showed a large up-sloping of isotherms

(Fig.5.3.2a). Thus, the shallow MLD could be explained in terms of this negative sea-level anomaly, which drives the cyclonic circulation and upwelling leading to shallow mixed layer. The deep MLD between 11°N to 13°N was due to the effect of warm core eddy as seen from the positive sea-level anomaly (Fig.5.3.2a) that drives the downwelling and results in deep mixed layer. The shoaling of mixed layer from 14° to 20°N was the result of decrease in salinity from 33 psu at 14°N to 28 psu at 20°N (Fig.5.3.1c). The presence of cold core eddy in the region of 16-18°N, though helped in decreasing the MLD, the rapid decrease of salinity towards the north made the upper layers highly stratified. The comparatively weaker winds (~5-6 m/s) during fall intermonsoon (Fig.4.3.3a&b) inhibited wind-driven mixing and there by making the mixed layer shallow.

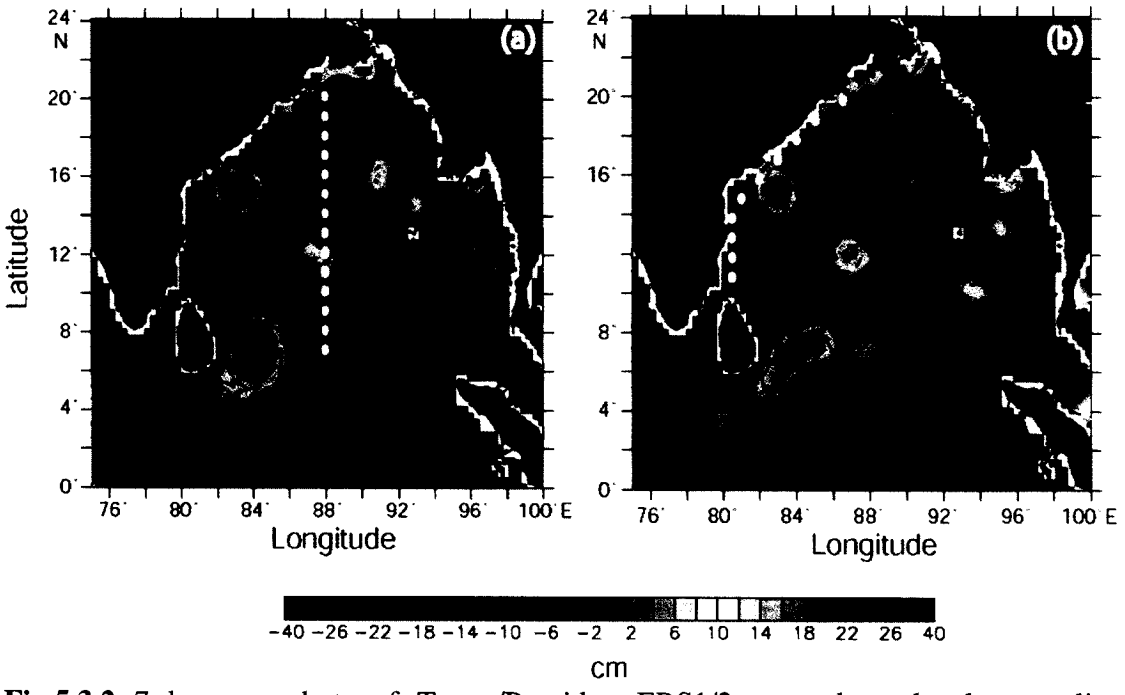

Fig.5.3.2 7-day snap-shots of Topex/Poseidon ERS1/2 merged sea-level anomalies overlaid with geostrophic velocities during (a) 18-24 September 2002 and (b) 2-8 October 2002. The white filled circles denote the location of CTD stations. The CTD stations along the central Bay were occupied during 15-27 September 2002 and that along the western boundary was during 30 September-11 October 2002.

Along the western boundary the stations at 11°N and 18°N were in the vicinity of cold core eddies (negative sea-level anomaly), while 16°N was in the vicinity of a warm core (positive sea-level anomaly) eddy (Fig.5.3.2b). As a result, the thermal structure showed shoaling at 11°N and 18°N, while a deepening at 16°N (Fig.5.3.1b). Thus, the deepening and shoaling of MLD at these locations were driven by the eddy-induced downwelling and upwelling. However, in the north, the rapid decrease of salinity from about 33 psu at 16°N to about 22 psu at 20°N had much greater influence on MLD. The strong stratification associated with the low salinity waters in the north lead to the shallow MLD.

5.4 Winter monsoon (25 November 2005 to 4 January 2006)

During winter season MLD along the open ocean transect showed shoaling and deepening consistent with the isotherm oscillations (Fig.5.41a). The MLD was about 30 m at 7°N, which deepened to 45 m at 8°N. From 8° to 13°N, MLD was about 40 m. A steep decrease in MLD was noticed from 14° to 15°N where MLD decreased to 30 m. Once again MLD showed a sharp deepening north of 16°N, with maximum value of 75 m at 19°N. Along the western boundary MLD was 50 m at 11°N, which showed a decreasing trend from 11° to 13°N reaching a value of 30 m (Fig.5.4.1b). From 13° to 15°N MLD varied between 30 to 40 m and from 15° to 17°N MLD showed a sharp increase of about 30 m. Again from 17° to 18°N MLD showed a drastic decrease of 40 m and then on remained shallow north of 18°N with a value of ~20 m.

An examination of sea-level anomaly map showed a number of cyclonic and anti-cyclonic circulation features during winter near the central Bay of Bengal as well as along the western boundary (Fig.5.4.2 a&b). The deep MLD observed between 8° and

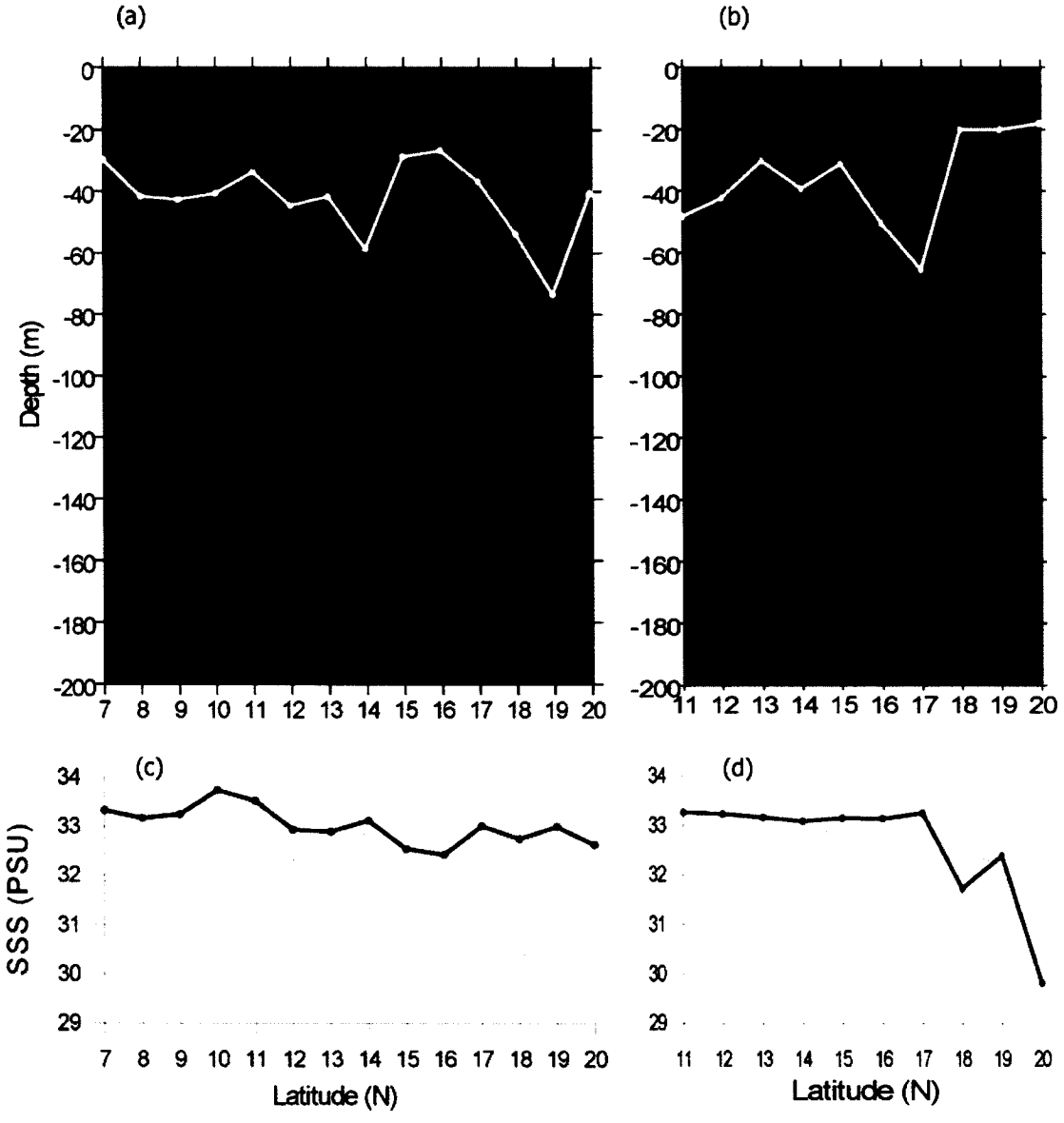

Fig.5.4.1 Vertical distribution of temperature (°C) in the upper 200 m along the (a) central Bay of Bengal (88°E) and (b) western boundary during winter monsoon (25 November 2005 to 4 January 2006). The white line indicates the MLD (m). Distribution of surface salinity (psu) along the (c) central Bay and (d) western boundary during the same period.

10°N and between 13° and 14°N was driven by the warm core eddy (positive sea-level anomaly) located in this region. The anti-cyclonic circulation associated with the warm core eddy and the downwelling led to the deepening of mixed layer. In the north, the surface salinity was about 33 psu (Fig.5.4.1c), which would lead to strong stratification and prevent any deepening of MLD. On the contrary a deepening of mixed layer between 16° and 19°N was noticed. This could be explained with the help of sea-level anomaly. The sea-level anomaly map showed the CTD sampling stations from 16° to 20°N was very close to the positive sea-level anomaly and the associated anti-cyclonic circulation. In fact CTD station at 19°N was much closer to the warm core eddy than the rest of the station and hence showed the highest deepening of MLD.

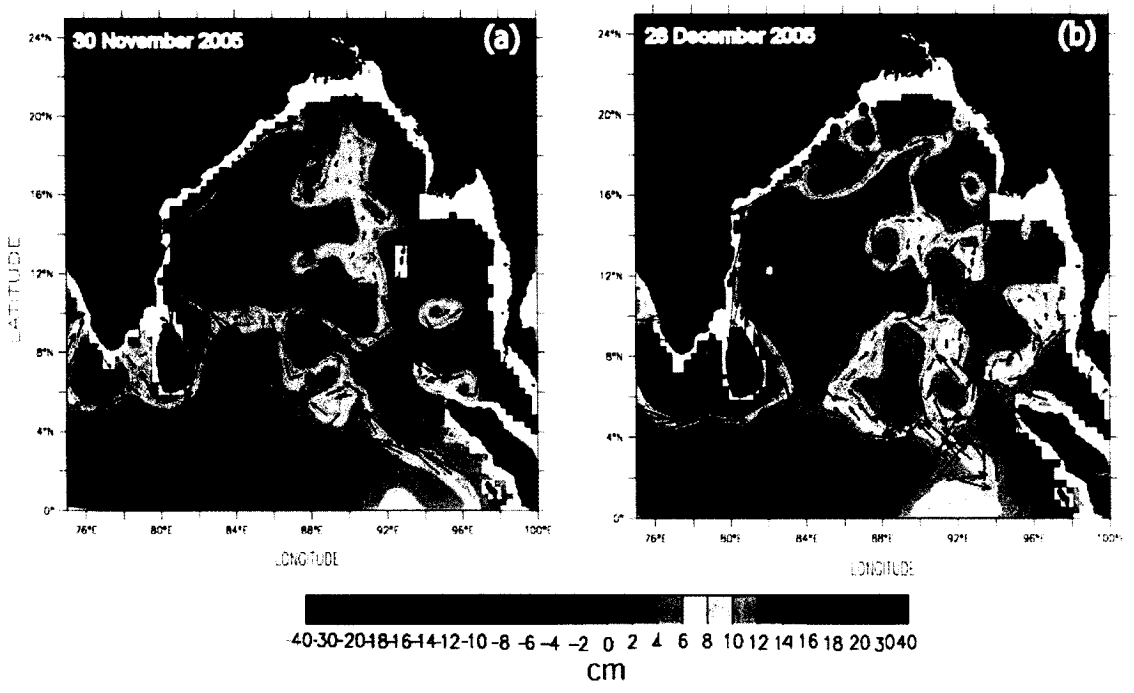

Fig.5.4.2 7-day snap-shots of Topex/Poseidon ERS1/2 merged sea-level anomalies overlaid with geostrophic velocities during (a) 30 November -6 December 2005 and (b) 28 December 2005 -3 January 2006. The black filled circles denote the location of CTD stations. The CTD stations along the central Bay were occupied during 29 November-10 December 2005 and that along the western boundary was during 11 December 2005-1 January 2006.

Along the western boundary, the shallow MLD from 13° to 15°N was due to the proximity of the station close to an elongated cold core eddy (negative sea-level anomaly) which drove upwelling associated with cyclonic circulation (Fig.5.4.2b) as well as the vertical thermal structure (Fig.5.4.1b). Similarly, the deep MLD of more then 60 m at 17°N was due to the presence of warm core eddy (positive sea-level anomaly) and the associated downwelling due to the anti-cyclonic circulation. North of 17°N, the shallow MLD was due to the rapid decrease of salinity from 33 to 29.8 psu (Fig.5.4.1d). This very low salinity led to strong stratification and the moderate winds (4-5 m/s, Fig.4.3.1) were unable to break this stratification to deepen the mixed layer by wind-driven mixing.

In summary, meso-scale eddies were seen as an integral part of the Bay of Bengal as they occurred in all over the basin in all the 4 seasons during which the Bay of Bengal was sampled along the central and the western boundary. The cyclonic circulation associated with the cold core eddies drive the upwelling which reduced the depth of the mixed layer. The anti-cyclonic circulation associated with the warm core eddy drive downwelling and resulted in the deepening of the mixed layer. However, in summer and fall intermonsoon the low salinity water in the north had more influence on mixed layer depth as they increased the upper ocean stratification, which the prevailing winds were unable to break and initiate strong wind-driven mixing.

Chapter 6 – Nitrate and Chlorophyll

Having analyzed and understood about the variability of the upper ocean, the mixed layer and the barrier layer, it is important to analyze the water-column nutrients and biology to understand how they respond to these changes. Towards this, the nitrate and chlorophyll *a* at 10, 20, 50, and 100 m were analyzed and presented below. Surface values are not presented since the nitrate concentrations are generally in the undetectable levels. Only three seasons namely spring intermonsoon (March-April-May), summer monsoon (June-July-August), and winter monsoon (November-December-January-February) were considered as data in the fall intermonsoon (September-October) was very few as mentioned in Chapter 2. In addition, the satellite derived chlorophyll pigment concentrations were also analyzed during the four seasons to decipher the seasonal cycle.

6.1 Nitrate

6.1.1 Spring intermonsoon

During spring intermonsoon the nitrate concentrations at 10 m in most part of the basin was very low ~ 0.5 μM (Fig.6.1.1.1a). Along the northern and western Bay a high concentration was seen and the values were in excess of 1 μM. The region around Sri Lanka as well as a large patch in the central Bay also showed nitrate concentrations in the range of 1-1.5 μM. At 20 m high nitrate concentrations in the range of 1-2 μM were seen along the western and northeastern boundary (Fig.6.1.1.1b). The highest nitrate concentration of 3 μM was noticed north of Sri Lanka. Except the regions south of Sri

Lanka and southeastern Bay, the nitrate concentrations were less then 0.5 μM. The distribution pattern at 50 m depth was similar to that of 20 m, but concentration levels were much higher (Fig.6.1.1.1c). The nitrate concentrations ranged between 4 to 12 μM in the southwestern and northern Bay, with concentrations increasing towards the coast. Concentration in most part of the Bay was about 2 μM . At 100 m depth nitrate varied between 8 to 24 μM (Fig.6.1.1.1d).

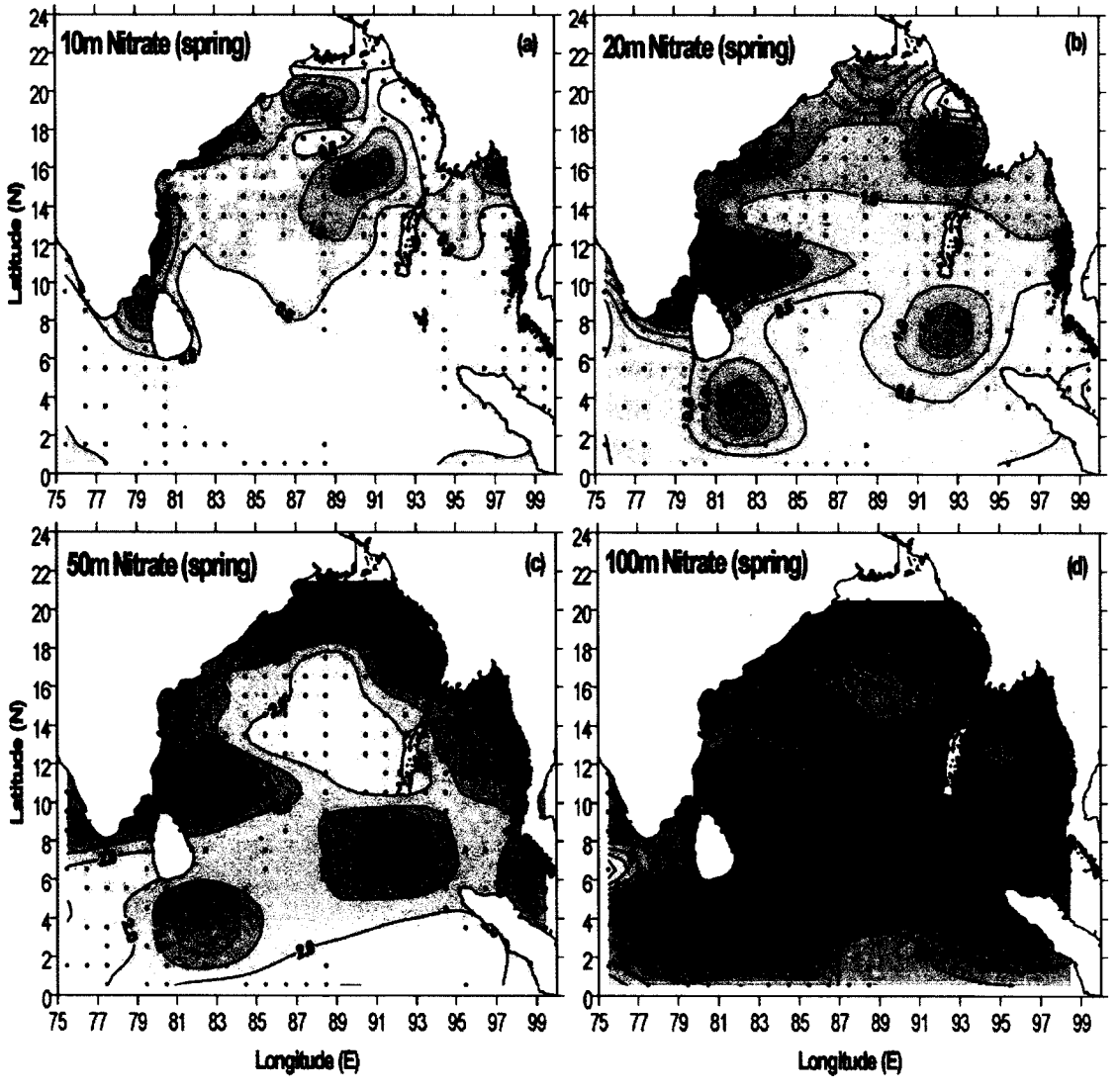

Fig.6.1.1.1 Spatial distribution of nitrate (μM) at (a) 10 m, (b) 20 m, (c) 50 m, and (d) 100 m during spring intermonsoon. Note the change in contour interval in (c) and (d).

6.1.2 Summer monsoon

The spatial distribution of nitrate at 10 m during summer showed very high concentrations in the Indo-Sri Lankan region where the values were as high as 6 μM near peninsular India and 3 μM off Sri Lanka (Fig.6.1.2.1a). Another region of high concentration, ~2.5 μM was found near the head Bay. The rest of the basin had nitrate concentrations less than 0.5 μM. At 20 m the pattern was similar to that of 10 m, except

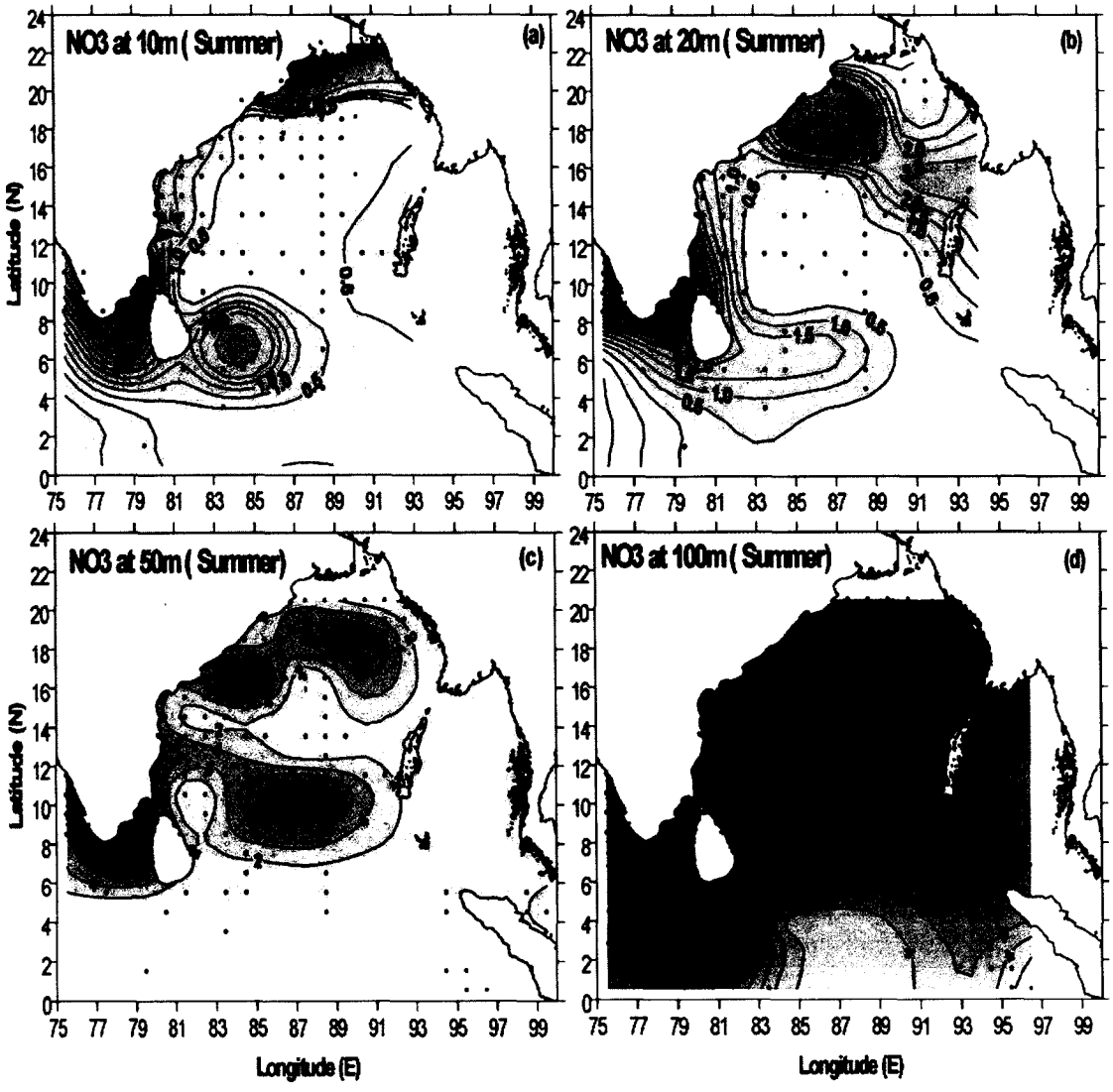

Fig.6.1.2.1 Spatial distribution of nitrate (μM) at (a) 10 m, (b) 20 m, (c) 50 m, and (d) 100 m during sumer monsoon. Note the change in contour interval in (c) and (d).

that the high nitrate concentrations seen near the head Bay at 10 m shifted towards the northwestern Bay and the concentrations increased to ~ 4 μM (Fig.6.1.2.1b). At 50 m the region of high concentrations of nitrate seen off east coast of Sri Lanka extended further to north and east and the core concentration was 10 μM (Fig.6.1.2.1c). The northern Bay north of 18°N showed high nitrate concentrations of 8-10 μM. At 100 m the northwestern Bay showed higher concentrations while the southeastern Bay showed lower concentrations (Fig.6.1.2.1d). The maximum concentration of nitrate was 24 μM.

6.1.3 Winter monsoon

The nitrate distribution at 10 m during winter season showed very less concentrations (0.2-0.4 μM) in the entire Bay except near the eastern equatorial region off Sumatra which had a maximum value of 2.5 μM (Fig.6.1.3.1a). At 20 m the nitrate concentrations near the eastern equatorial region off Sumatra reduced drastically to 0.8 μM (Fig.6.1.3.1b). This was one-third of the value seen at 10 m in the southeastern Bay indicating that the source of this is from the surface ocean. Near the head Bay as well as west of Sri Lanka the nitrate concentration showed slight enhancement. At 50 m the nitrate concentrations were in excess of 2 μM and the highest values were encountered near the southwestern (12 μM) and northeastern (10 μM) Bay (Fig.6.1.3.1c). At 100 m the nitrates over entire Bay showed high values and varied between 2 –24 μM (Fig.6.1.3.1d).

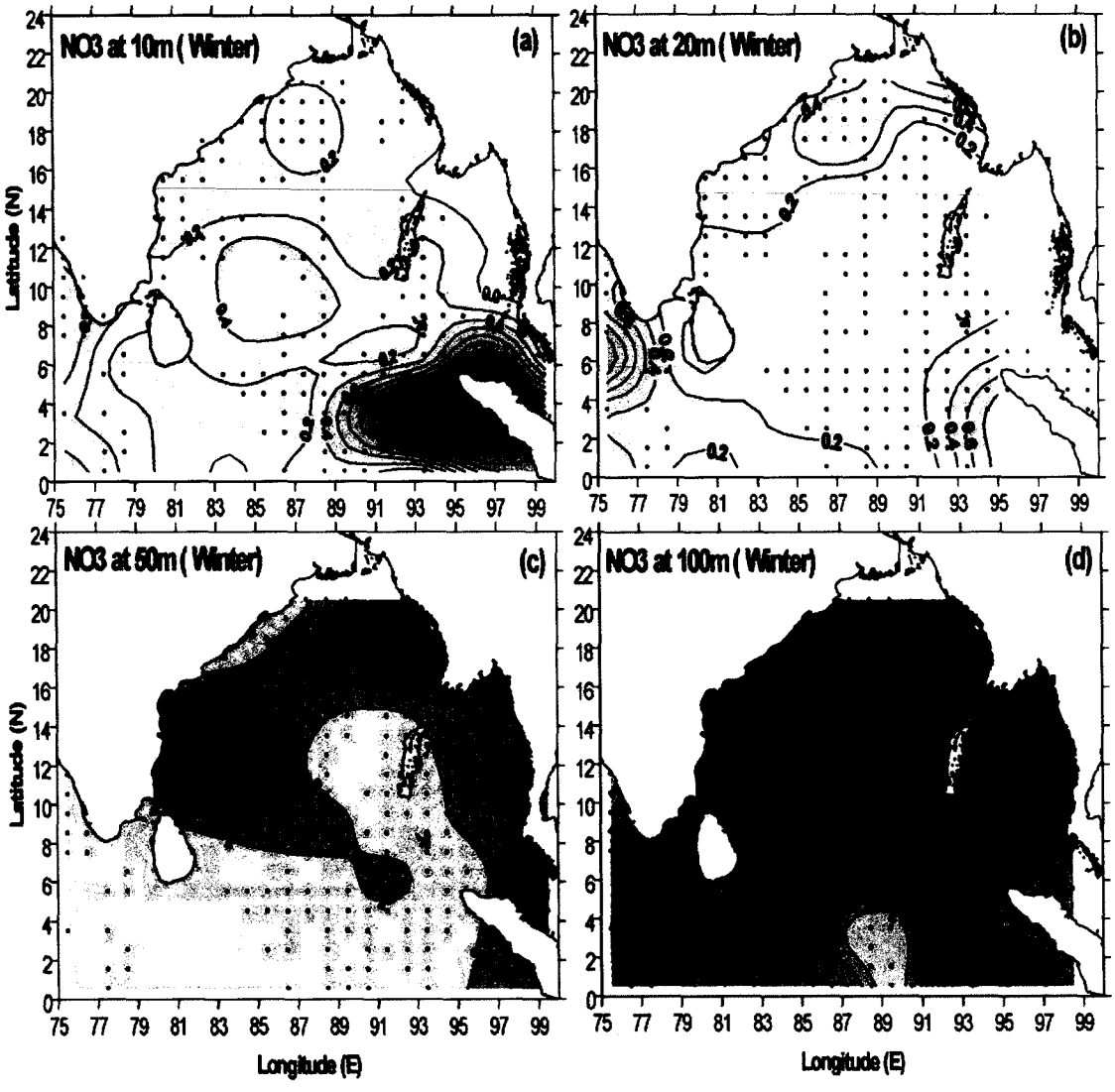

Fig.6.1.3.1 Spatial distribution of nitrate (μM) at (a) 10 m, (b) 20 m, (c) 50 m, and (d) 100 m during winter monsoon. Note the change in contour interval in (c) and (d).

6.2 Chlorophyll *a*

6.2.1 Spring intermonsoon

The chlorophyll *a* concentration at 10 m during spring intermonsoon was high along the southern tip of India, along the western boundary and also along the northeastern Bay

(Fig.6.2.1.1a). The region between 91 to 98°E and 4 to 10°N also showed highest chlorophyll *a* concentrations with maximum value of 0.7 mg/m^3. In the central and southern Bay the chlorophyll *a* was least and the value varied between 0.1 – 0.2 mg/m^3.

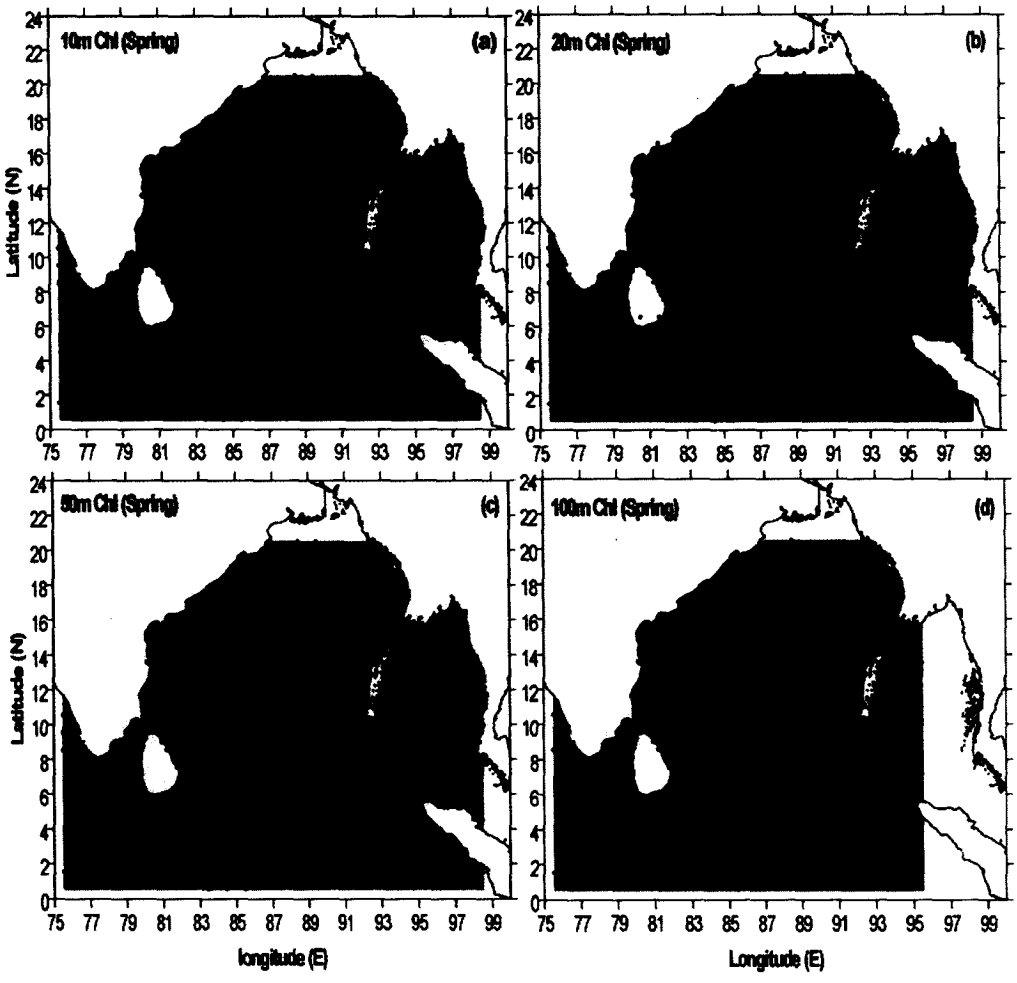

Fig.6.2.1.1 Spatial distribution of chlorophyll *a* (mg/m^3) at (a) 10 m, (b) 20 m, (c) 50 m, and (d) 100 m during spring intermonsoon.

At 20 m the chlorophyll showed the same pattern as that at 10 m with increased concentrations (Fig.6.2.1.1b). At 50 m the chlorophyll *a* along the western boundary and southern tip of India was high and showed an increase towards the coast (Fig.6.2.1.1c). The value varied between 0.2 – 0.7 mg/m^3. At 100 m the chlorophyll *a* concentrations in

the entire Bay was less then 0.2 mg/m^3 except in the southeastern Bay where it showed an increase from 0.2 to 0.7 mg/m^3 (Fig.6.2.1.1d).

6.2.2 Summer monsoon

The spatial distribution of chlorophyll *a* during summer monsoon at 10 m showed highest concentration of 0.5 mg/m^3 in the northern Bay compared to all other season (Fig.6.2.2.1a). The chlorophyll *a* concentrations along the southern part of the western

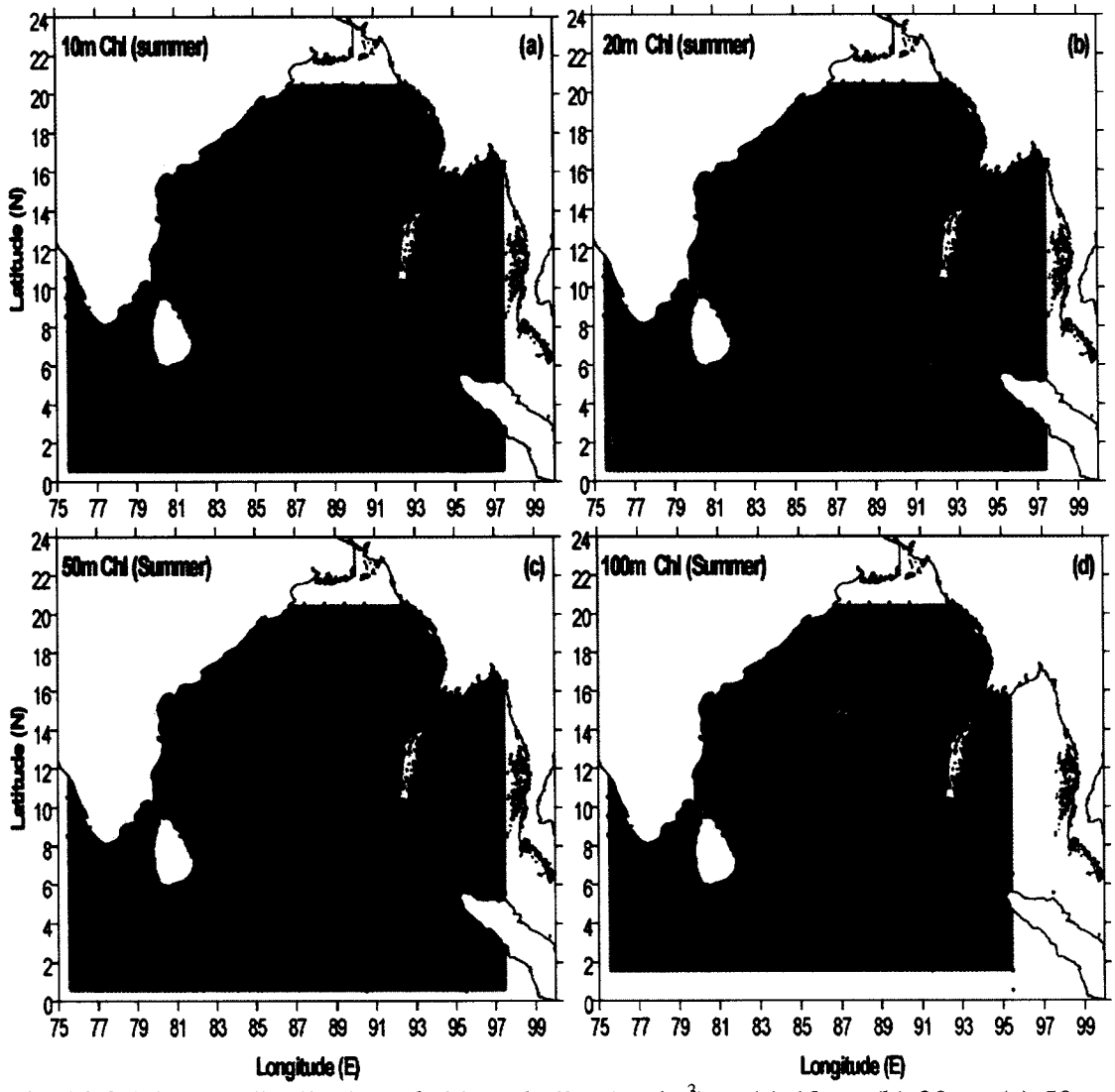

Fig.6.2.2.1 Spatial distribution of chlorophyll *a* (mg/m^3) at (a) 10 m, (b) 20 m, (c) 50 m, and (d) 100 m during summer monsoon. Note the change in contour interval in (b).

boundary also showed a value of about 0.5 mg/m^3 close to the coast, while in the rest of the Bay the chlorophyll *a* was between 0.1 to 0.2 mg/m^3. At 20 m the chlorophyll was the highest in the Indo-Sri Lanka with a value of ~ 2 mg/m^3 (Fig.6.2.2.1b). In the rest of the Bay the chlorophyll *a* was less then 0.2 mg/m^3. At 50 m (Fig.6.2.2.1c) and 100 m (Fig.6.2.2.1d) chlorophyll *a* distribution was similar to that at 20 m with higher concentrations around Sri Lanka and very less concentrations in the rest of the Bay.

6.2.3 Winter monsoon

During winter the chlorophyll *a* at 10 m in the Bay varied between 0.2 – 0.4 mg/m^3 except in the southeastern Bay where it was less then 0.1 mg/m^3 (Fig.6.2.3.1a). The highest concentration of 0.4 mg/m^3 occurred close to the western boundary. At 20 m the distribution of chlorophyll *a* showed a similar pattern as that of 10 m, except that the values along the western boundary was higher and varied between 0.3 – 0.6 mg/m^3 (Fig.6.2.3.1b). At 50 m the chlorophyll *a* over the Bay varied between 0.1 to 0.3 mg/m^3 except along the western boundary where it was more than 0.4 mg/m^3 (Fig.6.2.3.1.c). At 100 m most of the Bay showed low chlorophyll *a* with concentrations was about 0.1 mg/m^3, except a patch near the southern part of the western Bay where the concentration was ~0.5 mg/m^3 (Fig.6.2.3.1d). Similarly near Sumatra coast the vale was 0.3mg/m^3.

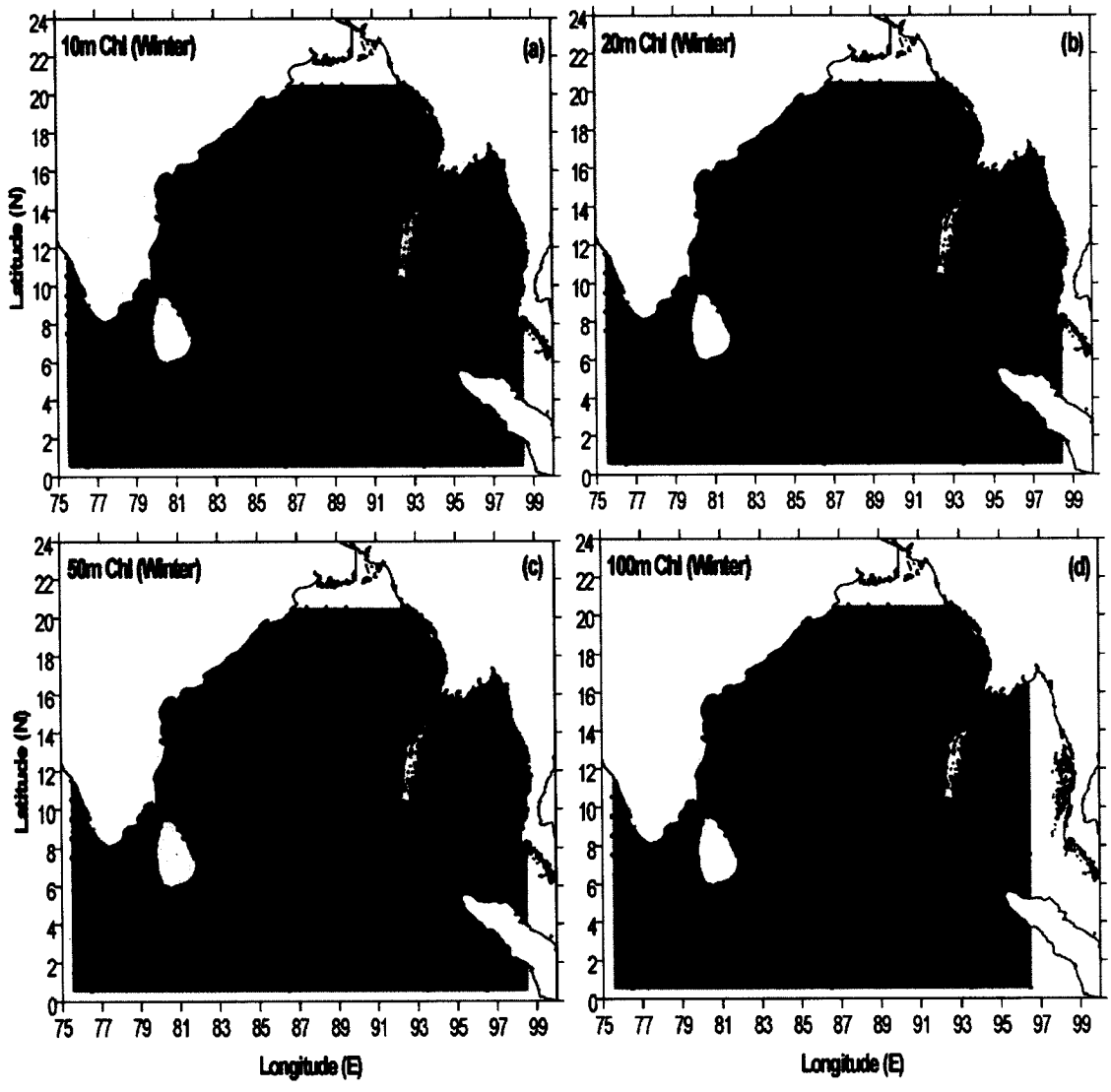

Fig.6.2.3.1 Spatial distribution of chlorophyll *a* (mg/m^3) at (a) 10 m, (b) 20 m, (c) 50 m, and (d) 100 m during winter monsoon.

6.3 Satellite-derived chlorophyll pigment concentrations

The satellite-derived chlorophyll pigment concentrations showed the least value during spring intermonsoon compared to the rest of the 3 seasons (Fig.6.3.1a). The pigment concentrations within the Bay varied over a very narrow range of 0.1 to 0.2 mg/m^3, except in the head Bay and close to peninsular India and Sri Lanka where it marginally

increased to 0.3 mg/m^3. The chlorophyll pigment concentrations were the highest in the Bay during summer monsoon around Indo-Sri Lanka region as well as in the northwestern Bay (Fig.6.3.1b). These values were comparable with the *in situ* concentrations seen in the earlier section. The Northern Bay showed a maximum value of

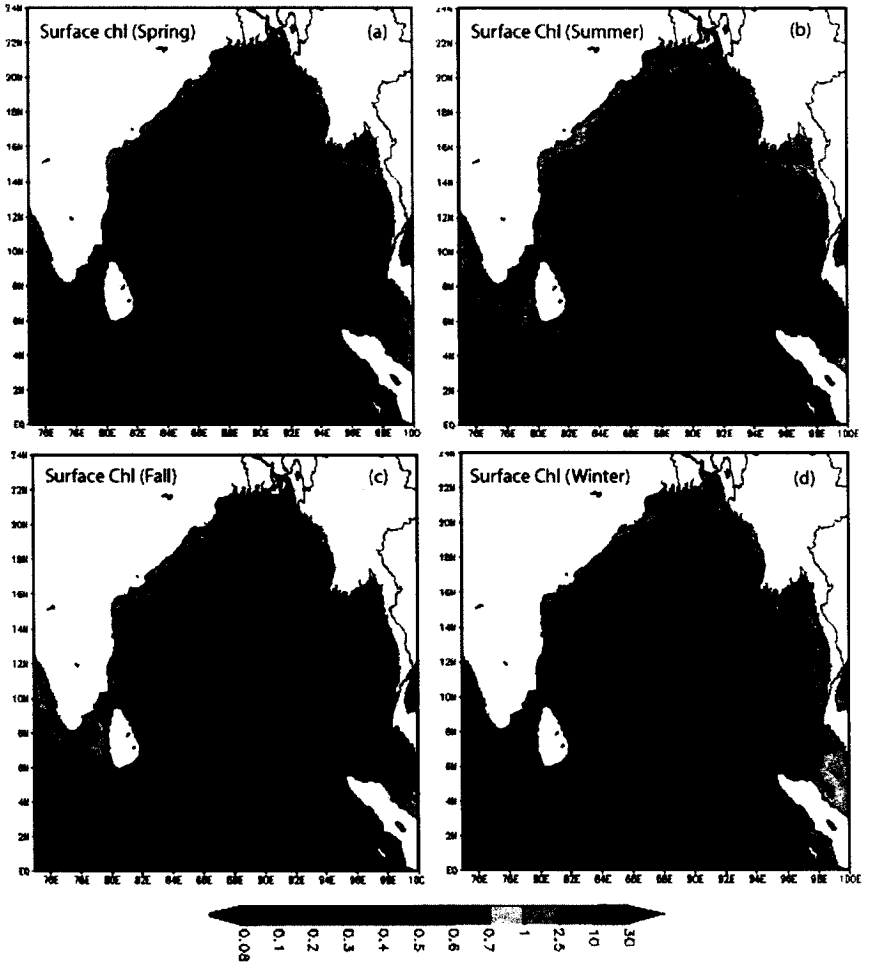

Fig.6.3.1 Seasonal mean climatology of chlorophyll pigment concentrations (mg/m^3) derived from SeaWiFS during (a) spring intermonsoon, (b) summer monsoon, (c) fall intermonsoon, and (d) winter monsoon.

about 1 mg/m^3, while near the Indo-Sri Lanka region it varied between 0.5 – 10 mg/m^3. In fall intermonsoon the chlorophyll pigment concentrations showed a reduction in their concentration, but the pattern remained similar to that of summer monsoon. The pigment

concentrations varied between 0.1 to 2.5 mg/m^3 (Fig.6.3.1c). During winter the chlorophyll pigment concentration showed a further reduction with most of the basin the values ranging between 0.1 to 0.3 mg/m^3 (Fig.6.3.1d). However, close to the western and eastern boundary the values varied between 0.3 – 2.5 mg/m^3.

In summary, the nitrate concentrations of the upper layer were the least during spring intermonsoon compared to the rest of the seasons. The highest concentrations in spring intermonsoon were along the western boundary. Consistent with this, the chlorophyll *a* concentrations, both in situ as well as satellite-derived, were also the least. The nitrate concentrations during summer monsoon were the highest and it occurred in the region of peninsular India and Sri Lanka and near the northern Bay. Accordingly, the chlorophyll concentrations were the highest. In fall intermonsoon, though the nutrient data and in situ chlorophyll *a* data were not available, the satellite-derived chlorophyll pigment concentrations showed pattern similar to that of summer monsoon with a reduced concentration indicating the tapering effect of summer monsoon. In winter, both the nitrate concentrations and the chlorophyll *a* concentrations were high along the western boundary. It is to be noted that the number of chlorophyll *a* data for any given season is much less in comparison with the nitrate data. Also the spatial coverage of chlorophyll *a* data also is less adequate compared to nitrate data. Hence it is quite possible that this data were unable to resolve all the characteristics of the seasonal variability. Nevertheless, the salient features such as summer monsoon high concentrations in the northern Bay as well as near the Indo-Sri Lanka region, the comparatively high concentrations along the western boundary and the lowest concentrations during spring intermonsooon were all captured.

Chapter 7 – Summary and conclusions

The variability of the upper ocean including the mixed layer and the barrier layer has been studied in the context of atmospheric forcing and remote forcing, and its role in regulating the nutrients and chlorophyll in the Bay of Bengal on a seasonal scale. For this a suite of *in situ* as well as remote sensing data were used. The *in situ* data consisted of temperature and salinity profiles derived from (1) World Ocean Data Base [*Boyer et al.*, 2006] consisting of Hydro-cast during the period 1919-2003 and CTD for the period 1972-2003, (2) Responsible National Oceanographic Data Centre (RNODC) at National Institute of Oceanography which has data from Hydro-cast during 1972-1996 and CTD during 1979-2006 collected from Indian research ships and (3) Argo data during 2002-2007. From the above 3 sources 7197 profiles of temperature and salinity from Hydro-cast, 2714 profiles from CTD and 4569 profiles from Argo were extracted. The nitrate data were extracted from the World Ocean Data Base during 1906-1999 and RNODC for the period 1973-2006, while chlorophyll data were taken from the RNODC during the period 1951-2006. In all there were 7406 nitrate profiles and 1060 chlorophyll *a* profiles. All the above hydrographic data were quality controlled to first eliminate duplicate profiles and then each profile were visually checked for obvious errors and removed. Finally profiles with depth less than 50 m were removed as the mixed layer in the Bay of Bengal is expected to exceed more than 50 m. This quality control procedure reduced the total number of Temperature-Salinity profiles from Hydro-cast to 5328, CTD to 2656 and Argo to 4203. The quality control reduced the nitrate profiles to 2653 and chlorophyll *a* profiles to 1030. The temperature and salinity profiles were used to calculate the density

(sigma-t). From these profiles the monthly mean climatology of temperature, salinity and sigma-t were prepared on a 1^{o} x 1^{o} grid.

As the salinity changed rapidly in the upper layers in the Bay of Bengal due to freshening by river runoff as well as precipitation, density criteria was used to define mixed layer for the present study. Mixed layer was defined as the depth at which the density (sigma-t) exceeds 0.2 kg m^{-3} from its surface value. The barrier layer was numerically calculated by subtracting the mixed layer depth (MLD) from the isothermal layer. The isothermal layer for the present study was defined as the depth at which the temperature decreased by $1^{o}C$ from its surface value.

Since adequate nitrate and chlorophyll *a* profiles were not available to create a monthly mean climatology, they were prepared as a seasonal climatology on a 1^{o} x 1^{o} grid. The seasons considered for this purpose were spring intermonsoon (March-May), summer monsoon (June-August), fall inter-monsoon (September-October), and winter monsoon (November-February). However, as the nitrate as well as chlorophyll *a* data were extremely limited during the fall intermonsoon, this season was not considered for the analysis.

The monthly mean climatology of discharge of 6 major rivers Ganges, Brahmaputra, Irrawady, Godavari, Krishna and Cauvery were taken from Global Runoff data Centre, Germany to examine the river discharge in the context of low surface salinity distribution in the Bay of Bengal.

In addition to the monthly mean climatology, the high resolution *in situ* data collected during Bay of Bengal Process Studies (BOBPS) has also been utilized to delineate the effect of meso-scale variability on mixed layer depth. The temperature and salinity profiles were obtained using CTD at 1-degree from 7°N to 20°N along the central (88°E) and from 11°N to 20°N along the western boundary of the Bay of Bengal. The measurements were carried out during summer (6 July to 2 August, 2001), fall intermonsoon (14 September to 12 October, 2002), spring intermonsoon (12 April to 7 May, 2003), and winter (25 November 2005 to 4 January 2006).

The atmospheric data used were monthly mean climatology of the incoming short wave radiation, wind speed, evaporation, precipitation and net heat flux on 1° longitude by 1° latitude grid obtained from National Oceanographic Centre (NOC), Southampton for the period 1980-1993. The remote sensing data used for the study were the chlorophyll pigment concentrations from SeaWiFS during the period September 1997 to December 2007 and the merged sea-level anomalies of Topex/Poseidon ERS1/2 series of satellites obtained from AVISO live access server during the period October 1992 to January 2006. From the sea-level height anomalies, velocities were computed assuming geostrophic balance.

The amplitude of the seasonal cycle of incoming short wave radiation (SWR) was about 120 W/m^2 with lowest during November – December (~165 W/m^2) and highest during March-April (~285 W/m^2). The seasonal cycle showed two warming and cooling periods. The highest SWR was during March-April followed by September, while the lowest was during November-February followed by June-August. The highest spatial variability

occurred in May when SWR varied 80 W/m^2 from south to north within the basin. The least spatial variability occurred in January and October which was about 20 W/m^2.

The amplitude of the seasonal cycle of net heat flux (NHF) was 220 W/m^2 with highest net heat gain by the ocean during April (~160 W/m^2) and the highest net heat loss by the ocean in December (~60 W/m^2). The NHF showed a seasonal cycle with two periods of high heat gain by the ocean, the highest during March-April followed by October. The ocean lost heat of about 20 W/m^2 during November-December from the northern Bay while the gain was the least in June. The highest spatial variability was in December (~140 W/m^2) and the least was in September (~50 W/m^2).

Consistent with the seasonality of the SWR and NHF, the sea surface temperature (SST) showed a strong seasonal cycle with two periods of warm and two periods of cool SST. The warming occurred during spring (April-May) and fall (October) intermonsoons, while cooling was in winter (January-February) and summer (August). There was a time lag of about a month between the atmospheric forcing by way of SWR and NHF and corresponding ocean's response in terms of SST. The amplitude of the seasonal cycle was about 6°C with coldest SST of about 25°C in the north during January and warmest SST of about 31°C in the central part of the eastern boundary during May. The highest spatial variability occurred during January when SST varied 4°C from south to north. The spatial variability was the least in October, which was about 1.5°C. Note that the highest and least spatial variability in SST was also closely coupled to that of atmospheric forcing. A characteristic feature in the time evolution of the spatial distribution of SST was the appearance of a thermal front with a region of cold water around Sri Lanka in

May. The thermal front developed further in June-July with expansion of cold water region towards the peninsular India. The thermal front was the strongest in August with coldest SST of 26.5°C and with a gradient of about 3°C from southern tip of peninsular India to south of Sri Lanka. The thermal front dissipated by September. This feature was not associated with atmospheric forcing due to SWR or NHF, but with the wind.

The amplitude of the seasonal cycle of wind speed within the basin was 6 m/s with lowest wind speed of about 4 m/s in March and October, and highest wind speed of 10 m/s in June. The highest spatial variability occurred during June when wind speed varied by 6 m/s from south to north. The least spatial variability occurred during March, which was 1 m/s. The seasonal cycle of wind speed in the northern Bay (north of 15°N) showed semiannual cycle with high wind speed during summer followed by winter, while low wind speed was during spring and fall intermonsoons. The wind stress curl showed highest positive value of 20 x 10^{-8} Pascal/m along the eastern part of Sri Lanka during June to August. This positive wind stress curl was capable of driving an upward Ekman pumping which in turn could transport cold sub-surface waters to the surface layer. Thus, the observed cold waters and the thermal front around Sri Lanka and the southern part of the peninsular India during June to August were linked to the process of upwelling in the Indo-Sri Lanka region.

The sea surface salinity (SSS) showed very strong seasonality, especially in the northern Bay. The amplitude of the annual cycle was about 8.5 psu with lowest salinity of 26.5 psu in the north during October and highest SSS of about 35 psu in the southern Bay during June-November. The highest spatial variability occurred during October when SSS varied

by 8.5 psu from north to south while the least spatial variability occurred in May, which was about 2 psu. The observed annual cycle of SSS could be understood in the light of the fresh water flux (E-P) and the freshwater discharge from rivers emptying into the Bay of Bengal.

The freshwater flux showed an annual cycle with the basin receiving excess precipitation over evaporation. The basin received highest excess precipitation of 440 mm/month in July and the highest evaporation of 120 mm/month was in December. The highest spatial variability occurred during July when E-P varied from 40 mm/month to –440 mm/month. The least spatial variability occurred during May, when E-P varied from 80 mm/month to –60 mm/month. The annual variability of E-P in the northern Bay (north of 15°N) showed a net evaporation from December-April and net precipitation from June-September. The monthly mean climatology of river discharge of 5 major rivers Ganges, Brahmaputra, Irrawady, Godavari, and Krishna showed the dominance of freshwater discharge during July to October. Thus, the observed rapid decrease of SSS in the northern Bay during June to October was tightly coupled to the freshening of the surface waters by the negative fresh water flux as well as the river water discharge into the northern Bay. The seasonal circulation redistributed the fresher water influencing the ambient salinity. In the southern Bay salinity remained almost same except during June to October when the high salinity waters (35 psu) of the Arabian Sea origin is advected into the Bay of Bengal. Since the freshwater input was from the peninsular rivers, which are located in the northern part of the Bay along the eastern and western boundaries, it is important to decipher the variability of the northern and southern Bay separately. In the northern Bay, north of 15°N, the amplitude of the annual cycle of SSS was about 6.5 psu

with the highest salinity in May (~33 psu) and lowest (~26.5 psu) in October. In the southern Bay the amplitude of the annual signal was about 0.5 psu and this was associated with the intrusion of the high salinity waters from the Arabian Sea.

The mixed layer and barrier layer variability were examined in the light of heat flux, momentum flux (wind-stress curl) and fresh water flux (evaporation-precipitation) to decipher the factors that are responsible for their changes.

The mixed layer depth during the spring intermonsoon (March-April-May) was the shallowest in the Bay of Bengal compared to the rest of the season. It varied between 10 and 25 m in March and April. In May, however, the shallow MLD was confined to the region north of 16°N. Another region of comparatively shallow MLD (~25 m) was seen in a band between 6° and 9°N. The rest of the basin, however, showed deep MLD (30-35 m). The observed MLD variability could be understood in the light of the prevailing ocean-atmospheric conditions. The incoming solar radiation peaked during March-April with a value of 280-290 W/m^2 and the net heat flux also was the highest 150-160 W/m^2. The basin-wide winds were the weakest during this period (~4 – 5 m/s), except near the western boundary in April where a core of high wind speed was noticed and a strong negative wind stress curl. The shallow MLD in March-April was driven by the strong stratification induced by peak solar heating and subsequent highest net heat gain by the ocean. The low salinity waters (< 32.5 psu) in the northern Bay (north of 18°N) during March-April made the upper ocean highly stratified. The weak winds during this period were unable to drive deep wind-mixing due to strong stratification and hence led to the formation of shallow mixed layer.

In the south, the comparatively deeper mixed layer (~ 35 m) seen west of 90°E was due to the presence of high salinity waters (>34.5 psu) which made the water column less stable and the moderate winds were able to initiate greater mixing leading to the observed deep MLD. However, the deep MLD east of Sri Lanka was linked to the development of anti-cyclonic circulation associated with the formation of subtropical gyre which begins in May. This anti-cyclonic circulation drives downwelling and deepens the mixed layer. The co-location of comparatively deep MLD (>25 m) and strong negative wind stress curl (~ -20 x 10^{-8} Pascal/m) along the western boundary in April suggested the role of wind stress curl in deepening the mixed layer. Note that the subtropical gyre was well developed in April in the central and western Bay of Bengal, which also leads to downwelling and augments the deepening of the mixed layer.

The shallow MLD in the northeastern Bay in May was due to the presence of low salinity waters (~ 32.5 psu) along with the high incoming solar radiation (270-280 W/m^2) which increased the stratification. The moderate winds (5 – 5.5 m/s) in the northeastern region were unable to drive strong wind-mixing and hence the MLD was shallow. Comparatively shallow MLD in a band between 6° and 10°N east of Sri Lanka and southern tip of India was due to the upward Ekman pumping associated with the positive wind stress curl in this region. The deep MLD in May in the south, south of 4°N, was related to the downward Ekman pumping due to the negative wind stress curl. In addition to this the time-longitude plot of sea-level height anomaly along 4°N showed the propagation of Rossby waves during spring intermonsoon, which also contributed in deepening the mixed layer.

During summer monsoon a band of deep MLD between equator and 6°N joined the deep MLD region seen closer to the western boundary towards the end of spring intermonsoon. However, the northern and eastern part of the Bay had shallow MLD. With the progress of summer monsoon, the region of deep MLD expanded towards the central and northern Bay. The region around Sri Lanka showed a progressively shallow mixed layer with time during summer monsoon which also showed eastward expansion with time. The observed pattern of MLD variation could be explained in the following manner. Though the wind speed was the highest during summer monsoon in the entire basin, the MLD was the shallowest in the northern Bay (~ 5m). An examination of E-P showed that it was negative and the highest of all the season, implying excess precipitation (in excess of 440 mm/month), in the northern Bay. In addition to the oceanic precipitation, the influx of freshwaters from the rivers adjoing the Bay of Bengal also contributed towards freshening of the surface waters of the Bay. An examination of the monthly mean climatology of river discharge of 5 major rivers Ganges, Brahmaputra, Irrawady, Godavari, and Krishna showed that the freshwater discharge dominated during July to October. The spreading of low salinity waters (<32 psu) were seen from the northern Bay towards the south and east with the progress of summer monsoon. The vertical profiles of stability parameter showed that these low salinity waters strongly stratified the upper ocean. Note that the upper ocean was very warm with SST in excess of 28.5°C, which also contributed towards strengthening the stratification. Hence, the winds though were the strongest of all the season, were unable to break the stratification to initiate wind-driven mixing and deepen the mixed layer. The shallow MLD seen around Sri Lanka was driven by the positive wind stress curl. The positive wind stress curl was seen developing

in May, which peaked in June and collapsed by September. The upwelling associated with the positive wind stress curl drives an upward Ekman pumping and this led to the observed shallow mixed layer during summer monsoon. This process of upwelling was also evident from the cold SST and the observed thermal front seen around Sri Lanka and southern part of the peninsular India. The band of deep mixed layer seen extending from the southwestern region into the central Bay was linked to the advection of high salinity waters from the Arabian Sea. An examination of SSS showed that the high salinity waters from the Arabian Sea were progressively advected into the central Bay around Sri Lanka during summer monsoon. This high salinity waters reduced the stratification of the upper ocean as could be inferred from the stability parameter. Thus, the strong winds of the summer monsoon combined with the less stratified upper ocean in the southern Bay due to the intrusion of high salinity waters from the Arabian Sea were able to drive strong wind-driven mixing. This was the mechanism which led to the formation of deep MLD in the south. In addition to this, the high sea-level anomaly in the central and eastern part of the southern Bay associated with the propagating Rossby waves also contributed towards deep MLD.

As the summer monsson tapers off and the fall intermonsoon sets in, the shallow MLD which was confined to northern Bay, north of 18°N, was seen extending southward to 15°N in October. This could be explained in the context of changing atmospheric forcing from summer monsoon to fall intermonsoon. The short wave radiation as well as net heat flux showed a secondary heating of the upper ocean during fall intermonsoon and accordingly the SST was in excess of 29°C in October. Though the E-P showed a rapidly decreasing precipitation, the surface salinity showed a progressive decrease from that of

summer monsoon and also a further southward extension of the low salinity waters. This indicated that the shallow MLD in the northern Bay and its further southward extension was linked to the presence of low salinity waters and its advection southward. As seen from the data, the river discharge was dominant during July to October and hence the low salinity of the surface water was the manifestation of this influence. The winds over the Bay showed a drastic reduction in their speed in the north during fall intermonsoon with the high wind speed confined to the southern Bay. Thus, the deep MLD in the southern Bay was driven by a combination comparatively high wind speed and the presence of high salinity waters both of which destabilized the water column.

The winter monsoon, in general, showed comparatively deep MLD (~30-40 m) all over the Bay except in the north and eastern Bay. The shallow MLD (~5-15 m) in the north and eastern Bay could be explained in the context of the presence of low salinity waters (<32 psu) during November-December and associated strong stratification. As the winter progressed, the E-P showed a net evaporation and with no substantial input from river discharge the low salinity waters were confined to the northern part during January-February. As a result the area of deeper mixed layer expands further towards eastern boundary. The shallow MLD observed near the Sumatra coast in January was driven by the strengthened positive wind stress curl and the associated upward Ekman pumping. The deep MLD in the rest of the Bay was related to the weakest stratification that occurred in the Bay during winter monsoon compared to all other seasons. The wind speed, which showed a secondary peak in winter were able to initiate deeper wind-mixing as the stratification of the water column was the weakest and this gave rise to the deep mixed layer.

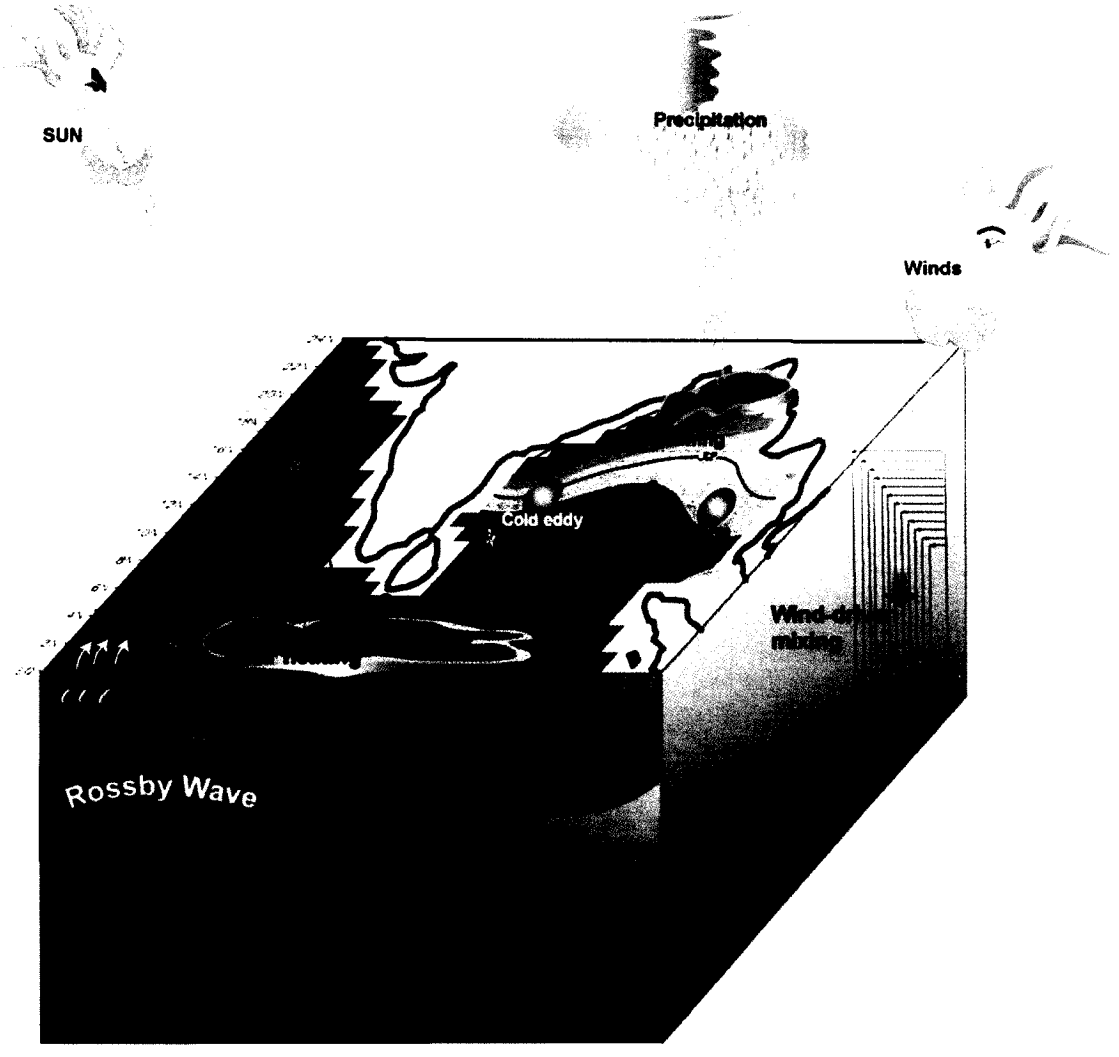

Fig.7.1 Schematic representation of local and remote forcing that influence the depth of the mixed layer. Colour shading is the climatological monthly mean salinity for August from WOA05 [*Antonov et al.*, 2006] showing the intrusion of high salinity waters from the Arabian Sea. The local forcing that affect the MLD are the precipitation and river runoff, solar heating, wind-mixing and meso-scale eddies (cold-core eddy in blue and warm-core eddy in red). The remote forcings are the intrusion of high salinity waters from the Arabian Sea and propagation of Rossby waves.

Thus, the mixed layer depth in the Bay of Bengal was controlled by a combination of local forcing as well as remote forcing. Local forcing were freshening of the surface waters due to excess precipitation over evaporation (fresh water flux) and river runoff,

surface heating due to incoming short wave radiation (heat flux) and wind-driven mixing (momentum flux). In addition to this, the meso-scale eddies which are ubiquitous in the Bay of Bengal also influenced the MLD. The remote forcing included advection of high salinity waters from the Arabian Sea and propagating Rossby waves. These local and remote forcing that influenced the MLD in the Bay of Bengal is depicted in Fig.7.1.

The seasonal variability of the barrier layer (BL) thickness showed strong coupling with wind stress curl, freshwater flux and prevailing circulation of the basin. On a basin-scale the thickness of the BL was the least in spring intermonsoon compared to the rest of the season and also the spatial variability was the least. This was primarily because the fresh water input into the Bay during spring intermonsoon either by river run-off or by precipitation was the least. The prevailing weak winds and very strong thermal stratification due to peak heating reduced the BL thickness to minimum. However, the negative wind stress curl near the northwestern Bay during March lead to an increase in the BL. Along the equator the spring-time Wyrtki jet flowing from west to east as well as the negative wind stress curl drove down-welling and sinking which increased the BL close to equator.

During summer the thick BL along the equator, especially towards the eastern region, was driven by the negative wind stress curl which increased towards east. Along the eastern boundary the thick BL was due to a combination of large negative wind stress curl and negative fresh water flux.

In fall intermonsoon the eastward flowing fall-time Wyrtki jet seen during October-November drives the down-welling and sinking of waters along the equator. The excess

precipitation seen from the freshwater flux makes the waters of the equatorial region fresher and the sinking due to Wyrtki jet increased the thickness of BL. In contrast, the thick BL seen in northern Bay was driven by the large negative freshwater flux.

In winter the thick BL in the northern Bay was in the region of low salinity (< 32.5 psu) waters and the southward expansion of the region of thick BL was associated with the development of EICC. In November the EICC starts flowing southward from the northern Bay carrying along with it the low salinity waters. During December-January, the EICC flows southward along the western boundary of the Bay transporting the low salinity waters into the eastern Arabian Sea. Thus, the observed spreading of thick BL from the northeastern Bay towards the south along the western boundary and into the west coast of India was driven by the EICC. Along the equator the thick BL during November-December was due to the negative freshwater flux and sinking.

Having deciphered the seasonal variability of the upper ocean, the mixed layer and the barrier layer, the variability of water-column nitrate and chlorophyll *a* were analyzed to understand how they are linked to the upper ocean variability. The nitrate concentrations showed close correspondence with chlorophyll *a* concentrations in the upper ocean. The nitrate concentrations of the upper layer were the least during spring intermonsoon compared to the rest of the seasons. Similarly, the *in situ* chlorophyll *a* as well as the satellite-derived chlorophyll pigment concentrations was also the least varying from 0.1 to 0.2 mg/m^3. The highest concentrations in spring intermonsoon were along the western boundary. Consistent with this, the chlorophyll *a* concentrations, both *in situ* as well as satellite-derived, were also the least ranging from 0.1 to 0.3 mg/m^3. The low levels of

nitrate could be understood in the context of prevailing upper ocean conditions. During spring intermonsoon the upper ocean was strongly stratified due to the peak heating by incoming shortwave radiation. The mixed layer was very shallow as the weak winds during spring intermonsoon were unable to initiate strong wind-driven mixing. As a result there was no vertical transport of nutrients to the surface layer from subsurface making the upper ocean oligotrophic. The observed low chlorophyll *a* concentrations were strongly coupled to mixed layer variability. The nitrate concentrations during summer monsoon were the highest and it occurred in the region of peninsular India and Sri Lanka and near the northern Bay. Accordingly, the chlorophyll concentrations were the highest. The observed high nitrate as well as the chlorophyll *a* concentrations was driven by the upwelling that occurs in the Indo-Sri Lanka region during summer. The upward Ekman pumping associated with upwelling transports sub-surface nutrients from the nitracline to the surface layers and supports high biological productivity. In the northern Bay the river runoff supplies nutrients along with sediments and freshwater. The observed enhanced chlorophyll *a* was supported by this nutrient input. Away from this region, the high stratification of the upper layers due to the freshwater input from precipitation as well as river runoff inhibits wind-driven mixing though the winds were strongest in summer monsoon. Accordingly, the nutrient input from sub-surface to the upper ocean also was curtailed. Thus, the shallow MLD and the oligotrophic upper ocean lead to the observed low chlorophyll concentrations (~ 0.2 mg/m^3) in the rest of the Bay. In fall intermonsoon, though the nutrient data and *in situ* chlorophyll *a* data were not available, the satellite-derived chlorophyll pigment concentrations showed pattern similar to that of summer monsoon with a reduced concentration indicating the tapering effect of

summer monsoon. In winter, both the nitrate concentrations and the chlorophyll *a* concentrations were high along the western boundary. The EICC which moved southward during winter was capable of transporting some of the nutrients from the northern Bay towards the south along the western boundary and could explain the nutrient enhancement which in turn supported observed chlorophyll *a* concentrations. Thus, the observed chlorophyll *a* concentrations in the Bay of Bengal were strongly coupled to mixed layer variability.

It is quite possible that all the characteristics of the seasonal variability of chlorophyll *a* were not fully resolved as the chlorophyll *a* data for any given season was much less in comparison with the nitrate data, both spatially and temporally. Nevertheless, the salient features such as summer monsoon high concentrations in the northern Bay as well as near the Indo-Sri Lanka region, the comparatively high concentrations along the western boundary and the lowest concentrations during spring intermonsooon were all captured.

Future Work

The research work presented in this thesis was an attempt to understand the basin-scale variability of the mixed layer and then probe into the causative factors that brings about the observed variability using a variety of *in situ* and remote sensing data. The aim of the research was also to understand how these changes in the upper ocean regulate nutrients and chlorophyll in the Bay of Bengal. The study could bring out the role of atmospheric forcing such as heat, momentum and freshwater flux in controlling the mixed layer depth on a seasonal scale. In addition to these local atmospheric forcing, the study also brought out the role of advection of high salinity waters from the Arabian Sea, propagating Rossby waves, and the meso-scale eddies in mediating the changes in the mixed layer depth.

Though the thesis advanced our understanding of the mixed layer variability and its coupling to nutrients and biology in the Bay of Bengal, there is ample scope to explore further. For example, the role of each of the above mechanisms can be determined quantitatively using a physical-biogeochemical model. Another area which needs urgent attention is the generation of quality biogeochemical data. The limitation of this study was the lack of adequate chlorophyll and nutrient data, which did not allow to fully resolve all the characteristics of the seasonal variability.

References

Antonov, J. I., R. A. Locarnini, T. P. Boyer, A. V. Mishonov, and H. E. Garcia, (2006), *World Ocean Atlas 2005, Volume 2: Salinity,* edited by S. Levitus, NOAA Atlas NESDIS 62, U.S. Government Printing Office, Washington, D.C., 182 pp.

Bathen, K.H., (1972), On the seasonal changes in the depth of mixed layer in the north Pacific Ocean, *Journal of Geophysical Research*, 77, 7138-7150.

Behera, S.K., A.A. Deo, and P.S. Salvekar, (1998), Investigation of mixed layer response to bay of Bengal cyclone using a simple Ocean Model, *Meteorology and Atmospheric Physics*, 65, 77-91.

Boyer, T. P., J. I. Antonov, H. Garcia, D. R. Johnson, R. A. Locarnini, A. V. Mishonov, M. T. Pitcher, O. K. Baranova, and I. Smolyar, (2006), *World Ocean Database 2005, Chapter 1: Introduction*, NOAA Atlas NESDIS 60, Ed. S. Levitus, U.S. Government Printing Office, Washington, D.C., 182 pp, DVD.

Brainerd, K.E. and M.C. Gregg, (1995), Surface mixed and mixing layer depths, *Deep-Sea Research I*, 42, 1521-1543.

Conkright, M., S. Levitus, T. O'Brien, J. Antonov, C. Stephens, (1998), *World Ocean Atlas 1998 CD-ROM Data Set Documentation*, Technical Report 15, National Oceanographic Data Center, Silver Spring, Md.

de Boyer Montegut, C., G. Madec, A.S. Fischer, A. Lazar, and D. Iudicone, (2004), Mixed layer depth over the global ocean: An examination of profile data and a profile based climatology, *Journal of Geophysical Research*, 109, C12003, doi:10.1029/2004JC002378.

de Boyer Montegut, C., J. Mignot, A. Lazar and S. Cravatte, (2007a), Control of salinity on the mixed layer depth in the world ocean: 1. General description, *Journal of Geophysical Reearch*, 112, C06011, doi:10.1029/2006JC003953.

de Boyer Montegut, C., J. Vialard, S.S.C. Shenoi, D. Shankar, F. Durand, C. Ethe, G. Madec, (2007b), Simulated seasonal and interannual variability of the mixed layer heat budget in the northern Indian Ocean, *Journal of Climate*, 20(13), 3249-3268.

Eigenheer, A., and D. Quadfasel, (2000), Seasonal variability of the Bay of Bengal circulation inferred from TOPEX/Poseidon altimetry, *Journal of Geophysical Research*, 105, 3243-3252.

Fischer, A.S., (1997), Arabian Sea mixed layer deepening during the monsoon: Observations and dynamics, M.S.thesis, MIT, Cambridge, MA.

Fischer, A.S., (2000), The upper ocean response to the monsoon in the Arabian Sea. Ph.D. thesis, MIT/WHOI Joint Program, Cambridge MA, 222 pp.

Gopalakrishna, V.V., Y. Sadhuram, V. Ramesh Babu, (1988), Variability of mixed layer depth in the northern Indian Ocean during 1977 and 1979 summer monsoon seasons, *Indian Journal of Marine Sciences*, 17, 258-264.

Gopalakrishna, V.V., V.S.N. Murty, D. Sengupta, Shenoy. Shrikant, N. Araligidad, (2002), Upper ocean stratification and circulation in the northern Bay of Bengal during southwest monsoon of 1991, *Continental Shelf Research*, 22, 791-802.

Han, W., J.P. McCreary, K.E. Kohler, (2001), Influence of precipitation minus evaporation and Bay of Bengal rivers on dynamics, thermodynamics, and mixed layer physics in the upper Indian Ocean, *Journal of Geophysical Research*, 106, 6895-6916.

Kara, A.B., P.A. Rochford and H.E. Hurburt, (2003), Mixed layer depth variability over the global ocean, *Journal of Geophysical Research*, 108(C3), 3079, doi:10.1029/2000JC000736.

Kraus, E.B., (1977), Modelling and prediction of the upper layers of the Ocean, Pergamon Press, Oxford, England.

Levitus, S., (1982), *Climatological Atlas of the World Ocean*, NOAA Professional paper 13, National Oceanic and Atmospheric Administration, Rockville Md, 173 pp.

Levitus, S., T. Boyer, (1994), *World Ocean Atlas 1994*, Vol. 4: Temperature. NOAA Atlas NESDIS 4, U.S. Gov. Printing Office, Wash., D.C., 117 pp.

Levitus, S., R.Gelfeld, T. Boyer, D. Johnson, (1994), *Results of the NODC Oceanographic Data Archaeology and Rescue Projects*, Key to Oceanograhic Records Documentation No. 19, NODC, Washington, D.C., 73pp.

Longhurst, A.,(1995), Seasonal cycles of pelagic production and consumption, *Progress in Oceanography*, 36, 77-167.

Lukas, R., and E. Lindstrom, (1991), The mixed layer of the western equatorial Pacific Ocean, *Journal of Geophysical research*, 96, 3343-3357.

Maheswaran, P.A., (2004), Mixed layer characteristics and hydrography off the west and east coasts of India, Ph.D thesis, Cochin University of Science and Technology, 203pp.

McCreary, J.P., P. K. Kundu, R. L. Molinari, (1993), A numerical investigation of dynamics, thermodynamics and mixed layer processes in the Indian Ocean, *Progress in Oceanography*, 31, 181-244.

McCreary,J. P., W. Han, D. Shankar, S.R. Shetye, (1996), Dynamics of the East India Coastal Current, 2, Numerical solutions, *Journal of Geophysical Research*, 101, 13993-14010.

Monterey, G., and S. Levitus, (1997), *Seasonal variability of mixed layer depth for the world ocean*, NOAA atlas NESDIS 14, U.S. Gov. Printing Office, Washington, D.C., 87 figures & 96pp.

Morel, A., and J.M. Andre, (1991), Pigment distribution and primary production in the western Mediterranean as derived and modeled from coastal zone colour scanner observations, *Journal of Geophysical Research*, 96, 685-698.

Murty, V.S.N., Y.V.B. Sarma, D.P. Rao, (1996), Variability of the Oceanic boundary layer characteristics in the northern Bay of Bengal during MONTBLEX-90, *Proceedings of the Indian Academy of Sciences (Earth and Planetary Sciences)*, 105,41-61.

Narvekar, J., and S. Prasanna Kumar, (2006), Seasonal variability of the mixed layer in the central Bay of Bengal and associated changes in nutrients and chlorophyll, *Deep-Sea Research I*, 53, 820-835.

Nuncio, M., (2007), Role of eddies in the Bay of Bengal circulation and hydrography and in the distribution of nutrients and chlorophyll, Ph.D thesis, Goa University, 118pp.

Perigaud, C., P. Delecluse, (1993), Interannual sea level variations in the tropical Indian Ocean from Geosat and shallow water simulations, *Journal of Physical Oceanography*, 23(1), 916-1934.

Pond, S., and G. L. Pickard, Introductory dynamical oceanography, Pergamon Press, New York, 241 pp, 1983.

Potemra, J.T., M.E. Luther, J.J. O'Brien, (1991), The seasonal circulation of the upper ocean in the Bay of Bengal, *Journal of Geophysical Research*, 96, 12667-12683.

Prasad, T.G., (1997), Annual and seasonal mean buoyancy fluxes for the tropical Indian Ocean, *Current Science*, 73, 667-674.

Prasad, T.G.,(2004), A comparison of mixed layer dynamics between the Arabian Sea and the Bay of Bengal:one dimensional model results, *Journal of Geophysical Research*, 109, doi:10.1029/2003JC002000.

Prasanna Kumar, S., and A.S. Unnikrishnan, (1995), Seasonal cycle of temperature and associated wave phenomena in the upper layers of the Bay of Bengal, *Journal of Geophysical Research*, 100, 13585-13593.

Prasanna Kumar, S., P.M Muraleedharan, T.G. Prasad, M. Gauns, N. Ramaiah, S.N. de Souza, S. Sardesai, M. Madhupratap (2002) hy is the Bay of Bengal less productive

during summer monsoon compared to the Arabian Sea? Geophys. Res. Lett., 29, 2235, doi:10.1029/2002GL016013, 88-1 to 88-4.

Prasanna Kumar, S., M. Nuncio, Jayu Narvekar, Ajoy Kumar, S. Sardesai, S.N. Desouza, Mangesh Gauns, N. Ramaiah, M. Madhupratap, (2004), Are Eddies nature's trigger to enhance biological productivity in the Bay of Bengal?, *Geophysical Research Letters*, 31, L07309, doi:10..1029/2003Gl019274.

Prasanna Kumar, S., and Jayu Narvekar, (2005), Seasonal variability of mixed layer in the central Arabian Sea and its implication to nutrients and primary productivity, *Deep-Sea Research II*, 52, 1848-1861.

Prasanna Kumar, S., M. Nuncio, N. Ramaiah, S. Sardesai, Jayu Narvekar, Veronica Fernandes, Jane T. Paul, (2007), Eddy-mediated biological productivity in the Bay of Bengal during fall and spring intermonsoons, *Deep-Sea Research I*, 54, 1619-1640.

Ramaswamy, V., R.R. Nair, (1994), Fluxes of material in the Arabian Sea and Bay of Bengal — Sediment trap studies. Proceedings of the Indian Academy of Sciences, *Earth and Planetary Sciences*, 103, 189–210.

Rao, R.R., R.L. Molinari, J.F. Festa, (1989), Evolution of the climatological near-surface thermal structure of the tropical Indian Ocean:1Description of mean monthly mixed-layer depth and sea-surface temperature, surface-current and surface meteorological fields, *Journal of Geophysical Research*, 94, 1081-10815.

Rao, R.R., R. Sivakumar, (2000), Seasonal variability of near-surface thermal structure and heat budget of the mixed layer of the tropical Indian ocean from a new global ocean temperature climatology, *Journal of Geophysical Research*, 105(C1), 995-1016.

Rao, R.R., R. Sivakumar, (2003), Seasonal variability of sea surface salinity and salt budget of the mixed layer of the north Indian Ocean, *Journal of Geophysical Research*, 108(C1), 3009, doi:10.1029/2001JC000907.

Schneider, N., P. Muller, (1990), The meridional and seasonal structures of the mixed layer depth and its diurnal amplitude observed during the Hawaii-to-Tahiti Shuttle Experiment, *Journal of Physical Oeanography*, 20, 1395-1404.

Schott, F.A., J.P. McCreary, (2001), The monsoon circulation of the Indian Ocean, *Progress in Oceanography*, 51, 1-123.

Shankar, D., J.P. McCreary, W. Han, S.R. Shetye, (1996), Dynamics of the East India Coastal Current, 1, Analytic solutions forced by interior Ekman pumping and local alongshore winds, *Journal of Geophysical Research*, 101, 13975-13991.

Shankar, D., P.V. Vinayachandran, A.S. Unnikrishnana, (2002), The monsoon currents in the north Indian Ocean, *Progress in Oceanography*, 52, 63-120.

Shenoi, S.S.C., D. Shankar, S.R. Shetye, (2002) Difference in heat budgets of the nearsurface Arabian Sea and Bay of Bengal: Implications for the summer monsoon, *Journal of Geophysical Research*, 107, doi:10.1029/2000JC000679.

Shetye, S.R., S.S.C. Shenoi, A.D. Gouveia, G.S. Michael, D. Sundar, G. Nampoothiri, (1991) Wind-driven coastal upwelling along the western boundary of the Bay of Bengal during the southwest monsoon, *Continental Shelf Research*, 11, 1397-1408.

Shetye, S.R., A.D. Gouveia, S.S.C. Shenoi, D. Sundar, G.S. Michael, G. Nampoothiri, (1993), The western boundary current of the seasonal subtropical gyre in the Bay of Bengal, *Journal of Geophysical Research*, 98, 945-954.

Shetye, S.R., A.D. Gouveia, D. Shankar, S.S.C. shenoi, P. Vinayachandran, D. Sundar, G.S. Michael, G. Namboothiri, (1996), Hydrography and circulation in the western Bay of Bengal during the north east monsoon, *Journal of Geophysical Research*, 101(6), 14011-14025.

Sprintall, J., M.Tomczak, (1992), Evidence of barrier layer in the surface layer of the tropics, *Journal of Geophysical Research*, 97, 7305-7316.

Subramanian, V., (1993), Sediment load of Indian Rivers, *Current Science*, 64, 928-930.

Swain, J., R.K. Shukla, A. Raghunadha Rao, J.K. Panigrahi, N.R. Venkitachalam, (2003), Observations of wind and waves in the central Bay of Bengal during BOBMEX-99 and their effect on mixed layer depth variability due to forced mixing, *Proceedings of the Indian Academy of Sciences (Earth and Planetary Sciences)*, 112, 255-266.

Thadathil, P., P.M. Muraleedharan, R.R. Rao, Y.K. Somayajulu, G.V. Reddy, C. Revichandran, (2007), Observed seasonal variability of barrier layer in the Bay of Bengal, *J. Geophys. Res.* (C: Oceans): 112(2); doi:10.1029/2006JC00365.

UNESCO., (1981), Technical papers in marine science, United Nations Educational, Scientific and Cultural Organization, Paris, 192pp.

Vinayachandran, P.N., S.R. Shetye, D. Sengupta, S. Gadgil, (1996), Forcing mechanisms of the Bay of Bengal circulation, *Current Science*, 71, 753-763.

Vinaychandran, P. N., V.S.N. Murthy, B.V. Ramesh,(2002), Observations on barrier layer formation in the Bay of Bengal during summer monsoon, *J. Geophysical Res*, 107 (C12):8018 Doi10:1029/200JC000831.

Vinaychandran, P.N., and J. Kurian, (2007), Hydrographic observations and model simulation of the Bay of Bengal freshwater plume, *Deep-Sea Research I*, 54, 471-486.

Varkey, M.J., V.S.N. Murty, A. Suryanarayana, (1996), Physical oceanography of the Bay of Bengal and Andaman Sea. Oceanography and Marine Biology: an Annual Review 34, 1-70.

Weller, R.A., and D.M. Farmer, (1992), Dynamics of the ocean mixed layer, *Oceans*, 35, 46-55.

Wyrtki, K., (1964), The thermal structure of the eastern Pacific Ocean, *Dtsch. Hydrogr. Ze*, Supplement A8, 6-84.

Yu, L., J.J. O'Brien, J. Yang, (1991), On the remote forcing of the circulation in the Bay of Bengal, Journal of Geophysical Research, 96, 20449-20454.